Overview of the Physics and Technological Challenges of (Inverse) Compton Sources

Luca Serafini – INFN-Milan and Univ. of Milan

- **Physics of Thomson/Compton back-scattering from 2-body kinematics (particle quantum treatment vs. classical electro-dynamics a'la synchrotron radiation)**
- **Effect of electron recoil on X/γ ray beam phase space quality (spectral density, bandwidth broadening) and on electron beam (emittance dilution in multiple scattering and incoherent energy spread due to scattering stochasticity)**
- **Challenges of *electron-(optical)photon colliders* as X/γ beam Sources using Compton back-scattering**

- **Need of *high peak brightness/high average current* electron beams (cmp. FEL's drivers) *fsec-class* synchronized and *μm-μrad-scale* aligned to *high peak/average power* laser beams**
- **Main goal for Nuclear Physics and Nuclear Photonics:**

  ***Spectral Densities* > 10^4 $N_{ph}/(s \cdot eV)$**

  photon energy range 1-20 MeV, *bandwidths* 10^{-3} class
- **Overview of Paradimgs for Thomson/Compton Sources: Linac based, Storage Ring based, ERL SuperConducting Linac based**
- **ELI-NP-GammaBeamSystem in construction by EuroGammaS as an example of new generation Compton Source**
- **STAR in construction at University of Calabria as an example of compact Thomson Source for countries under development**

- **BriXS as an example of an Ultra High-Flux Thomson Source with ambitions/potentialities to compete with Synchrotron Light Sources (context: Human Technopole Initiative)**
- **Main goal for *MeV-class* $\gamma-\gamma$ and *TeV* γ - nucleon colliders:**

  Peak Brilliance **$> 10^{21}$** $N_{ph}/(s \cdot mm^2 \cdot mrad^2 \cdot 0.1\%)$ **$10^9 < N_{ph} < 10^{13}$**

  Source spot size *μm*-scale (low diffraction, few *μrad*)

  Tunability, Mono-chromaticity, Polarization (H,V,C)
- **Photon-Photon scattering (+ Breit-Wheeler: pair creation in vacuum) is becoming feasible with this new generation γ-beams: a γ-γ low energy collider**

If the Physics of Compton/Thomson back-scattering is well known….

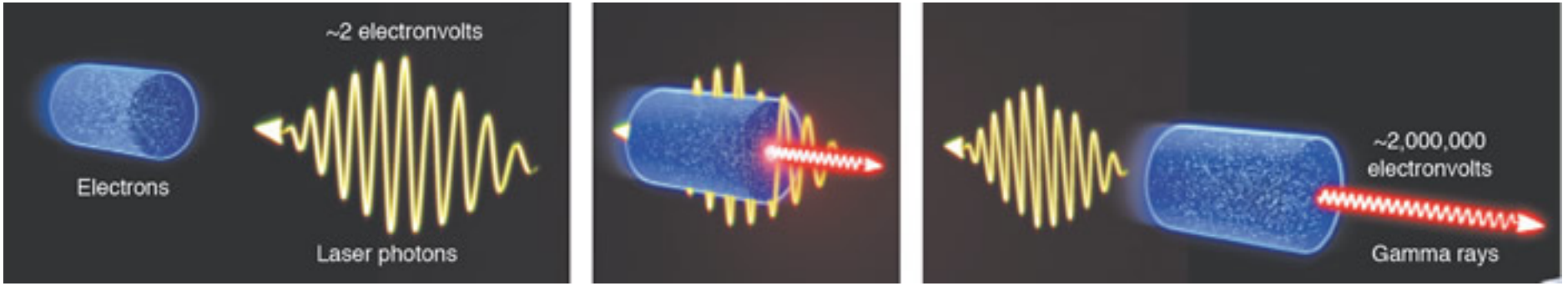

the Challenge of making a Compton Source running as an electron-photon Collider with maximum Luminosity, to achieve the requested Spectral Density, Brilliance, narrow Bandwidth of the generated *X/γ* ray beam, is a completely different issue/business !

Re-visiting the Physics of Compton back-scattering with an eye to effects impacting the quality and behavior of the photon (and electron) beam phase space distribution

Courtesy L. Palumbo

FEL's and Thomson/Compton Sources common mechanism:
collision between a relativistic electron and a (pseudo)electromagnetic wave

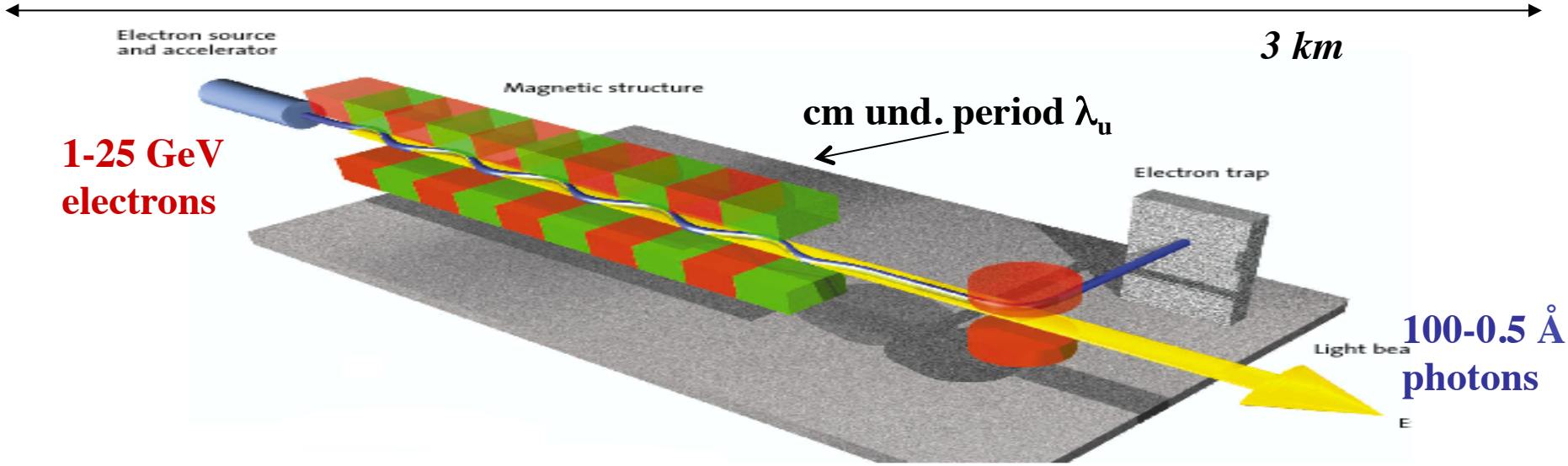

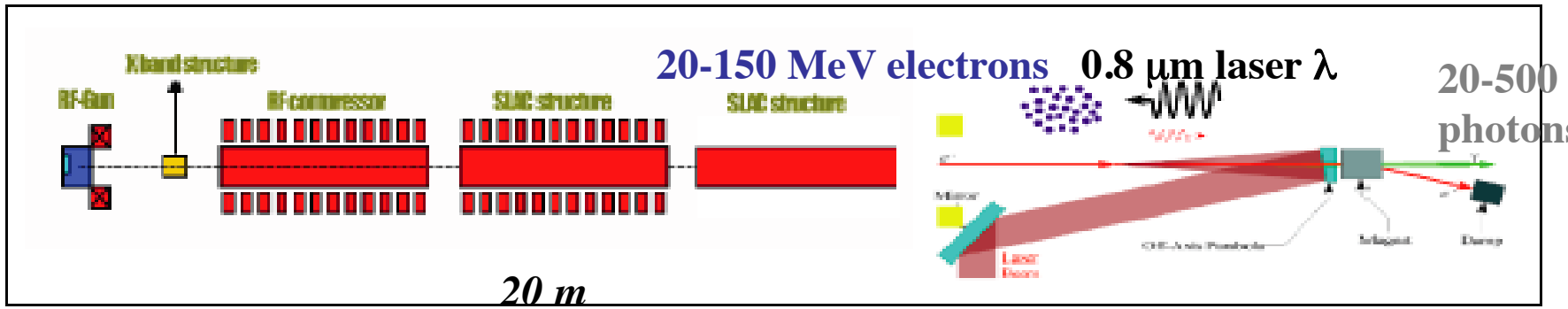

FEL resonance condition

$$\lambda_R = \lambda_w \frac{\left(1 + a_w^{\,2}\right)}{2\gamma^2}$$

(magnetostatic undulator)

Example : for λ_R=1A, λ_w=2cm, E=7 GeV

$$a_w = 0.93\lambda_w[cm]B_w[T]$$

$$\lambda_R = \lambda \frac{\left(1 + a_0^{\,2}/2\right)}{4\gamma^2}$$

(electromagnetic undulator)

Example : for λ_R=1A, λ=0.8μm, E=25MeV

Example : for $h\nu$=10 MeV, λ=0.4μm, E=530 MeV

L. Serafini et al., Proceedings of the SPIE, Volume 6634, article id. 66341G (2007)

$$a_0 \propto \frac{\lambda[\mu m]\sqrt{P[TW]}}{R_0[\mu m]}$$

laser power

laser spot size

Compton Inverse Scattering Physics is clear: recall some basics

Quantum model

Laboratory ref. system

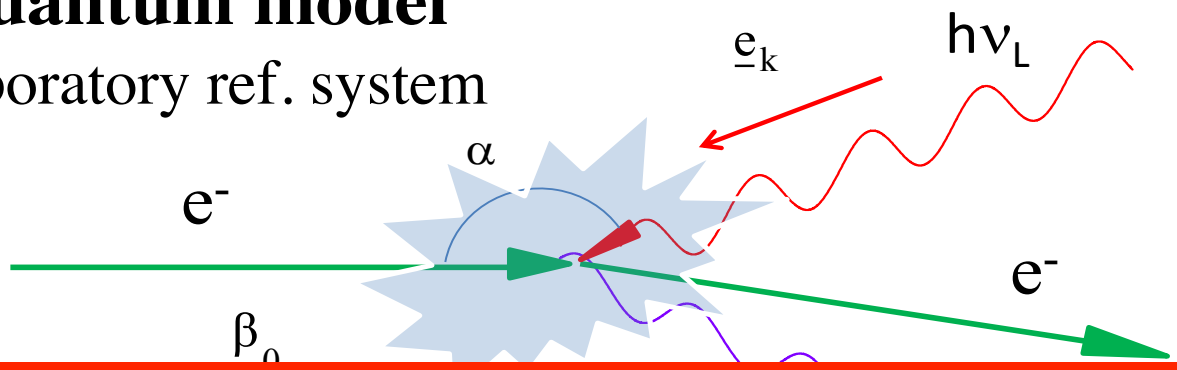

3 regimes: a) Elastic, Thomson b) Quasi-Elastic, Compton with Thomson cross-section c) Inelastic, Compton, recoil dominated

$$\begin{cases} mc^2(\gamma-\gamma_0)=-h(\nu-\nu_L) \\ mc(\underline{\beta}\gamma-\underline{\beta}_0\gamma_0)=-h(\underline{k}-\underline{k}_L)/2\pi \end{cases}$$

Energy and momentum conservation laws

γ_0:initial Lorentz factor

$$\nu = \nu_L \frac{1-\underline{e}_k\cdot\underline{\beta}_0}{1-\underline{n}\cdot\underline{\beta}_0+\frac{h\nu_L}{mc^2\gamma_0}(1-\underline{e}_k\cdot\underline{n})}$$

$$\lambda = \lambda_L \frac{1-\underline{n}\cdot\underline{\beta}_0}{1-\underline{e}_k\cdot\underline{\beta}_0} + \frac{h}{mc\gamma_0}\frac{1-\underline{e}_k\cdot\underline{n}}{1-\underline{e}_k\cdot\underline{\beta}_0}$$

Petrillo V. and al., NIM A **693** (2012)

Sun C. and Wu Y. K., PRSTAB **14** (2011) 044701

Quantum Model: a look at what happens in the Center of Mass reference system (kinematics)

Lab ref.

$$Assumptions: h_{\nu L} << E_e \; ; \; E_e = \gamma m_e c^2 \;\; \gamma >> 1$$

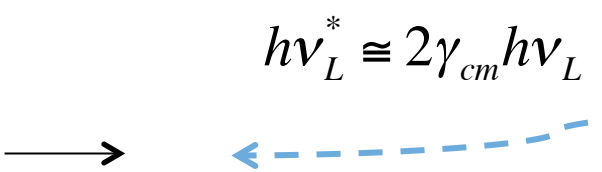

c.m. ref.

$$\vec{p}_{tot}^{\,*} = \vec{p}_e^{\,*} + \hbar\vec{k}_{h\nu}^{\,*} = \vec{0}$$

Recall some Basics

$$electron\ 4-vector\ \mathbf{P}_e = \left[E_e/c, p_{ex}=0, p_{ey}=0, p_{ez}=p_e=\sqrt{E_e^2/c^2 - m_e^2 c^2}\right]$$

$$photon\ 4-vector\ \mathbf{P}_{h\nu} = \left[h\nu_L/c, \hbar k_x = 0, \hbar k_y = 0, \hbar k_z = -h\nu_L/c\right]$$

Invariant Mass, Lorentz transformation from Lab to c.m. ref. system

$$Total\ \ 4-vector\ \ \mathbf{P} = \mathbf{P}_e + \mathbf{P}_{h\nu} = \left[E_e/c + h\nu_L/c, 0, 0, \sqrt{\frac{E_e^2}{c^2} - m_e^2 c^2} - h\nu_L/c \right]$$

$$Invariant\ \ Mass\ \ s \equiv \sqrt{c\mathbf{P} \bullet c\mathbf{P}} = E_{tot}^{2*} = E_{cm}^2$$

$$\left(4-vector\ \ product\ \ \mathbf{P}_1 \bullet \mathbf{P}_2 \equiv \left[E_1 E_2/c^2 - \vec{p}_1 \cdot \vec{p}_2 \right] \right)$$

$$E_{cm} \cong \sqrt{4E_e h\nu_L + m_e^2 c^4} = m_e c^2 \sqrt{1 + \frac{4\gamma h\nu_L}{m_e c^2}}$$

$$e^-\ \ recoil\ \ factor\ \ \Delta \equiv \frac{4\gamma h\nu_L}{m_e c^2}$$

from $\vec{p}^{\,*}_{tot} = \vec{p}^{\,*}_{e} + \hbar\vec{k}^{\,*}_{h\nu} = \vec{0}$ $\Rightarrow$ $\left|\vec{p}^{\,*}_{e}\right| = \hbar\left|\vec{k}^{\,*}_{h\nu}\right|$

and $E_{cm} = E^{*}_{e} + h\nu^{*} = m_e c^2\sqrt{1+\Delta}$

$$\begin{pmatrix} E^{*}_{e} = m_e^2 c^4 + \left|\vec{p}^{\,*}_{e}\right|^2 c^2 \\ h\nu^{*} = \hbar\left|\vec{k}^{\,*}_{h\nu}\right| c \end{pmatrix}$$

$$E^{*}_{e} = m_e c^2 \frac{2+\Delta}{2\sqrt{1+\Delta}}$$

$$h\nu^{*} = m_e c^2 \frac{\Delta}{2\sqrt{1+\Delta}}$$

$$\left|\vec{p}^{\,*}_{e}\right| = m_e c \frac{\Delta}{2\sqrt{1+\Delta}}$$

Holds before and after scattering (c.m ref. system!)

before scattering

$$\begin{pmatrix} p^*_{eIN} = [0,0,p^*_e] \\ \hbar\vec{k}^*_{IN} = [0,0,-h\nu^*/c] \end{pmatrix}$$

after scatt.

$$\begin{pmatrix} p^*_{eOUT} = [p^*_e \sin\vartheta^* \cos\varphi^*, p^*_e \sin\vartheta^* \sin\varphi^*, p^*_e \cos\vartheta^*] \\ \hbar\vec{k}^*_{OUT} = [-p^*_e \sin\vartheta^* \cos\varphi^*, -p^*_e \sin\vartheta^* \sin\varphi^*, -p^*_e \cos\vartheta^*] \end{pmatrix}$$

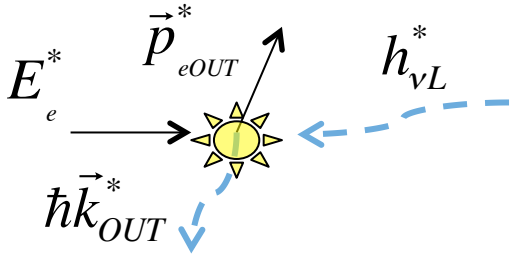

what is the probability of scattering at ϑ^*, φ^* ?

Klein-Nishina differential cross-section

$$\frac{d\sigma}{d\theta' d\phi'} = r_e^2 \left(\frac{2}{2+\Delta(1-cos\theta')}\right)^2 \left(\frac{1+cos^2\theta'}{2}\right) \cdot \left(1+\frac{\Delta^2(1-cos\theta')^2}{2(1+cos^2\theta')(2+\Delta(1-cos\theta'))}\right) sin\theta'$$

$$\vartheta^* = \vartheta'\sqrt{1+\Delta}$$

$\Delta \to 0$

$$\frac{d\sigma}{d\vartheta^* d\varphi^*} = r_e^2 \left(\frac{1+\cos^2\vartheta^*}{2}\right) \sin\vartheta^*$$

To transform to the Lab ref. system we need to compute γ_{cm}

$$\gamma_{cm} = \frac{E_{lab}}{E_{cm}} = \frac{E_e + h\nu_L}{m_e c^2 \sqrt{1+\Delta}} \cong \frac{\gamma}{\sqrt{1+\Delta}}$$

Then apply a Lorentz transformation

$$\begin{cases} E_{ph} = p^*_{ph}\gamma_{cm}\left(1 + \sqrt{1 - \frac{1}{\gamma^2_{cm}}}\cos\theta^*\right) \\ p_{phx} = p^*_{ph}\sin\theta^*\cos\phi^* \\ p_{phy} = p^*_{ph}\sin\theta^*\sin\phi^* \\ p_{phz} = p^*_{ph}\gamma_{cm}\left(\sqrt{1 - \frac{1}{\gamma^2_{cm}}} + \cos\theta^*\right) \end{cases}$$

$$\vartheta^* = \frac{2\gamma\vartheta}{\sqrt{1+\Delta}}$$

$$E_{ph} = m_e c^2 \frac{\Delta\gamma}{2(1+\Delta)}\left[1+\sqrt{1-\frac{1+\Delta}{\gamma^2}}\cos\left(\frac{2\gamma\vartheta}{\sqrt{1+\Delta}}\right)\right]$$

$\Delta << 1$ $\qquad$ $\gamma >> 1$ $\qquad$ $\gamma\vartheta < 1$

$$E_{ph} = 4\gamma^2 h\nu_L \frac{1-\frac{\gamma^2\vartheta^2}{1+\Delta}}{1+\Delta}$$

Thomson regime Δ=0 no recoil

$$E_{ph} = 4\gamma^2 h\nu_L \left(1-\gamma^2\vartheta^2\right)$$

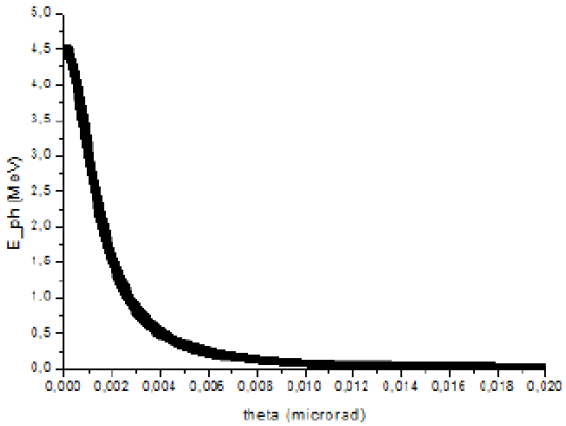

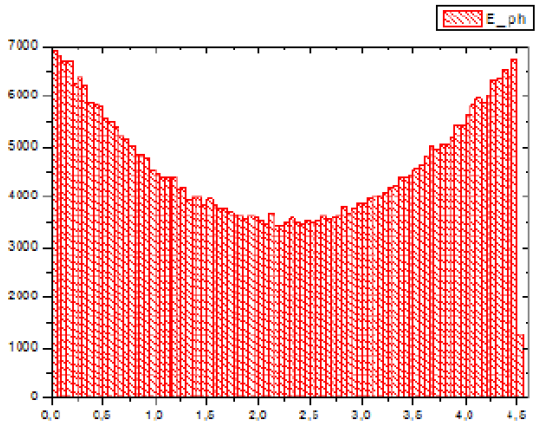

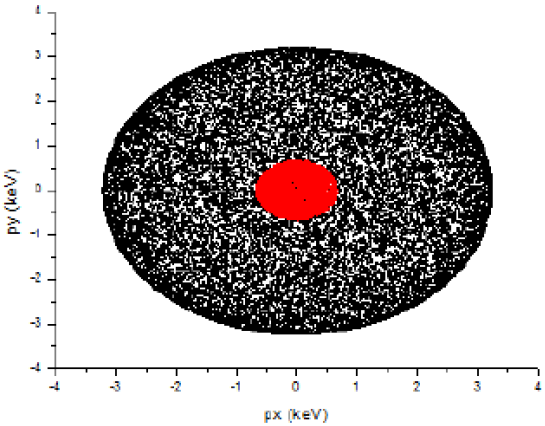

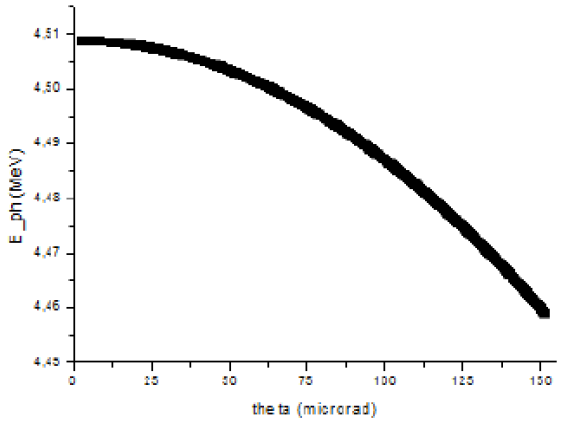

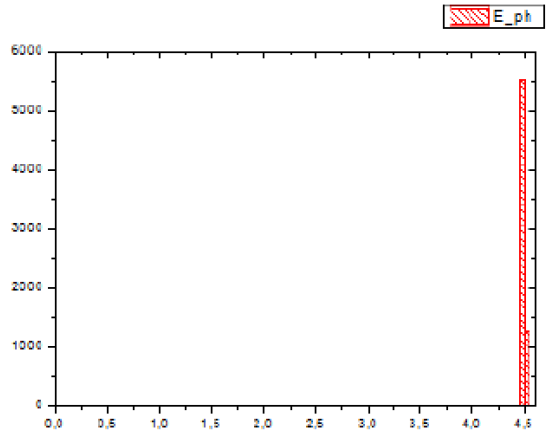

Energia elettroni 360 MeV
Energia fotoni 2.3 eV
Angolo alpha 0 gradi
Theta collimazione 151 microrad
Banda relativa 0.003

$$\gamma\vartheta = 0.11$$

If the electron has not null transverse components respect to the z axis, the Lorentz transformations in a generic direction have to be used:

$$\begin{cases} E_{ph} = p^*_{ph}\gamma_{cm} + p^*_{phx}\gamma_{cm}\beta_x + p^*_{phy}\gamma_{cm}\beta_y + p^*_{phz}\gamma_{cm}\beta_z \\ p_{phx} = p^*_{ph}\gamma_{cm}\beta_x + p^*_{phx}\dfrac{1+\gamma^2_{cm}\beta^2_x}{1+\gamma_{cm}} + p^*_{phy}\dfrac{\gamma^2_{cm}\beta_x\beta_y}{1+\gamma_{cm}} + p^*_{phz}\dfrac{\gamma^2_{cm}\beta_x\beta_z}{1+\gamma_{cm}} \\ p_{phy} = p^*_{ph}\gamma_{cm}\beta_y + p^*_{phx}\dfrac{\gamma^2_{cm}\beta_x\beta_y}{1+\gamma_{cm}} + p^*_{phy}\dfrac{1+\gamma^2_{cm}\beta^2_y}{1+\gamma_{cm}} + p^*_{phz}\dfrac{\gamma^2_{cm}\beta_y\beta_z}{1+\gamma_{cm}} \\ p_{phz} = p^*_{ph}\gamma_{cm}\beta_z + p^*_{phx}\dfrac{\gamma^2_{cm}\beta_x\beta_z}{1+\gamma_{cm}} + p^*_{phy}\dfrac{\gamma^2_{cm}\beta_y\beta_z}{1+\gamma_{cm}} + p^*_{phz}\dfrac{1+\gamma^2_{cm}\beta^2_z}{1+\gamma_{cm}} \end{cases}$$

See C. Curatolo, PhD Thesis, Univ. of Milan, 2016 (and references therein)

The transverse momentum of the incoming electron beam is linked to the emittance by the relation

$$\sigma_{p_x} = \frac{\epsilon_{n,x} M_e}{\sigma_x}$$

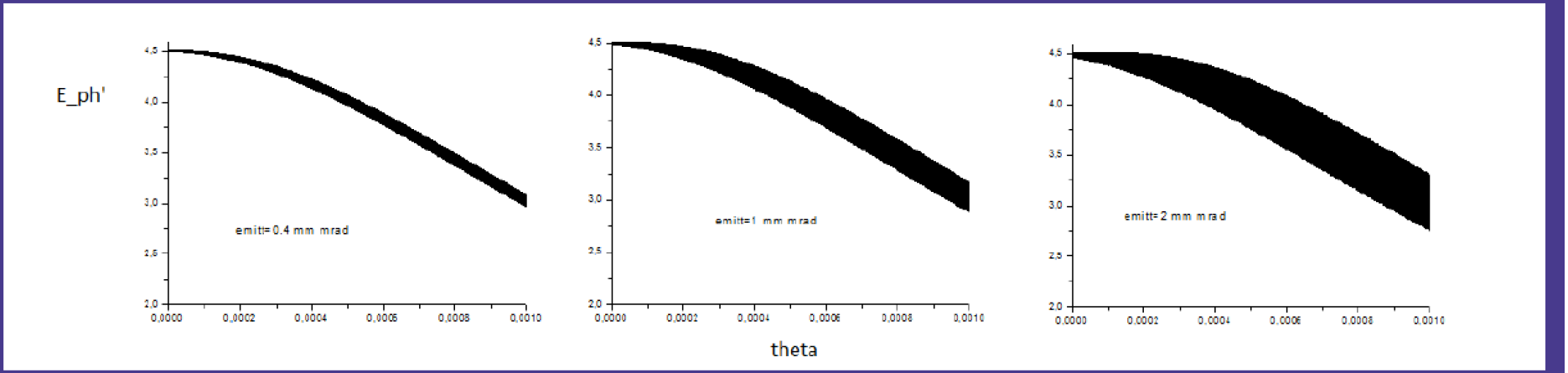

FIGURA : Energy of the emitted photons as a function of the emission angle in the lab θ for different values of the electron beam emittance.

$$\nu_\gamma = \frac{4\nu_0}{\frac{1}{2\gamma^2}\left(1+\frac{4\gamma h\nu_0}{mc^2}\right)} \Rightarrow + collective\ \ effects$$

$$\nu_\gamma \approx \frac{4\nu_0\gamma^2}{1+\gamma^2\theta^2+a_0^2/2}(1-\Delta)$$

$$\Delta = \frac{4\gamma h\nu_0}{mc^2} \quad \Delta << 1 \ \ Compton\ \ recoil$$

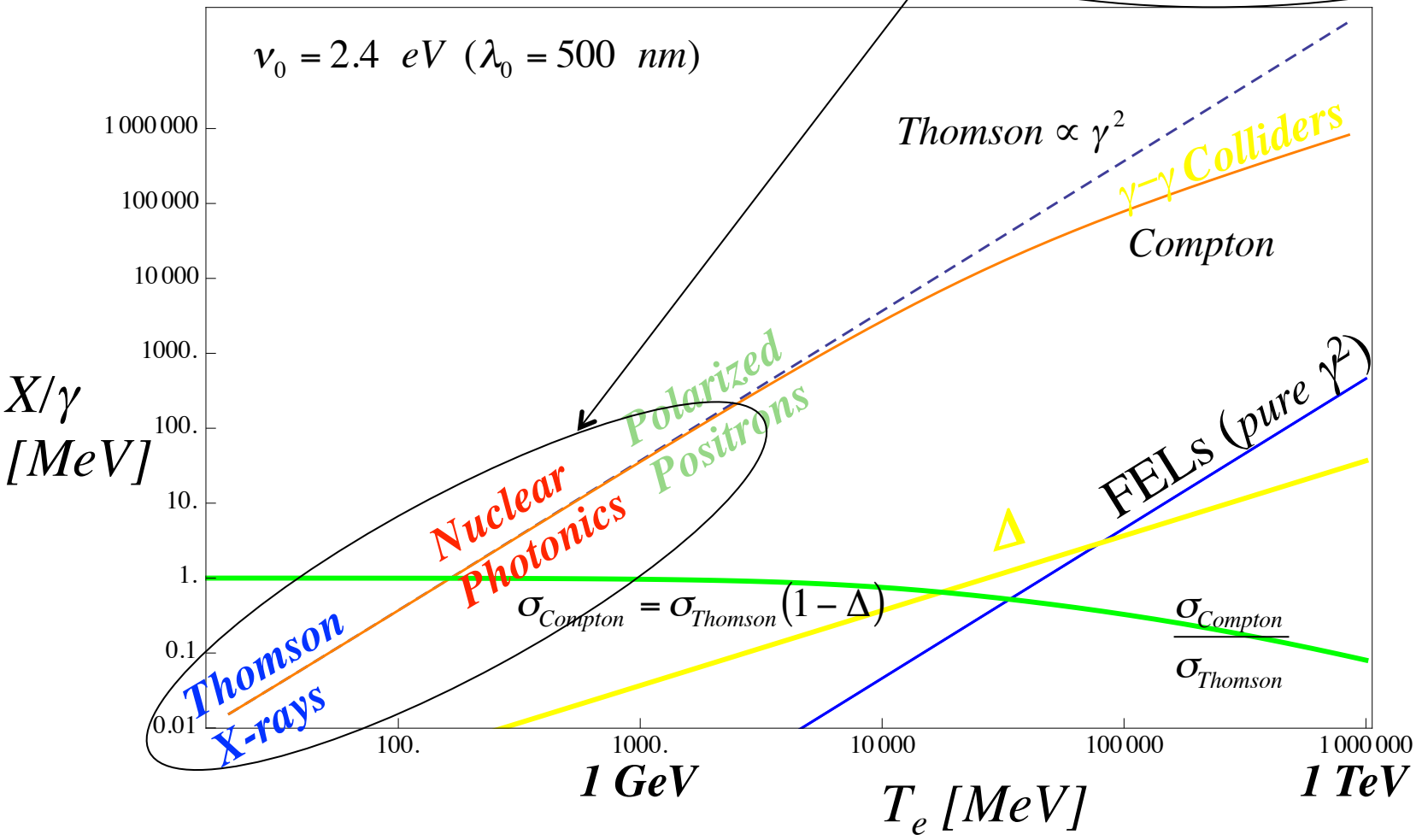

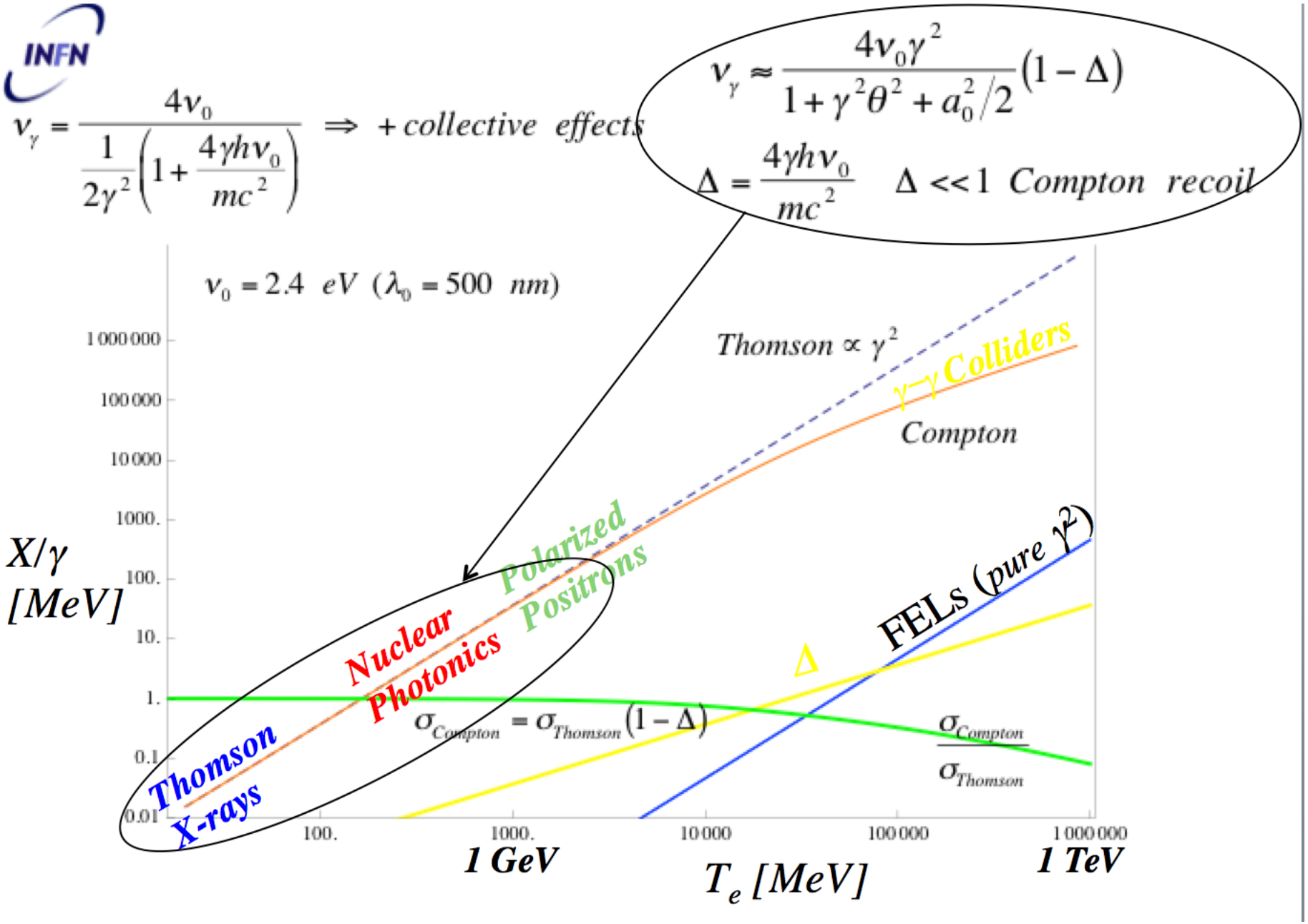
INFN
$\nu_\gamma = \frac{4\nu_0}{\frac{1}{2\gamma^2}\left(1+\frac{4\gamma h\nu_0}{mc^2}\right)} \Rightarrow +collective\ effects$
$\nu_\gamma \approx \frac{4\nu_0\gamma^2}{1+\gamma^2\theta^2+a_0^2/2}(1-\Delta)$
$\Delta = \frac{4\gamma h\nu_0}{mc^2}$ $\Delta << 1$ Compton recoil
$\nu_0 = 2.4\ eV\ (\lambda_0 = 500\ nm)$
Thomson $\propto \gamma^2$
γ–γ Colliders
Compton
Polarized Positrons
Nuclear Photonics
Thomson X-rays
Δ
FELs (pure γ^2)
$\sigma_{Compton} = \sigma_{Thomson}(1-\Delta)$
$\frac{\sigma_{Compton}}{\sigma_{Thomson}}$
X/γ [MeV]
1 000 000
100 000
10 000
1000.
100.
10.
1.
0.1
0.01
100.
1000.
10 000
100 000
1 000 000
1 GeV
1 TeV
T_e [MeV]

What happens to the recoiling electrons?

$$p_{e\perp}^{*} = m_e c \frac{\Delta \sin\vartheta^{*}}{2\sqrt{1+\Delta}} \qquad p_{ez}^{*} = m_e c \frac{\Delta \cos\vartheta^{*}}{2\sqrt{1+\Delta}}$$

Computing rms transverse momentum (emittance) and longitudinal momentum spread by averaging over the probabilty distribution (i.e. differential cross section)

$$\sqrt{\left\langle p_{e\perp}^{*2} \right\rangle} \cong \left[\frac{\int_0^{\pi} p_{e\perp}^{*2} \frac{d\sigma}{d\vartheta^{*} d\varphi^{*}} d\vartheta^{*}}{\int_0^{\pi} \frac{d\sigma}{d\vartheta^{*} d\varphi^{*}} d\vartheta^{*}} \right]^{1/2}$$

$$\frac{d\sigma}{d\vartheta^{*} d\varphi^{*}} \cong \sin\vartheta^{*} \left(\frac{1+\cos^2\vartheta^{*}}{2} \right)$$

Derivation of rms stochastic momentum induced on trasnv. and longit. phase space by Compton back-scattering

$$\sqrt{\langle p_{e\perp}^{*2}\rangle} \cong \sqrt{\frac{3}{5}}\frac{\Delta m_e c}{2\sqrt{1+\Delta}} \qquad \frac{\sqrt{\langle \delta p_{ez}^2\rangle}}{\langle p_{ez}\rangle} \cong \sqrt{\frac{2}{5}}\frac{\Delta}{1+\Delta}$$

$$\left.\frac{\Delta\varepsilon_n}{\varepsilon_n}\right|_{sc} \cong \sqrt{\frac{3}{5}}\frac{\Delta}{2}\sqrt{n_{sc}}\sigma_0\eta \qquad \left.\frac{\Delta\gamma}{\gamma}\right|_{sc} \cong \sqrt{\frac{2}{5}}\Delta\sqrt{n_{sc}}\eta \qquad \eta \equiv \frac{N_{ph}^{tot}}{N_e}$$

ELI – NP

$$\varepsilon_n = 0.3\ \mu m,\ \left.\frac{\Delta\gamma}{\gamma}\right|_{IN} = 5.\cdot 10^{-4},\ \eta = 0.025,\ \Delta = 0.03,\ bw = 0.003,\ \sigma_0 = 20\mu m \Rightarrow$$

$$\left.\frac{\Delta\varepsilon_n}{\varepsilon_n}\right|_{sc} = 0.006,\ \left.\frac{\Delta\gamma}{\gamma}\right|_{sc} = 4.7\cdot 10^{-4}$$

$n_{sc} \equiv scatt.\ multiplicity$

SPARC – LAB

$$\varepsilon_n = 1.5\ \mu m,\ \left.\frac{\Delta\gamma}{\gamma}\right|_{IN} = 2.\cdot 10^{-3},\ \eta = 0.9,\ \Delta = 0.003,\ bw = 0.05,\ \sigma_0 = 20\mu m \Rightarrow$$

$$\left.\frac{\Delta\varepsilon_n}{\varepsilon_n}\right|_{sc} = 0.02,\ \left.\frac{\Delta\gamma}{\gamma}\right|_{sc} = 1.7\cdot 10^{-3}$$

FEL and electron recoil

$$\Delta \equiv \frac{4\gamma h\nu_L}{m_e c^2} = \frac{h\nu}{\gamma m_e c^2} = \frac{\rho}{\bar{\rho}}$$

$$\left.\frac{\Delta\gamma}{\gamma}\right|_{sc} \cong \sqrt{\frac{2}{5}}\Delta\sqrt{n_{sc}\eta} \Rightarrow \left.\frac{\Delta\gamma}{\gamma}\right|_{sc} \cong \sqrt{\frac{2}{5}}\sqrt{n_{sc}}\frac{\rho}{\bar{\rho}} \Rightarrow \left.\frac{\Delta\gamma}{\gamma}\right|_{sc} \geq \frac{\rho}{\bar{\rho}}$$

$$\eta \equiv N_{ph}^{tot} / N_e \cong 1$$

A Letters Journal Exploring the Frontiers of Physics

January 2013

EPL, 101 (2013) 10008
doi: 10.1209/0295-5075/101/10008

www.epljournal.org

Phase space distribution of an electron beam emerging from Compton/Thomson back-scattering by an intense laser pulse

V. Petrillo[1], I. Chaikovska[2], C. Ronsivalle[3], A. R. Rossi[1], L. Serafini[1] and C. Vaccarezza[4(a)]

[1] *INFN, Università degli Studi Milano - Via Celoria, 16, 20133 Milano, Italy, EU*
[2] *LAL, Université Paris-Sud, IN2P3/CNRS - Orsay-Ville, France, EU*
[3] *ENEA - Via E. Fermi, 45, Frascati (Rm), Italy, EU*
[4] *INFN-LNF Via E. Fermi, 40, Frascati (Rm), Italy, EU*

received 14 November 2012; accepted in final form 16 December 2012
published online 21 January 2013

PACS 03.65.Nk – Scattering theory
PACS 41.60.Cr – Free-electron lasers

Abstract – We analyze the energy distribution of a relativistic electron beam after the Compton back-scattering by a counterpropagating laser field. The analysis is performed for parameters in the range of realistic X-γ sources, in the framework of the Quantum Electrodynamics, by means of the code CAIN. The results lead to the conclusion that, in the regime considered, the main effect is the initial formation of stripes, followed by the diffusion of the most energetic particles toward lower values in the longitudinal phase space, with a final increase of the electron energy bandwidth.

photon energy distribution near the Compton edge, showing that no photons are emitted with energy larger than 4.82 MeV.

point-particle collision between an electron and a photon. In the following, when the electrons undergo more colli-

We need to build a very high luminosity collider, that needs to maximize the *Spectral Luminosity*, *i.e.* Luminosity per unit bandwidth

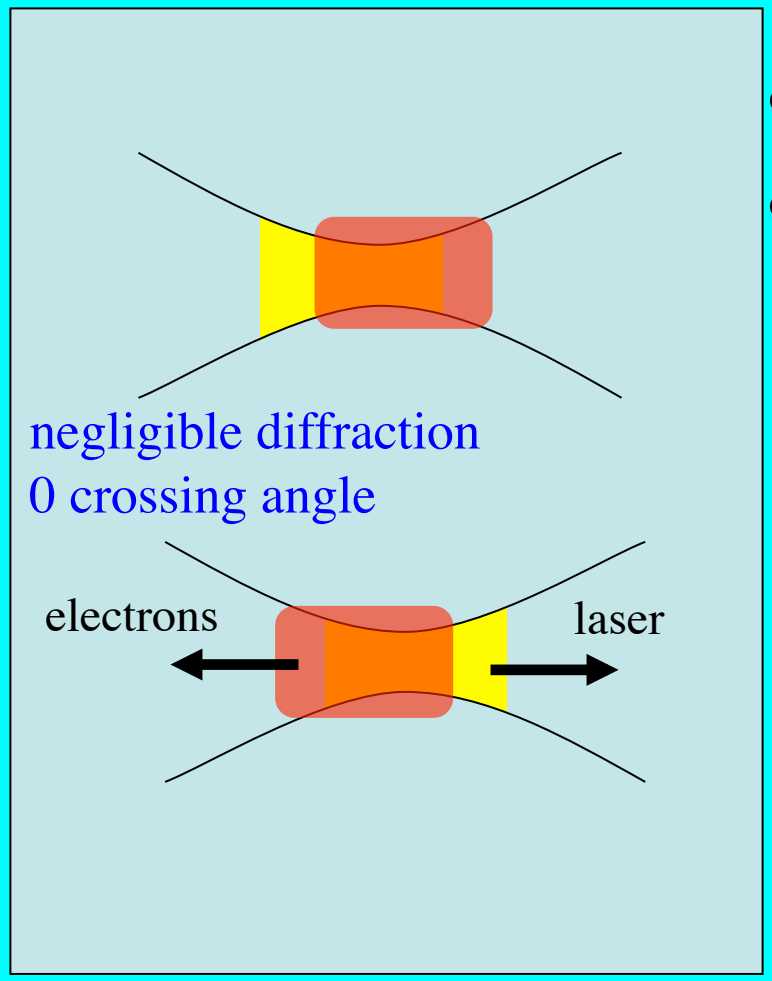

$$\sigma_T = 0.67 \cdot 10^{-24}\, cm^2 = 0.67\ \ barn$$

- Scattered flux $N_\gamma = \mathbf{L}\sigma_T$ $\sigma_T = \frac{8\pi}{3} r_e^2$
- Luminosity as in HEP collisions
  - Many photons, electrons
  - Focus tightly $\mathbf{L} = \frac{N_L N_{e-}}{4\pi\sigma_x^2} f$
  - ELI-NP

$$L_S \equiv \frac{L}{\Delta\nu_\gamma}$$

$$L = \frac{1.3 \cdot 10^{18} \cdot 1.6 \cdot 10^{9}}{4\pi(0.0015cm)^2} 3200(s^{-1}) = 2.5 \cdot 10^{35}\, cm^{-2} s^{-1}$$

cfr. LHC 10^{34}, Hi-Lumi LHC 10^{35}

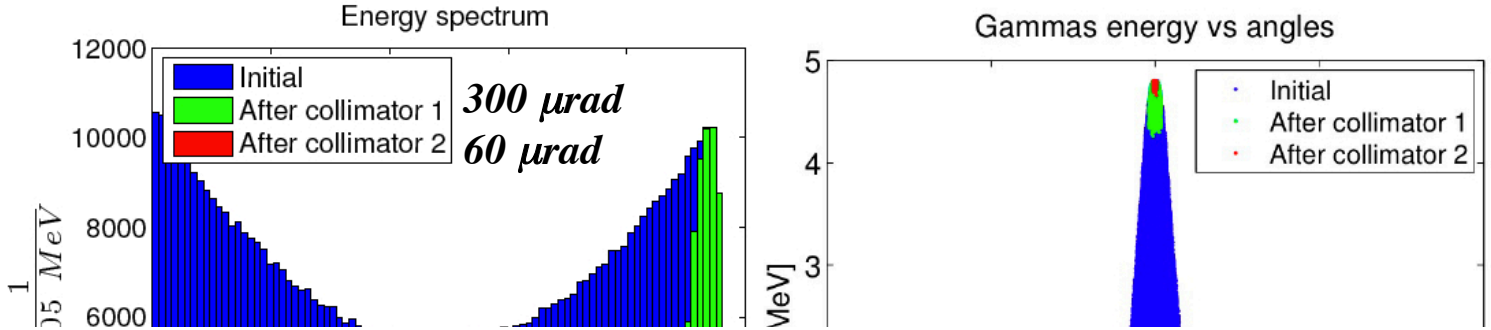

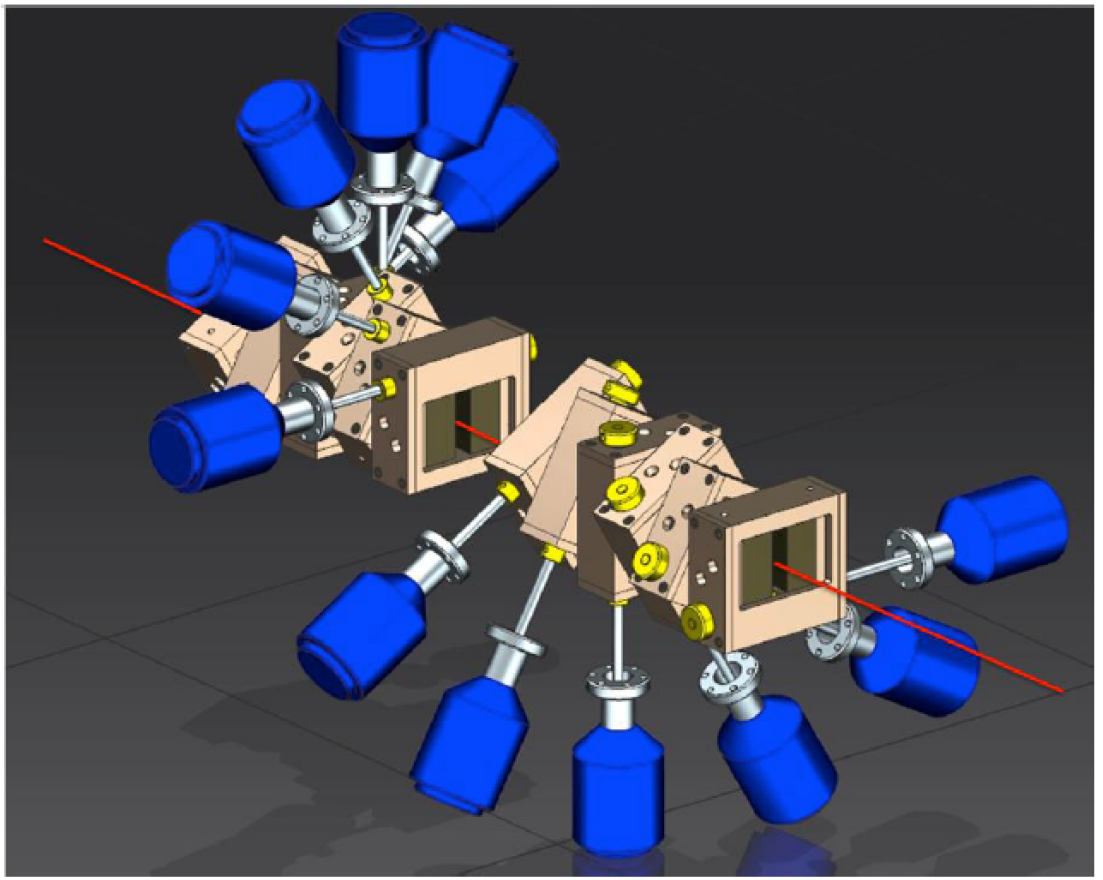

Fig. 184. **Drawing of the configuration of low energy collimator made up of 12 tungsten adjustable slits with a relative 30° rotation each**

Courtesy M. Gambaccini

Formulas derived from Luminosity extensively tested vs. ELI-NP-GBS simulations

$$N_\gamma^{bw} = 1.4 \cdot 10^9 \frac{U_L[J] Q[pC] f_{RF} \delta_\phi}{h\nu_L[eV]\left(\sigma_x^2[\mu m] + \frac{w_0^2[\mu m]}{4}\right)} \gamma^2 \theta^2$$

correction factor for collision angle $\phi << 1$

$$\delta_\phi = \frac{1}{}$$

Assumptions: weak diffraction $c\sigma_t < Z_0 \equiv \frac{\pi w_0^2}{\lambda}$

and $\sigma_{z-el} < \beta_0 \equiv \frac{\gamma \sigma_0^2}{\varepsilon_n}$ *and ideal time – space overlap*

implies: $\sigma_t <$ *a few psec* $\sigma_{z-el} < 300$ μm

EPJ Web of Conferences **117**, 05002 (2016) DOI: 10.1051/epjconf/201611705002
NN2015

High intensity X/γ photon beams for nuclear physics and photonics

L. Serafini[1], D. Alesini[2], A. Bacci[1], N. Bliss[5], K. Cassou[3], C. Curatolo[1], I. Drebot[1], K. Dupraz[3], A. Giribono, V. Petrillo[1], L. Palumbo[4], C. Vaccarezza[2], A. Variola[2], F. Zomer[3].

[1] INFN, Sezione di Milano and Università degli Studi di Milano, Milano, Italy
[2] LNF-INFN, Frascati (RM), Italy
[3] LAL-Orsay, Orsay, France
[4]Università la Sapienza, Roma, Italy
[5] STFC Daresbury Laboratory, Warrington, UK

and references therein

Workshop on Trends in FEL Physics, Erice, May 19th 2016

Efficiency η of a Comtpon Source (number of photons back-scattered per electron

$$\eta \equiv \left. \frac{N_\gamma^{bw}\big|_{fullspectrum}}{N_e} \right|_{shot} = 68 \frac{U_L[J]\delta_\phi}{h\nu_L[eV]\left(\sigma_x^2[\mu m] + \frac{w_0^2[\mu m]}{4}\right)}$$

$ELI - NP \quad \eta \cong 0.025$

$STAR \quad \eta \cong 0.4$

$SPARC - LAB \ \eta \cong 1$

can exceed 1 when multiple scattering regime is reached

ELI-NP-GBS T. D. R.,http://arxiv.org/abs/1407.3669, (2014)

Vaccarezza C. and al., Proc. IPAC2014, Dresden, Germany, (2014)

A Letters Journal Exploring the Frontiers of Physics

January 2013

EPL, 101 (2013) 10008
doi: 10.1209/0295-5075/101/10008

www.epljournal.org

Phase space distribution of an electron beam emerging from Compton/Thomson back-scattering by an intense laser pulse

V. Petrillo[1], I. Chaikovska[2], C. Ronsivalle[3], A. R. Rossi[1], L. Serafini[1] and C. Vaccarezza[4(a)]

[1] *INFN, Università degli Studi Milano - Via Celoria, 16, 20133 Milano, Italy, EU*
[2] *LAL, Université Paris-Sud, IN2P3/CNRS - Orsay-Ville, France, EU*
[3] *ENEA - Via E. Fermi, 45, Frascati (Rm), Italy, EU*
[4] *INFN-LNF Via E. Fermi, 40, Frascati (Rm), Italy, EU*

received 14 November 2012; accepted in final form 16 December 2012
published online 21 January 2013

PACS 03.65.Nk – Scattering theory
PACS 41.60.Cr – Free-electron lasers

Abstract – We analyze the energy distribution of a relativistic electron beam after the Compton back-scattering by a counterpropagating laser field. The analysis is performed for parameters in the range of realistic X-γ sources, in the framework of the Quantum Electrodynamics, by means of the code CAIN. The results lead to the conclusion that, in the regime considered, the main effect is the initial formation of stripes, followed by the diffusion of the most energetic particles toward lower values in the longitudinal phase space, with a final increase of the electron energy bandwidth.

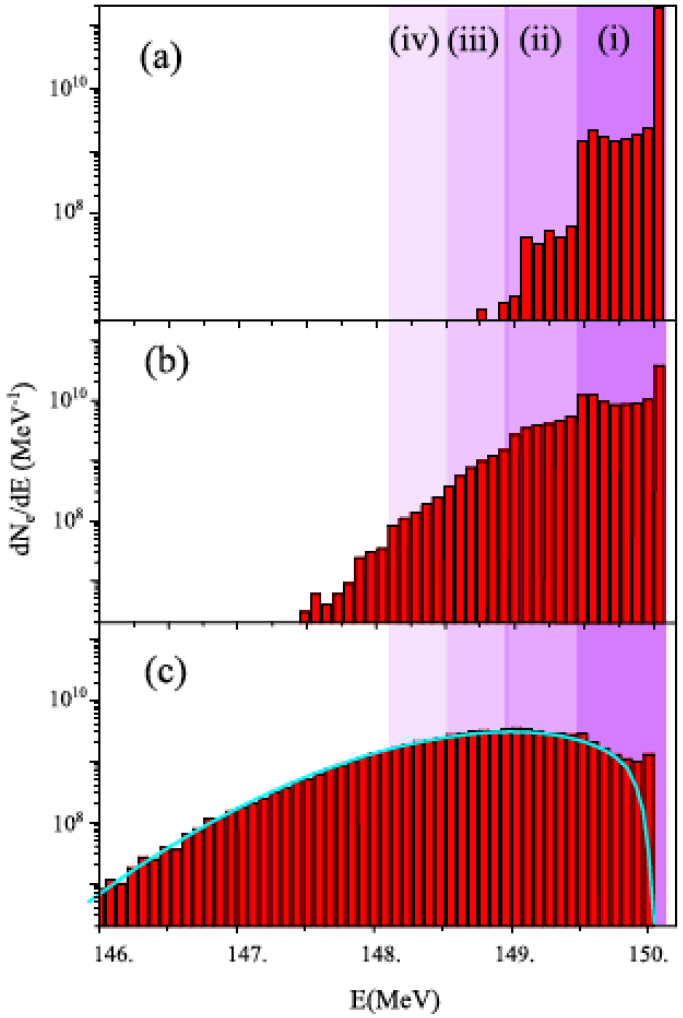

Fig. 2: (Colour on-line) Electron distribution $dN_e/dE(\mathrm{MeV}^{-1})$ *vs.* electron energy in MeV for the case without diffraction (Rayleigh length $L_R = 10\,\mathrm{mm}$) and for $a_0 = 0.083$. (a) $\Delta t = 0.083\,\mathrm{ps}$, $E_L = 1\,\mathrm{J}$ ($F_X = 0.0145$); (b) $\Delta t = 1.66\,\mathrm{ps}$, $E_L = 20\,\mathrm{J}$ ($F_X = 0.29$); (c) $\Delta t = 6.66\,\mathrm{ps}$, $E_L = 80\,\mathrm{J}$ ($F_X = 1.16$). The curve in panel (c) represents the Rayleigh distribution function associated to random walk for $N = 4.5$.

be much smaller than one. From a simple definition of the luminosity of the system [10],

$$L = \frac{N_L N_e}{2\pi(\sigma^2 + \sigma_e^2)}, \tag{2}$$

with $N_L = E_L/(\hbar\omega_L)$, N_e the total number of electrons and σ_e the transverse dimension of the electron beam, the number of emitted photons N can be introduced:

$$N = L\sigma_T, \tag{3}$$

where $\sigma_T = \frac{8}{3}r_e^2$ is the total Thomson cross-section, and r_e the classical electron radius. Finally, the number of emitted photons per electron is

$$F_X = \frac{N}{N_e} = \frac{E_L\sigma_T}{2\pi\hbar\omega_L(\sigma^2 + \sigma_e^2)}, \tag{4}$$

which, for the previous case, assumes values between $1.45 \cdot 10^{-2}$ and 1.16.

Starting from the case of shorter laser pulse (fig. 2(a)), the electron distribution develops a tail which is shaped in a complementary way with respect to the photon spectrum, thus forming a sort of plateau between 150 MeV and 149.5 MeV (zone (i)), with a flat peak in correspondence with the latter value (*i.e.*, 149.5 MeV), which is about 500 keV less than the Compton edge, due to this energy loss by most electrons in their first collision. Another low plateau appears below this value, down to 149 MeV (zone (ii)). It reveals the occurrence of cascaded emission from electrons that have already undergone a first scattering and that perform two successive collisions within $\Delta t = 0.083\,\mathrm{ps}$. Increasing the laser time duration (fig. 2(b) and (c)), these stripes become more populated, and a third zone, between 149 and 148.5 MeV, fills up by the electrons (zone (iii)) that participate to three collisions. Increasing further the time duration of the laser, the first zone begins to drain, the level of the lower stripes increases, then the

Bandwidth due to collection angle, laser and electron beam phase space distribution

$$\nu_\gamma = \nu \frac{4\gamma^2}{1+\gamma^2\theta^2 + a_0^2/2}(1-\Delta) \qquad \Delta = 4\gamma h\nu/mc^2 \quad \Delta << 1 \; Compton\ recoil$$

$$\left\langle \gamma^2\theta^2 \right\rangle \cong \left\langle \gamma^2\vartheta^2 \right\rangle + \left\langle \gamma^2\vartheta_e^2 \right\rangle \cong \gamma^2\vartheta_{rms}^2 + (\sigma_{p\perp}/mc)^2 \cong \gamma^2\vartheta_{rms}^2 + 2(\varepsilon_n/\sigma_x)^2$$

$$\frac{\Delta\nu_\gamma}{\nu_\gamma} \cong \sqrt{(\gamma\vartheta)_{rms}^4 + 4\left(\frac{\Delta\gamma}{\gamma}\right)^2 + \left(\frac{\sqrt{2}\varepsilon_n}{\sigma_x}\right)^4 + \left(\frac{\Delta\nu}{\nu}\right)^2 + \left(\frac{M^2\lambda_L}{2\pi w_0}\right)^4 + \left(\frac{a_{0p}^2/3}{1+a_{0p}^2/2}\right)^2}$$

$\gamma\vartheta$ = *normalized collection angle*

electron beam

laser

$$Optimized\ \ Bandwidth \cong 2(\varepsilon_n/\sigma_x)^2$$

$$Maximum\ \ Spectral\ \ Density \propto Luminosity/(\varepsilon_n/\sigma_x)^2 \propto Q/\varepsilon_n^2$$

$$Maximum\ \ Spectral\ \ Density \propto Phase\ \ Space\ \ density$$

FEL CONDITIONS FOR EXPONENTIAL GROWTH

The instability can develop only if the undulator length is much larger than the power gain length, and some other conditions are satisfied: $\Delta\nu_{FEL}/\nu_{FEL} \le \rho \quad \rho_{LCLS} = 5\cdot 10^{-4}$

a. Beam emittance of the order of or smaller than the wavelength:

$$\varepsilon \le \frac{\lambda}{4\pi} \qquad \textbf{(4.21)}$$

b. Beam relative energy spread smaller than the FEL parameter:

$$\sigma_E / E < \rho \qquad \textbf{(4.22)}$$

c. Power gain length shorter than the radiation Rayleigh range:

$$L_G < L_R \qquad \textbf{(4.23)}$$

where the Rayleigh range is defined as $L_R = 2\pi\sigma_0^2/\lambda_r$, and σ_0 is the radiation rms beam radius.

Independent on electron energy !

$$\frac{\Delta\nu_\gamma}{\nu_\gamma} \ge 2\frac{\varepsilon_n^2}{\sigma_x^2}$$

$$2\frac{\varepsilon_n^2}{\sigma_x^2} = p_{\perp rms}^2 = \left(\gamma\sigma_{x'}\right)^2$$

$$\frac{\Delta\nu_\gamma}{\nu_\gamma} \le 0.3\% \qquad \sigma_x = 15 \ \mu m \qquad \varepsilon_n \le 0.58 \ mm\cdot mrad$$

$$\frac{\Delta\nu_\gamma}{\nu_\gamma} \le 1\% \qquad \sigma_x = 1 \ \mu m \qquad \varepsilon_n \le 0.071 \ mm\cdot mrad$$

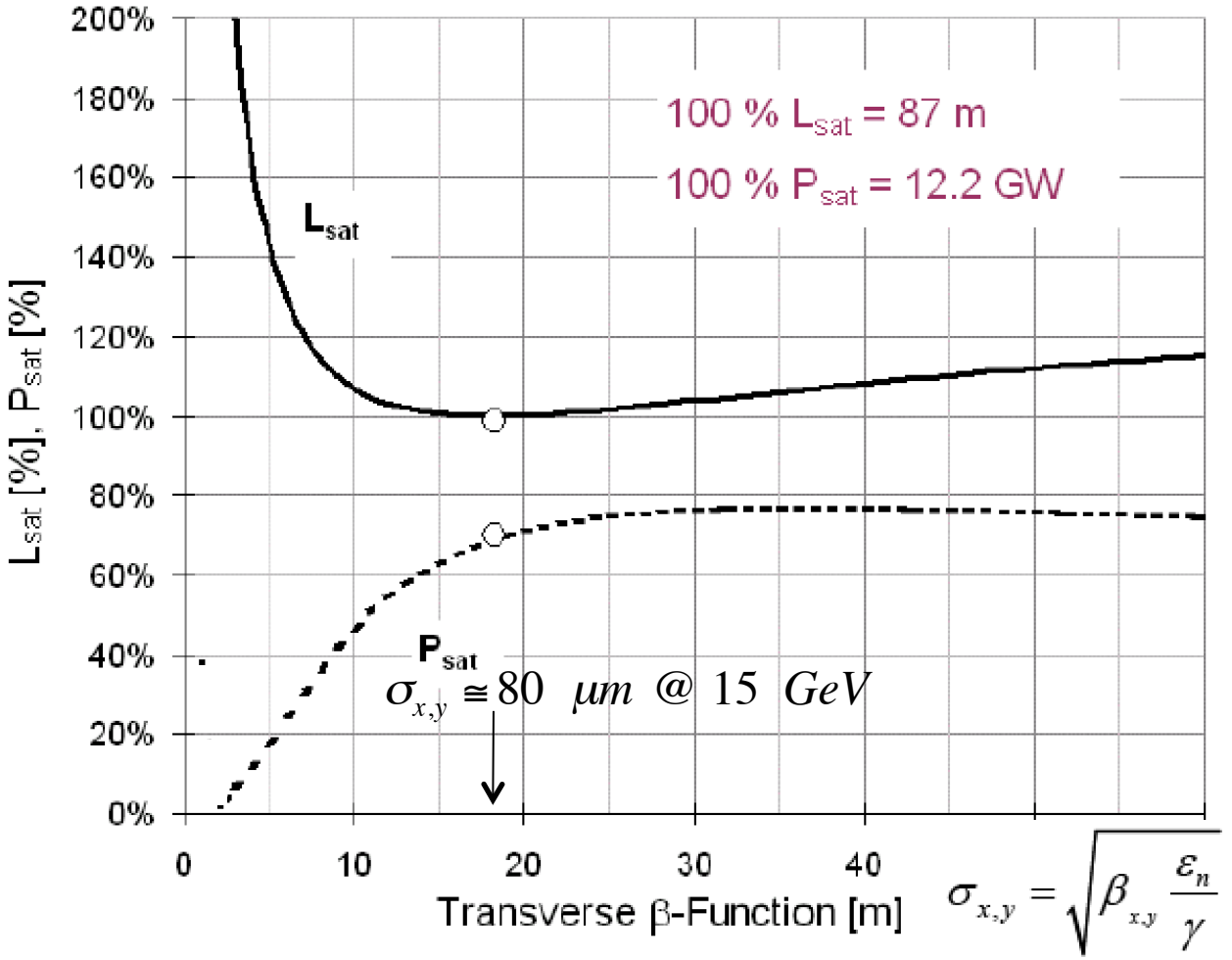

Figure 5.4 Power at saturation, P_{sat}, and saturation length, L_{sat}, as a percentage of 12.2 GW and 87 m, respectively, as a function of the average β-function at a radiation wavelength of 1.5 Å (14.35 GeV). The circles indicate the LCLS operating point.

Quantum red−shift ΔE due to electron recoil:
example ELI-NP-GBS, recoil factor = 0.025

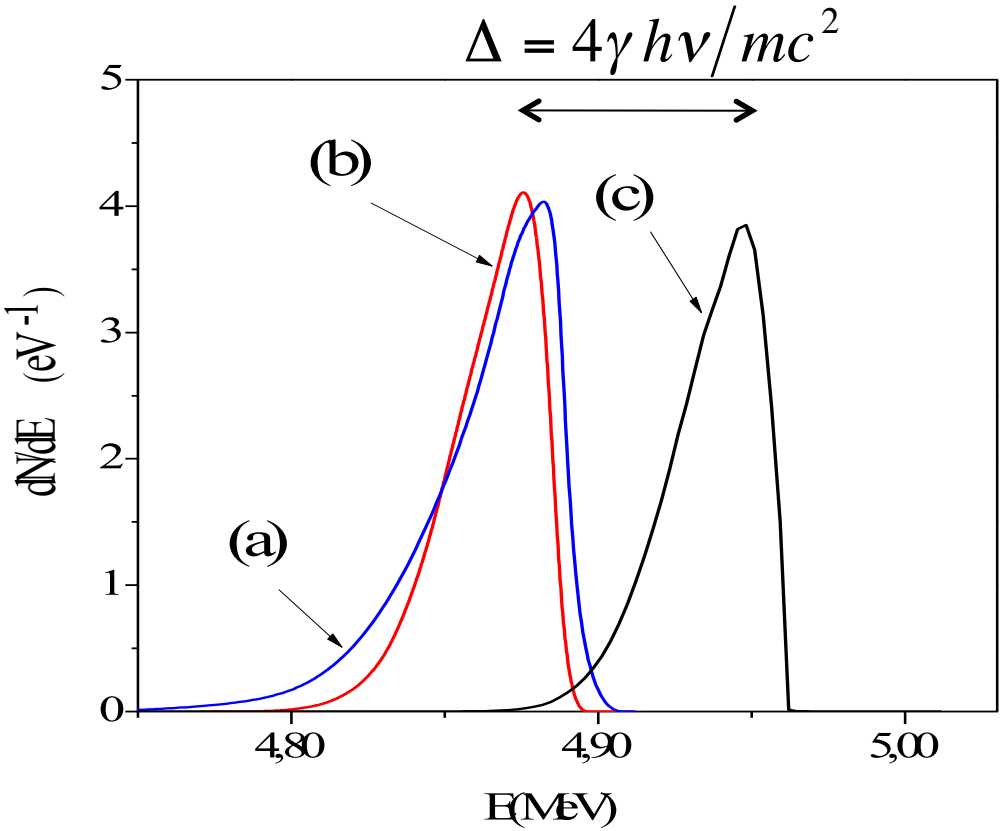

(a)CAIN
(b)Comp_Cross
(c)TSST

A part from quantum shift, the spectra are quite similar

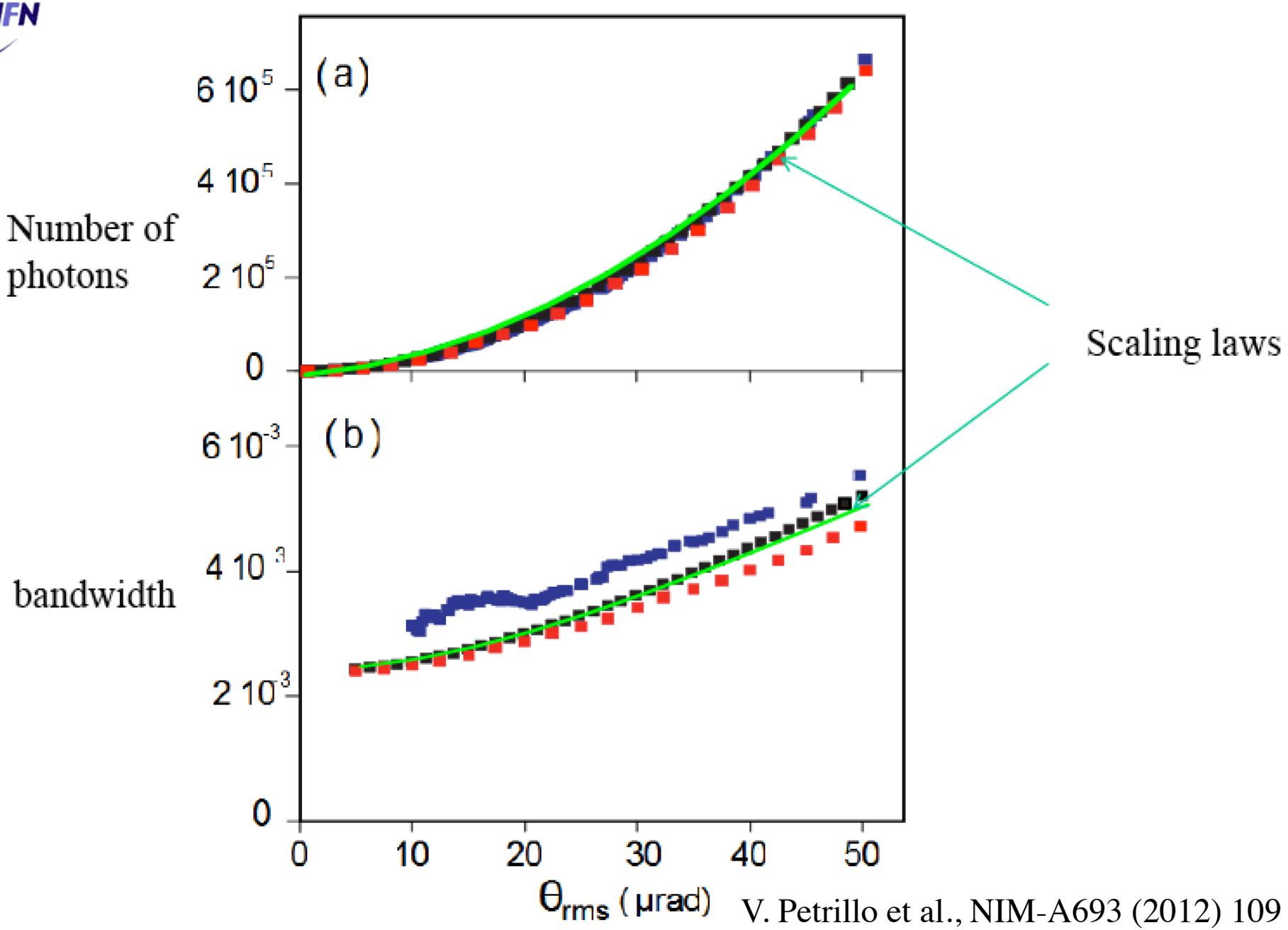

V. Petrillo et al., NIM-A693 (2012) 109

Angular and Frequency Spectrum
(560 MeV electrons)

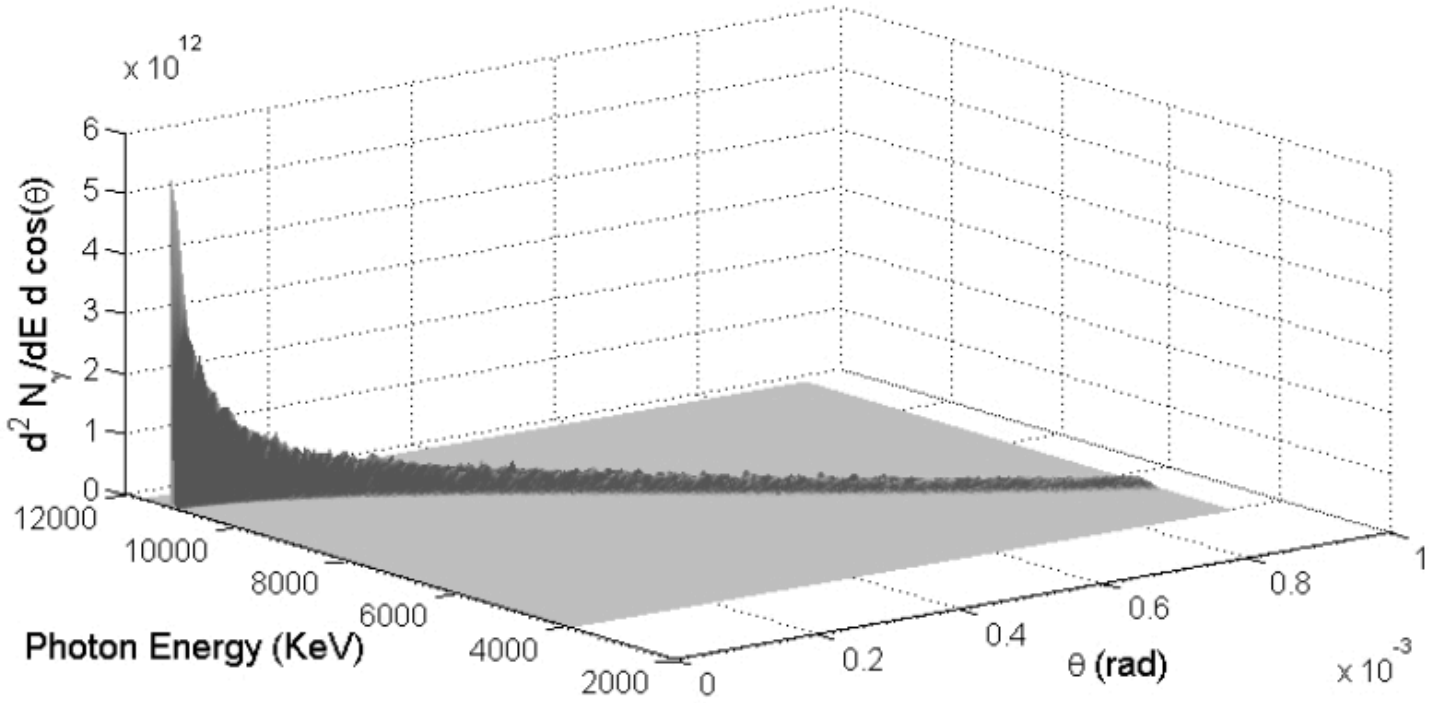

Figure 18: Spectrum versus photon energy and collection angle

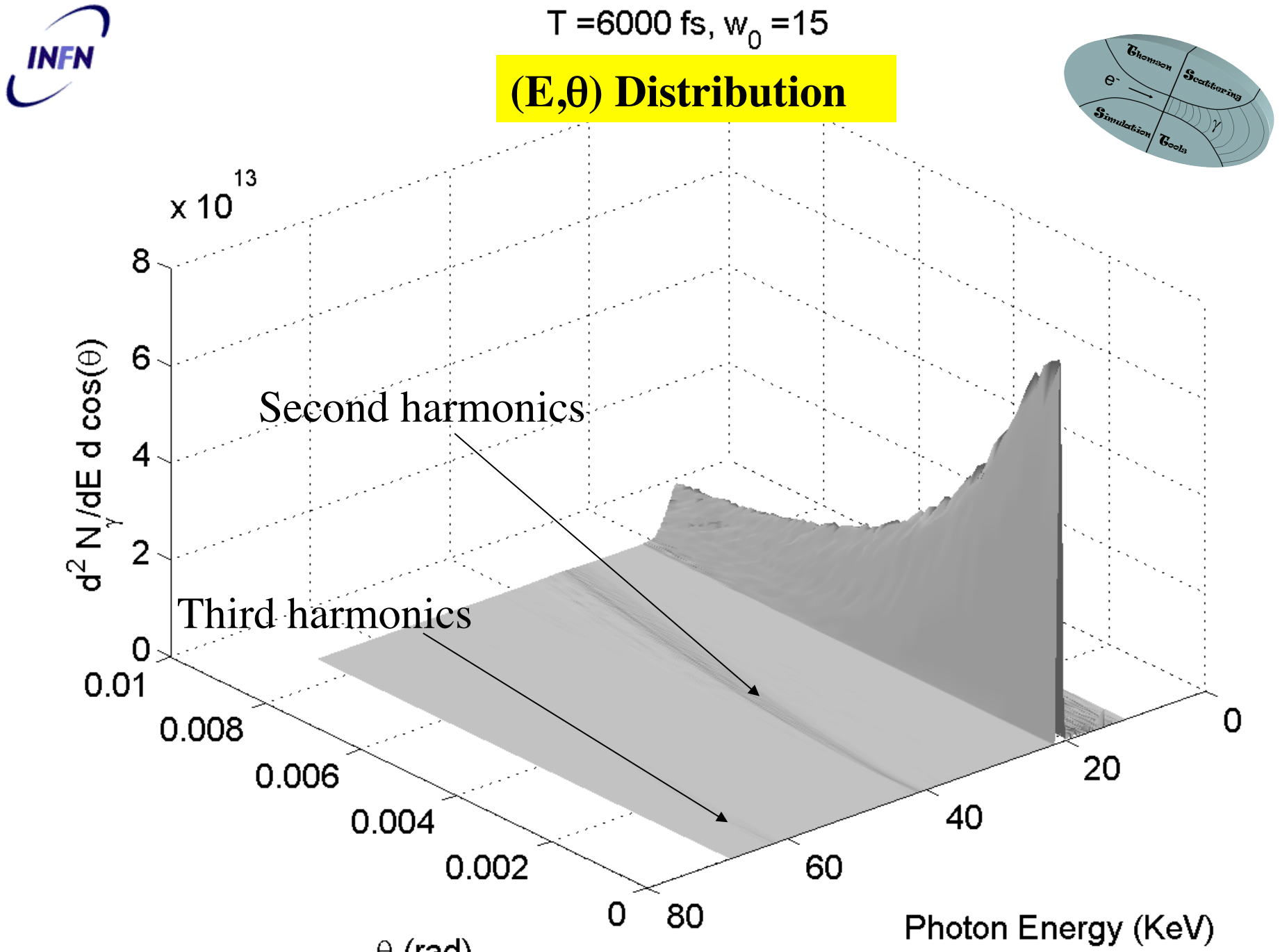
T =6000 fs, w0 =15
(E,θ) Distribution
Thomson Scattering
Simulation Tools
e-
γ
x 10^13
d^2 N_γ /dE d cos(θ)
8
6
4
2
0
Second harmonics
Third harmonics
0.01
0.008
0.006
0.004
0.002
0
θ (rad)
0
20
40
60
80
Photon Energy (KeV)

Example

Quasi head-on collision of a 5 MeV electron (θ_e = 50 mrad, $\phi_e = \pi/2$) on a flat-top pulse of normalized ampliude a_0=1.5, λ = 1μm and T = 20 fs

P. Tomassini et al., Appl. Phys. B 80, 419 (2005)

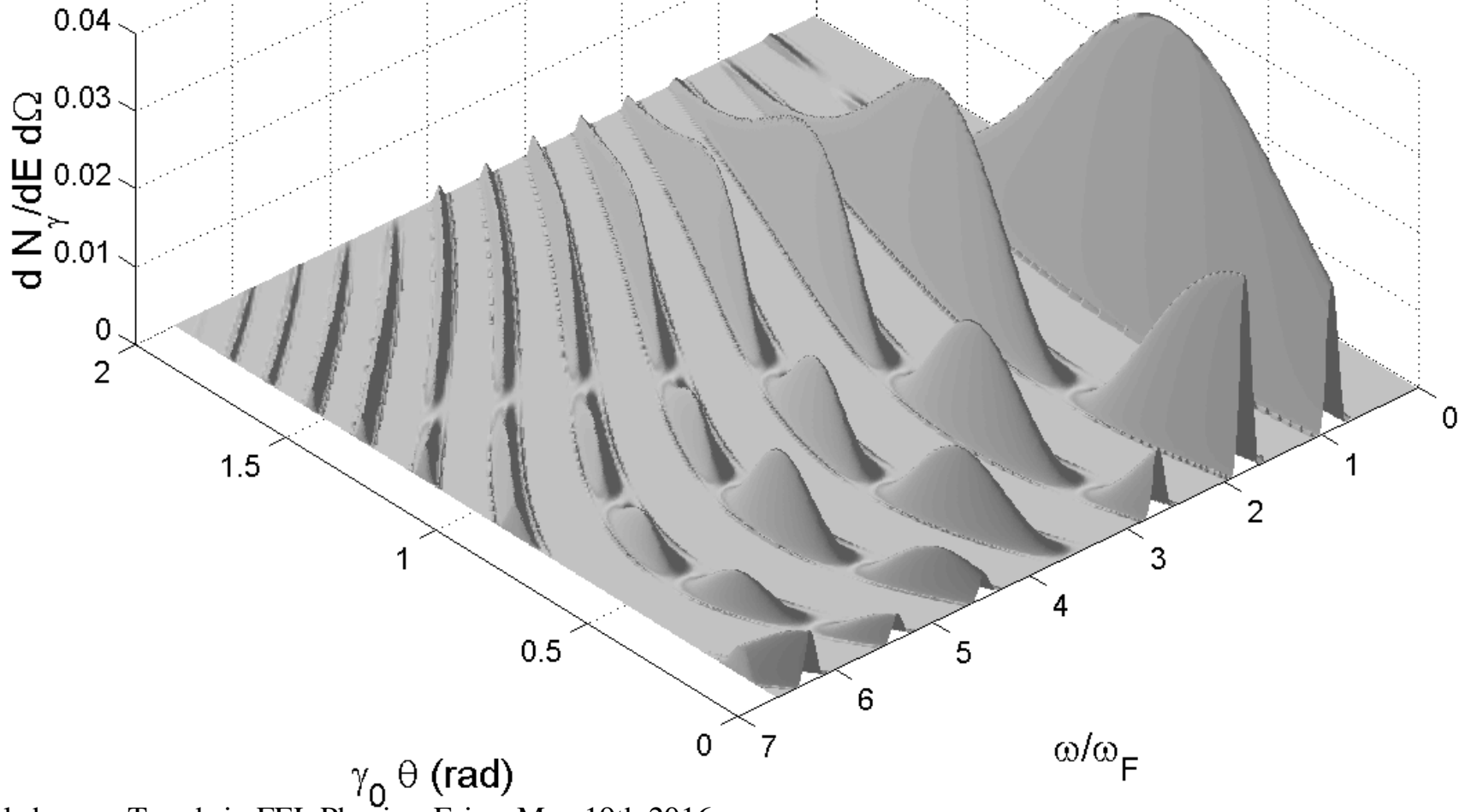

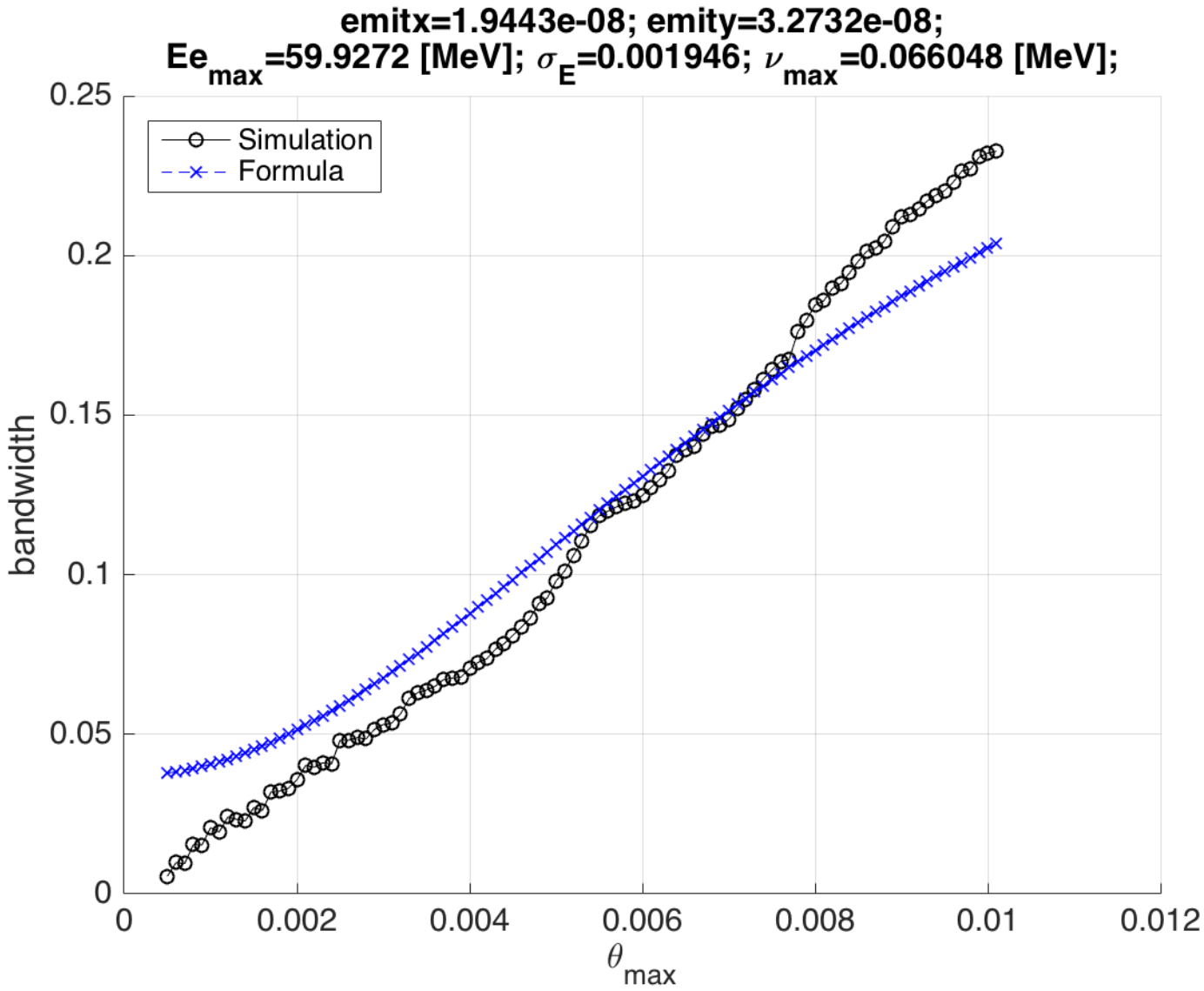
emitx=1.9443e-08; emity=3.2732e-08;
Ee_max=59.9272 [MeV]; σ_E=0.001946; ν_max=0.066048 [MeV];
Simulation
Formula
bandwidth
θ_max
0.25
0.2
0.15
0.1
0.05
0
0.002
0.004
0.006
0.008
0.01
0.012

Number of scattering photons:

$$N = \frac{A_y A_x A_z}{2\pi\sqrt{\sigma_{y1}^2+\sigma_{y2}^2}} \frac{\sigma N_1 N_2 f}{\sqrt{\sigma_{x01}^2+\sigma_{x2}^2+(\sigma_{z1}^2+\sigma_{z2}^2)\tan(\frac{\alpha_0}{2})^2}}$$

where

$$A_z = \exp\left(-\frac{\Delta z^2 \tan^2(\alpha_0)}{2(\sigma_{x1}^2+\sigma_{x2}^2+(\sigma_{z1}^2+\sigma_{z2}^2)\tan(\frac{\alpha_0}{2})^2)}\right)$$

$$A_x = \exp\left(-\frac{\Delta x^2}{2(\sigma_{x1}^2+\sigma_{x2}^2+(\sigma_{z1}^2+\sigma_{z2}^2)\tan(\frac{\alpha_0}{2})^2)}\right)$$

$$A_y = \exp\left(-\frac{\Delta y^2}{2(\sigma_{y1}^2+\sigma_{y2}^2)}\right)$$

I. Drebot (INFN-Milan) for STAR, to be published

Degradation of the flux due to initial angle.

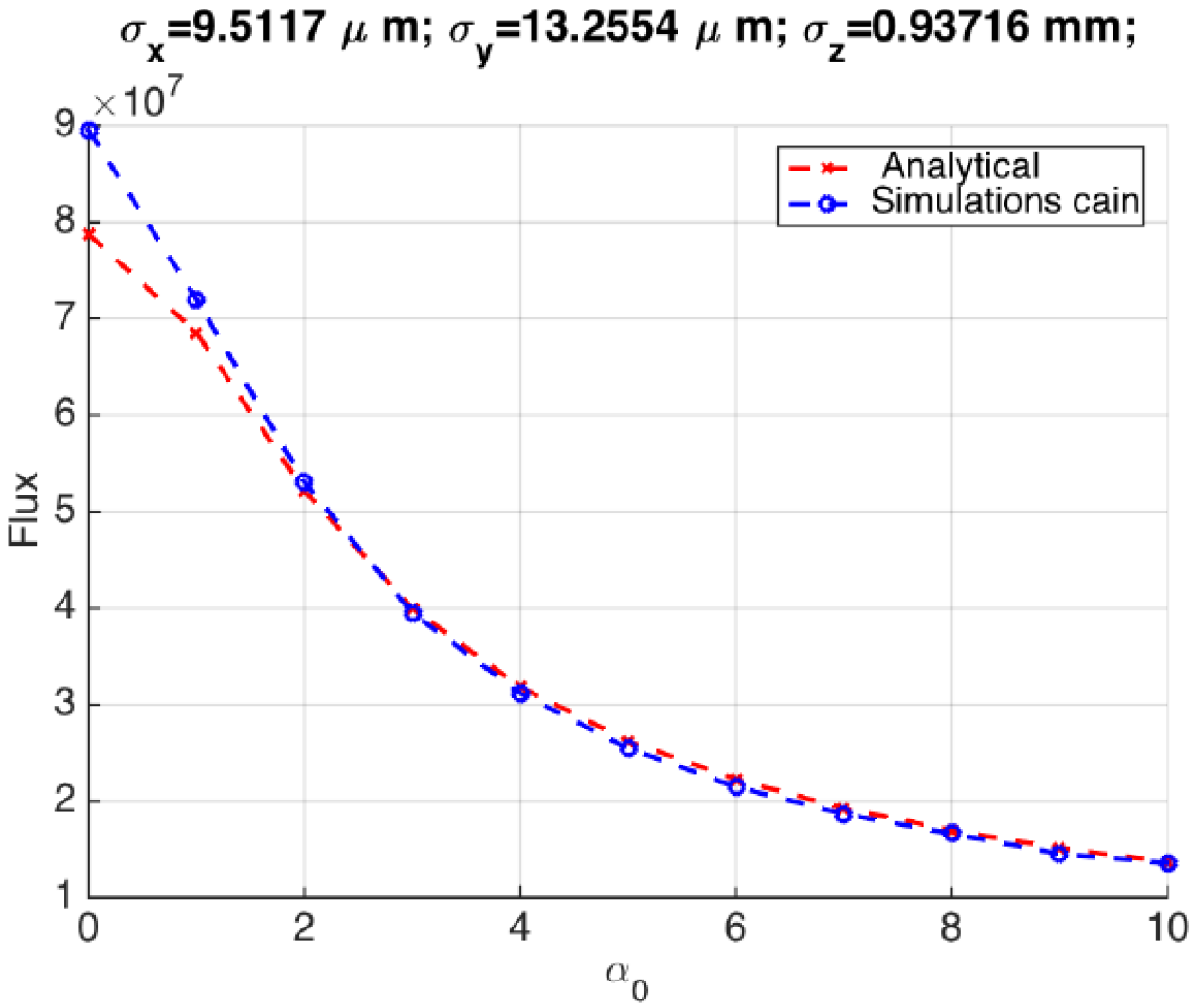

I. Drebot (INFN-Milan) for STAR, to be published

ELI-NP γ beam: the quest for narrow bandwidths (from 10^{-2} down to 10^{-3})

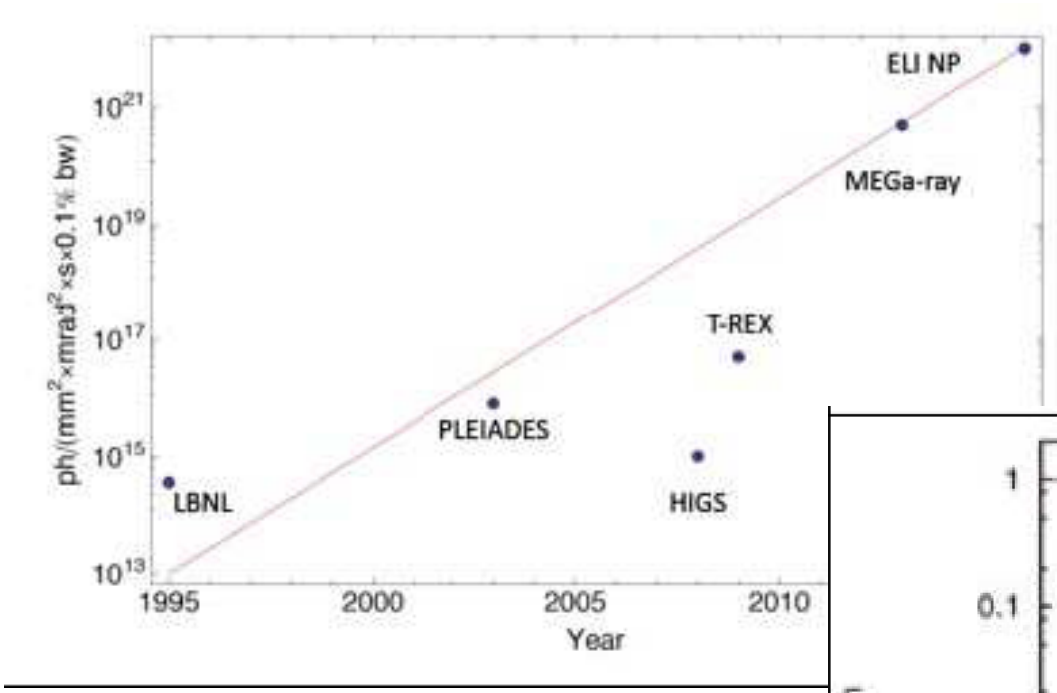

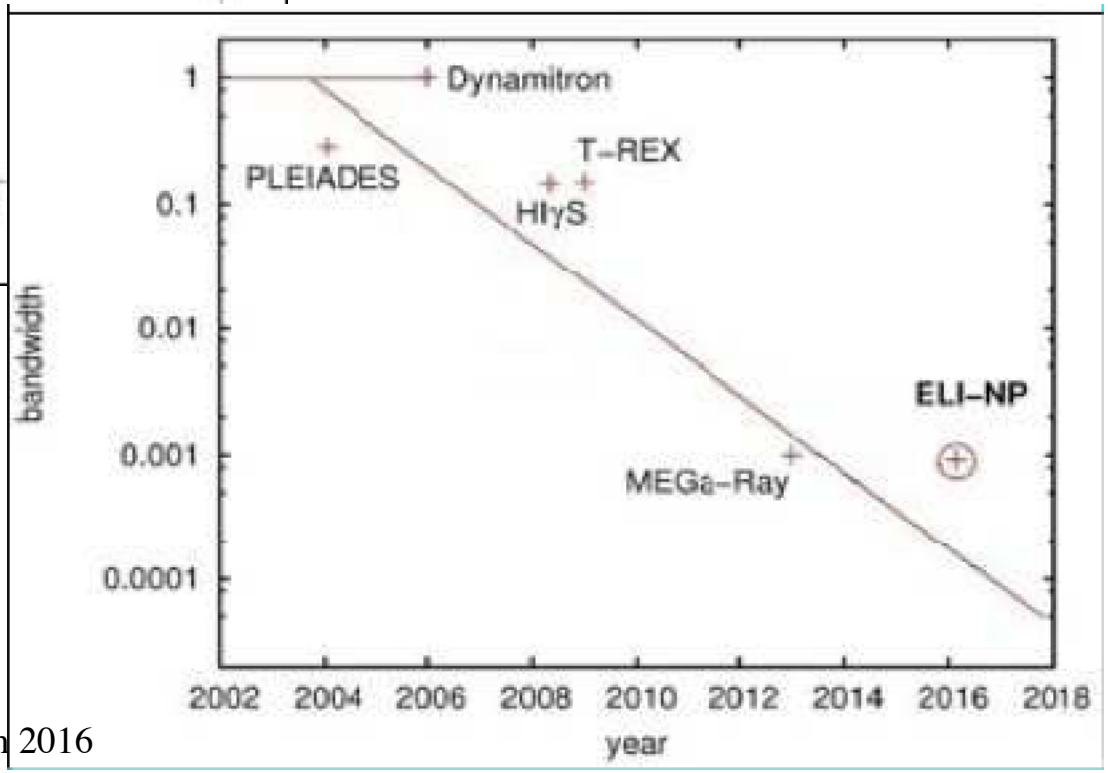

Courtesy V. Zamfir – ELI-NP

Nondestructive Assay by Nuclear Resonant Fluorescence

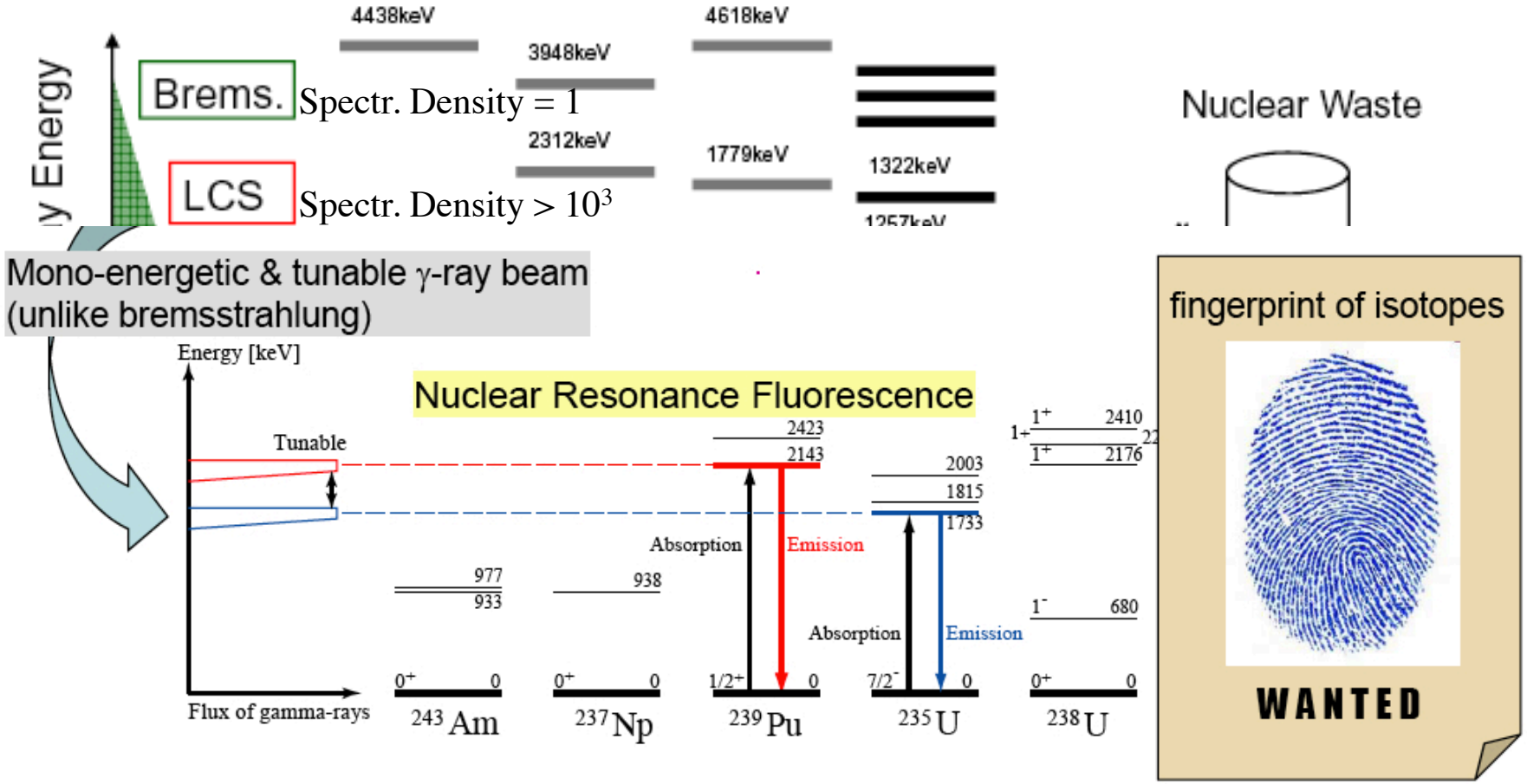

R. Hajima et al., J. Nuclear Science and Technology, 45, 441-451 (2008).

The IGS performance requirements are severe

Up to 10^{13}, 10 MeV gammas/sec

Producing 10 MeV gammas requires
~500 MeV electrons
(assuming green drive laser)

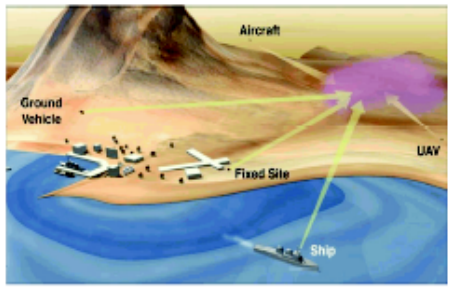

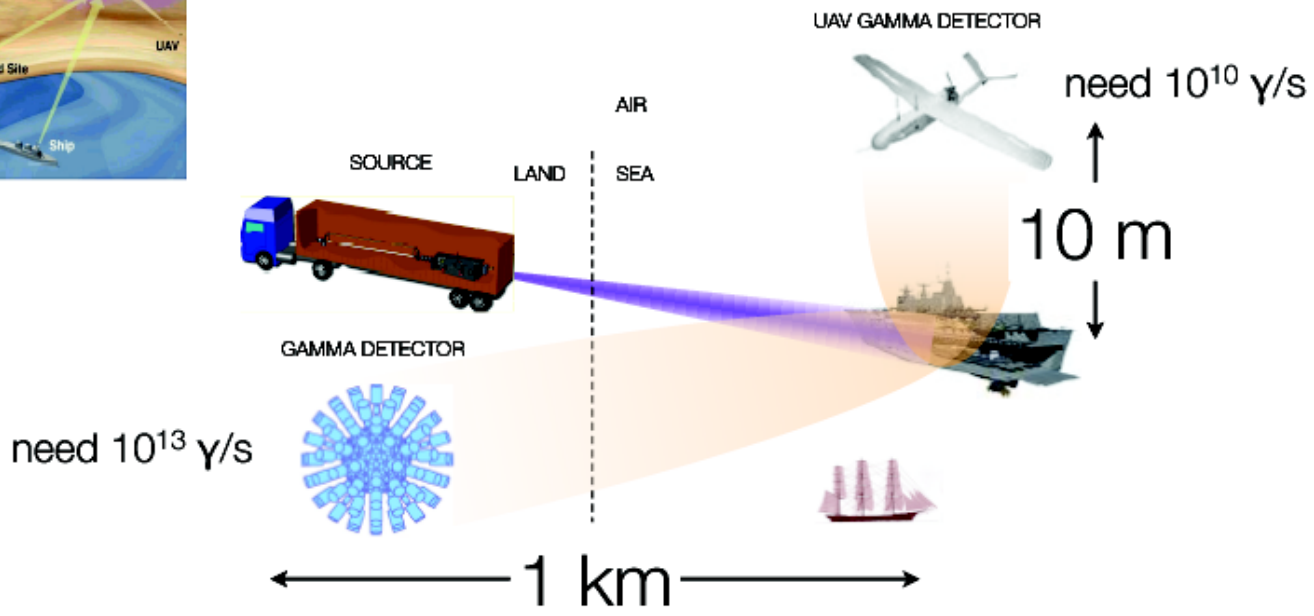

courtesy of G. Travish (UCLA)

ELI-NP GBS (Extreme Light Infrastrucutre Gamma Beam System) Main Parameters

$$\gamma - ray \;\; 1-20 \;\; MeV \;\; ; \;\; rms \;\; Bandwidth \;\; 3.-5.\,10^{-3}$$

$$Spectral \;\; Density: \;\; 10^{3}-10^{4} \;\; photons/s\cdot eV$$

$$needs \;\; 3.10^{5} \;\; photons/pulse \;\; @ \;\; 3 \;\; kHz \;\; rep \;\; rate$$

$$rms \;\; divergence \;\; 30 < \;\; 300 \;\; \mu ra$$

$$linear \;\; or \;\; circular \;\; polarization \;\; > \;\; 9 \;\; \%$$

outstanding electron beam @ 750 MeV with high ph e space density
(all values are projected, not slice! cmp. FE 's)

$$Q = 250\,pC \;\; ; \;\; \varepsilon_n = 4.10^{-7}\,m\cdot rad \;\; ; \;\; \Delta\gamma/\gamma = \cdot 10^{-4}$$

Back-scattering a high quality *J-class* ps laser pulse

$$U_L = 400 \;\; mJ \;\; ; \;\; M^2 = 1.2 \;\; ; \;\; \frac{\Delta\nu}{\nu} = 5\cdot 10^{-4}$$

not sustainable by RF, Laser!

Accelerator and Equipments in ELI-NP Building

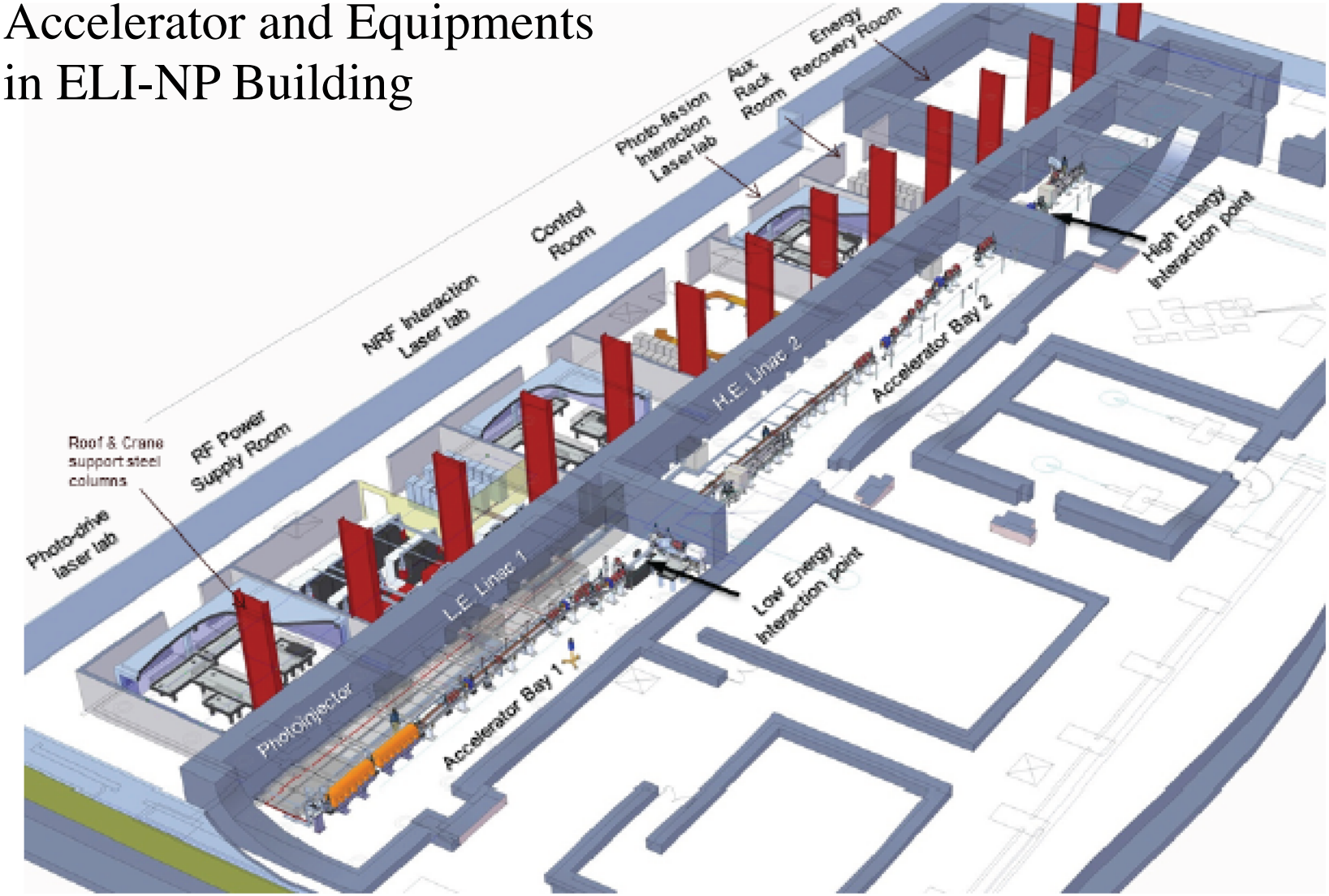

Fig. 197. Isometric 3D view of Building Layout of the Accelerator Hall & Experimental Areas

Technical Design Report

EuroGammaS proposal for the ELI-NP Gamma beam System

With 73 tables and 230 figures

O. Adriani, S. Albergo, D. Alesini, M. Anania, D. Angal-Kalinin, P. Antici, A. Bacci, R. Bedogni, M. Bellaveglia, C. Biscari, N. Bliss, R. Boni, M. Boscolo, F. Broggi, P. Cardarelli, K. Cassou, M. Castellano, L. Catani, I. Chaikovska, E. Chiadroni, R. Chiche, A. Cianchi, J. Clarke, A. Clozza, M. Coppola, A. Courjaud, C. Curatolo, O. Dadoun, N. Delerue, C. De Martinis, G. Di Domenico, E. Di Pasquale, G. Di Pirro, A. Drago, F. Druon, K. Dupraz, F. Egal, A. Esposito, F. Falcoz, B. Fell, M. Ferrario, L. Ficcadenti, P. Fichot, A. Gallo, M. Gambaccini, G. Gatti, P. Georges, A. Ghigo, A. Goulden, G. Graziani, D. Guibout, O. Guilbaud, M. Hanna, J. Herbert, T. Hovsepian, E. Iarocci, P. Iorio, S. Jamison, S. Kazamias, F. Labaye, L. Lancia, F. Marcellini, A. Martens, C. Maroli, B. Martlew, M. Marziani, G. Mazzitelli, P. McIntosh, M. Migliorati, A. Mostacci, A. Mueller, V. Nardone, E. Pace, D.T. Palmer, L. Palumbo, A. Pelorosso, F.X. Perin, G. Passaleva, L. Pellegrino, V. Petrillo, M. Pittman, G. Riboulet, R. Ricci, C. Ronsivalle, D. Ros, A. Rossi, L. Serafini, M. Serio, F. Sgamma, R. Smith, S. Smith, V. Soskov, B. Spataro, M. Statera, A. Stecchi, A. Stella, A. Stocchi, S. Tocci, P. Tomassini, S. Tomassini, A. Tricomi, C. Vaccarezza, A. Variola, M. Veltri, S. Vescovi, F. Villa, F. Wang, E. Yildiz, F. Zomer

109 Authors, 327 pages
published today on ArXiv
http://arxiv.org/abs/1407.3669

Electron beam is transparent to the laser (only 10^9 photons are back-scattered at each collision out of the 10^{18} carried by the laser pulse)

CIRCULATOR PRINCIPLE

- 2 high-grade quality parabolic mirrors
  - Aberration free
- Mirror-pair system (MPS) per pass
  - Synchronization
  - Optical plan switching
    - ⇒ Constant incident angle = small bandwidth

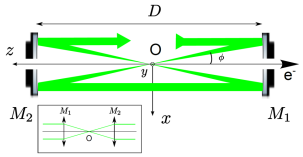

PARAMETERS = OPTIMIZED ON THE GAMMA-RAY FLUX

- Laser power = state of the art
- Angle of incidence ($\varphi = 7.54°$)
- Waist size ($\omega_0 = 28.3\mu m$)
- Number of passes = 32 passes

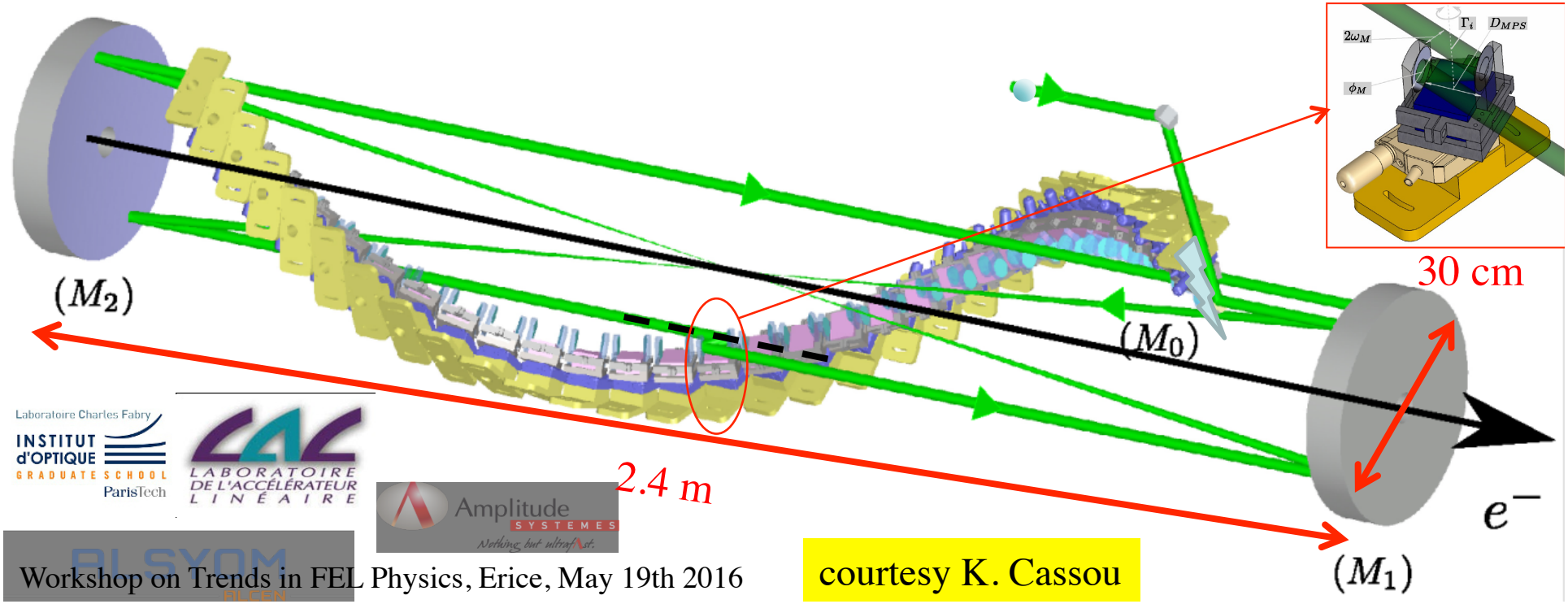

Laboratoire Charles Fabry INSTITUT d'OPTIQUE GRADUATE SCHOOL ParisTech

LABORATOIRE DE L'ACCÉLÉRATEUR LINÉAIRE

Amplitude SYSTEMES Nothing but ultrafast.

courtesy K. Cassou

PHYSICAL REVIEW SPECIAL TOPICS - ACCELERATORS AND BEAMS 17, 033501 (2014)

Design and optimization of a highly efficient optical multipass system for γ-ray beam production from electron laser beam Compton scattering

K. Dupraz,* K. Cassou, N. Delerue, P. Fichot, A. Martens, A. Stocchi, A. Variola, and F. Zomer
LAL, Université Paris-Sud, CNRS/IN2P3, Orsay, Bâtiment 200, BP 34, 91898 Orsay cedex, France

A. Courjaud and E. Mottay
Amplitude Systèmes, 6 allée du Doyen Georges Brus, 33600 Pessac, France

F. Druon
Laboratoire Charles Fabry de l'Institut d'Optique, UMR 8501 CNRS, Université Paris Sud, 91127 Palaiseau, France

G. Gatti and A. Ghigo
INFN-LNF, Via Enrico Fermi 40, 00044 Frascati Rome, Italy

T. Hovsepian, J. Y. Riou, and F. Wang
Alsyom, Parc des Algorithmes, Bâtiment Aristote, 9 Avenue du Marais, 95100 Argenteuil, France

A. C. Mueller
National Institute for Nuclear and Particle Physics, CNRS, 3 rue Michel-Ange, 75016 Paris, France

L. Palumbo
Universita di Roma La Sapienza, Dipartimento Energetica, Via Antonio Scarpa, 14-00161 Rome, Italy

L. Serafini and P. Tomassini
INFN-MI, Via Celoria 16, 20133 Milano, Italy
(Received 31 December 2013; published 26 March 2014)

A new kind of nonresonant optical recirculator, dedicated to the production of γ rays by means of Compton backscattering, is described. This novel instrument, inspired by optical multipass systems, has its design focused on high flux and very small spectral bandwidth of the γ-ray beam. It has been developed to fulfill the project specifications of the European Extreme Light Infrastructure "Nuclear Pillar," i.e., the Gamma Beam System. Our system allows a single high power laser pulse to recirculate 32 times synchronized on the radio frequency driving accelerating cavities for the electron beam. Namely, the polarization of the laser beam and crossing angle between laser and electrons are preserved all along the 32 passes. Moreover, optical aberrations are kept at a negligible level. The general tools developed for designing, optimizing, and aligning the system are described. A detailed simulation demonstrates the high efficiency of the device.

ELI-NP-GBS High Order mode Damped RF structure

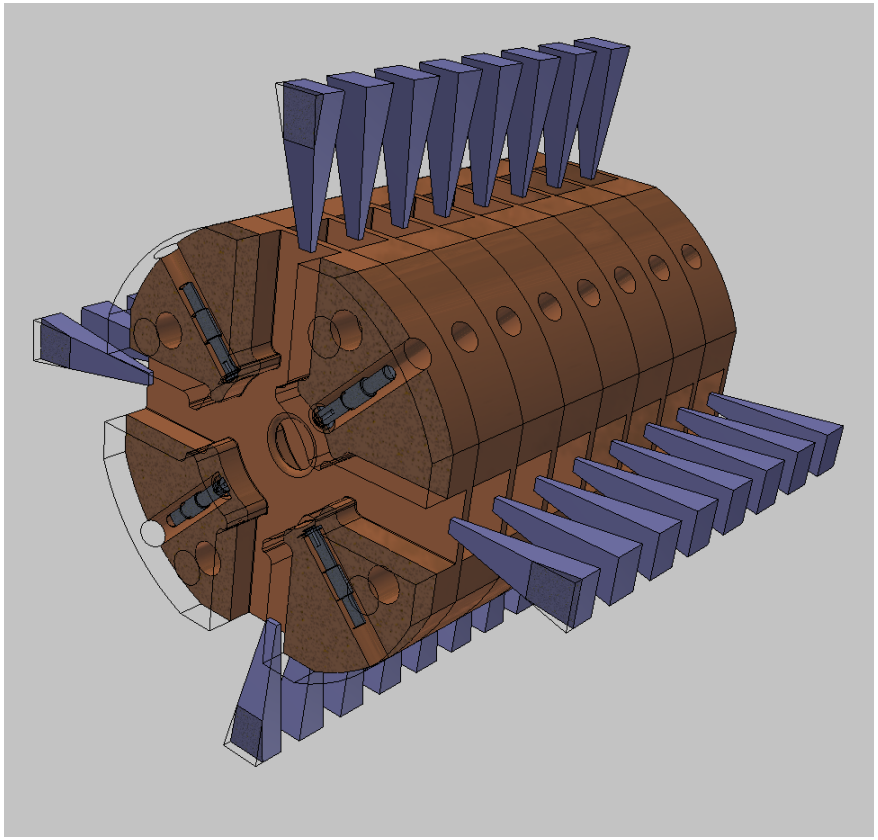

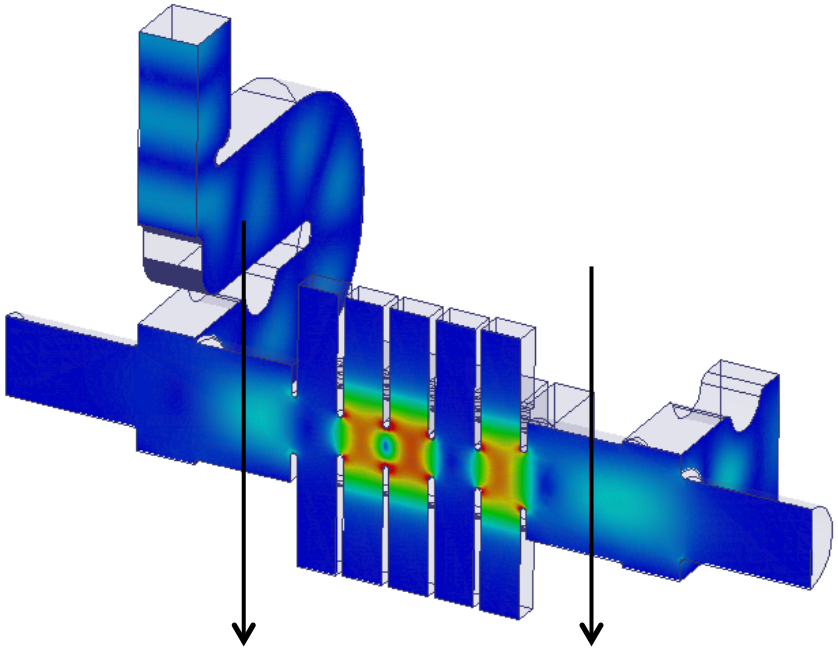

Unlike FEL's Linacs, ELI-NP-GBS is a multi-bunch accelerator, therefore we need to control the Beam-Break-Up Instability to avoid complete deterioration of the electron beam emittance, i.e. of its brightness and phase space density

courtesy David Alesini

C-BAND STRUCTURES: HIGH POWER TEST SETUP

The structure has been tested at **high power at the Bonn University under RI responsibility**.

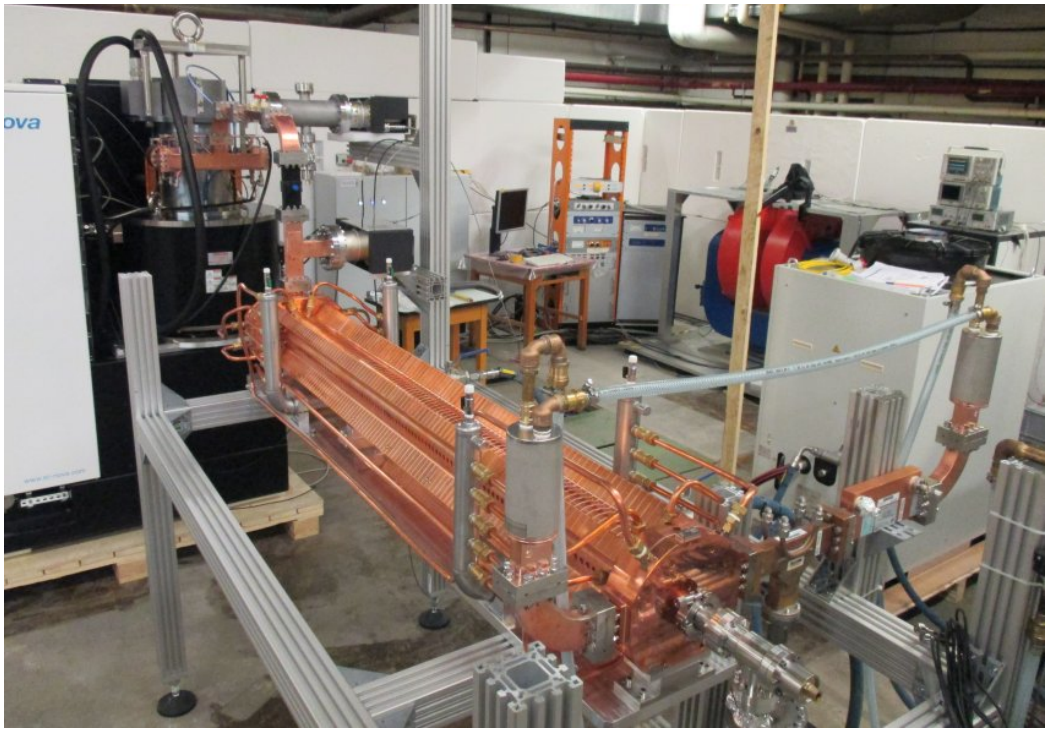

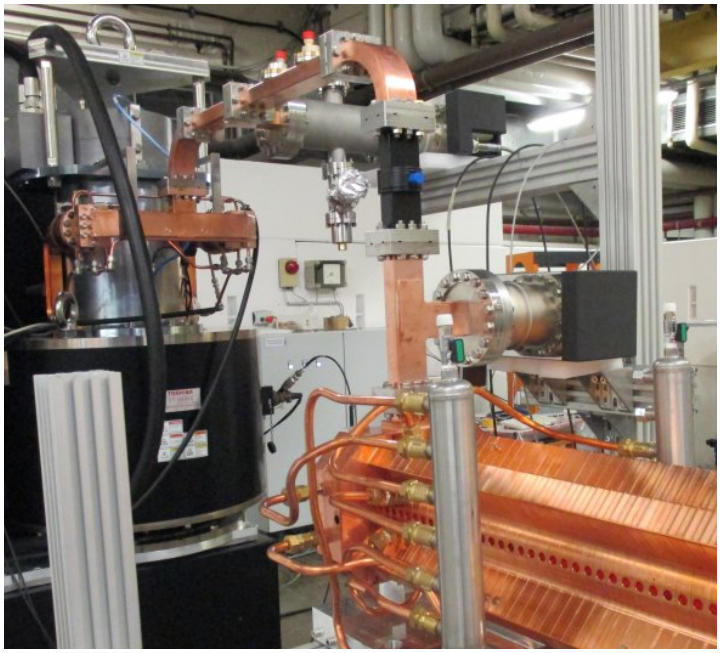

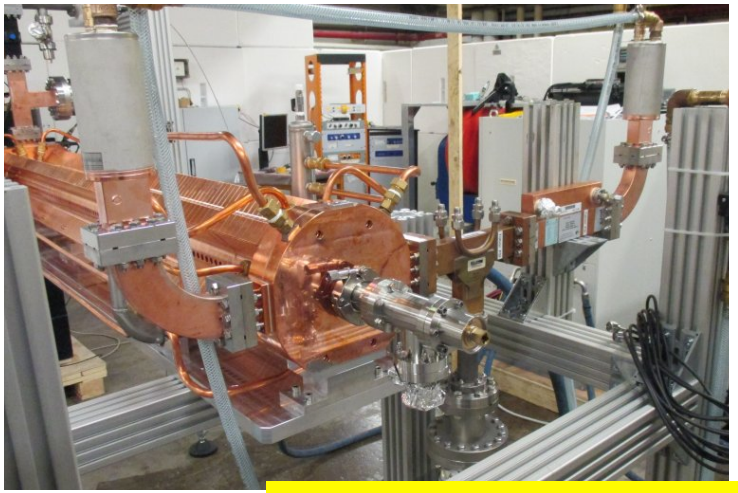

Successfully tested at full power (40 MW)

courtesy David Alesini

Brilliance of Lasers and X-ray sources

ELI

BELLA

$$N_{ph} = 10^{19} - 10^{20}$$

$$\sigma_t = 10 - 20 \quad fs$$

$$B = \frac{N_{ph}}{\sqrt{2\pi}\sigma_t \left(M^2\lambda\right)^2 \frac{\Delta\lambda}{\lambda}}$$

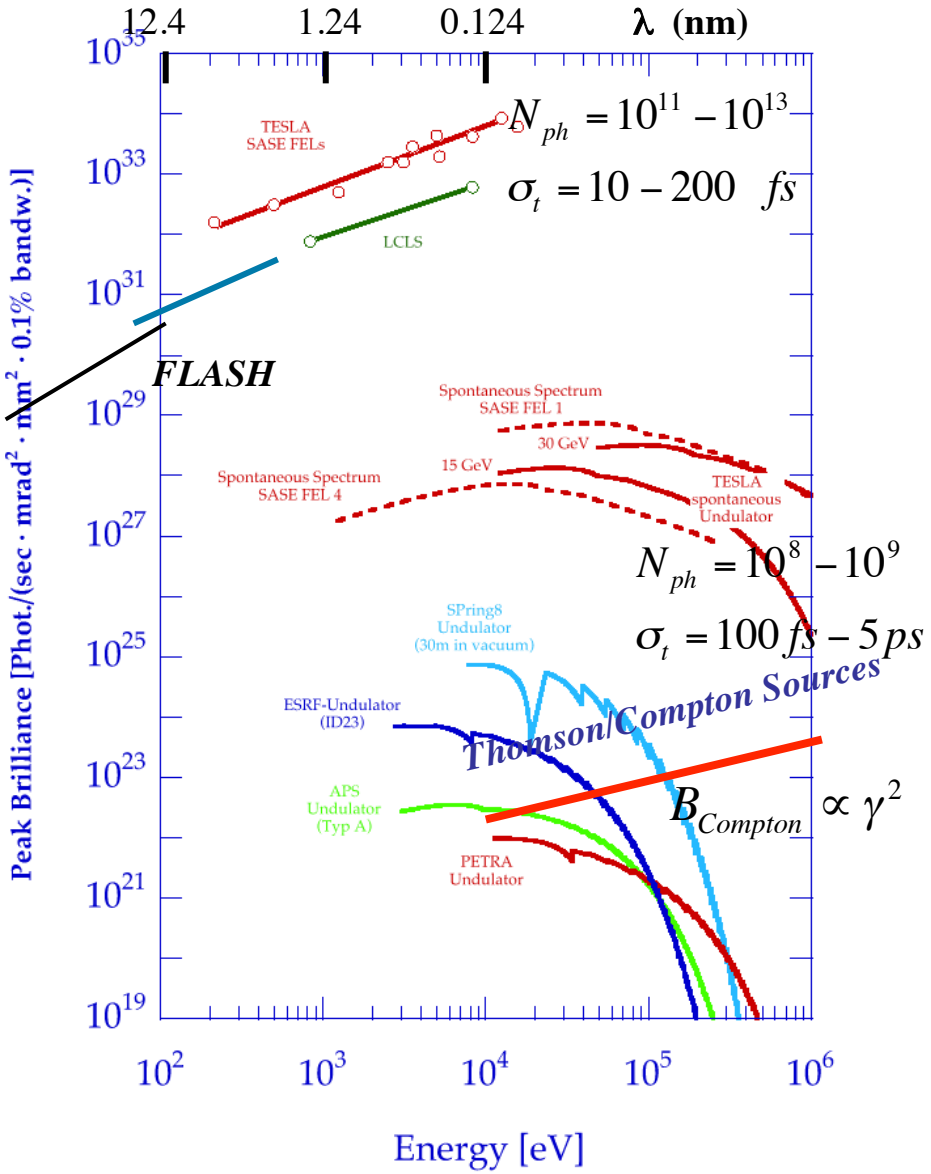

Outstanding X/γ photon beams for Exotic Colliders

Advancing Thomson X Ray Sources for Bio/Medical Imaging Applications and Matter Science

Proposal BriXS: BRIght and compact X-ray Source

NUCLEAR INSTRUMENTS & METHODS IN PHYSICS RESEARCH

Section A: accelerators, spectrometers, detectors and associated equipment

Volume 608 (2009), Issue 1S Supplement

COMPTON 2008

Compton sources for X/γ rays:
Physics and applications
Alghero, Sardinia, Italy, September 7–12, 2008

Edited by Massimo Carpinelli, Luca Serafini

Abstracted/Indexed in: Current Contents: Engineering, Computing and Technology; Current Contents: Physical, Chemical and Earth Sciences; EI Compendex Plus; Engineering Index; INSPEC. Also covered in the abstract and citation database SCOPUS®. Full text available on ScienceDirect®.

0168-9002(20090901)608:1s;1-V

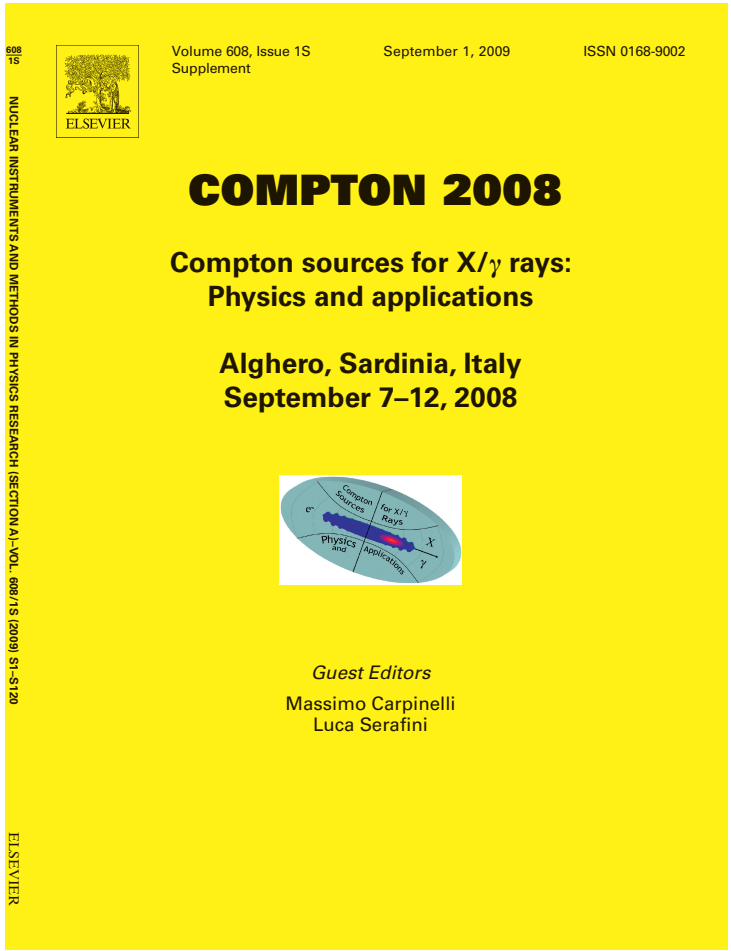

Biomedical imaging with the lab-sized laser-driven synchrotron source Munich Compact Light Source

Klaus Achterhold

Biomedical Physics, Physics-Department E17, Technische Universität München

Compact machine
10x10 m^2
In operation since
early 2015

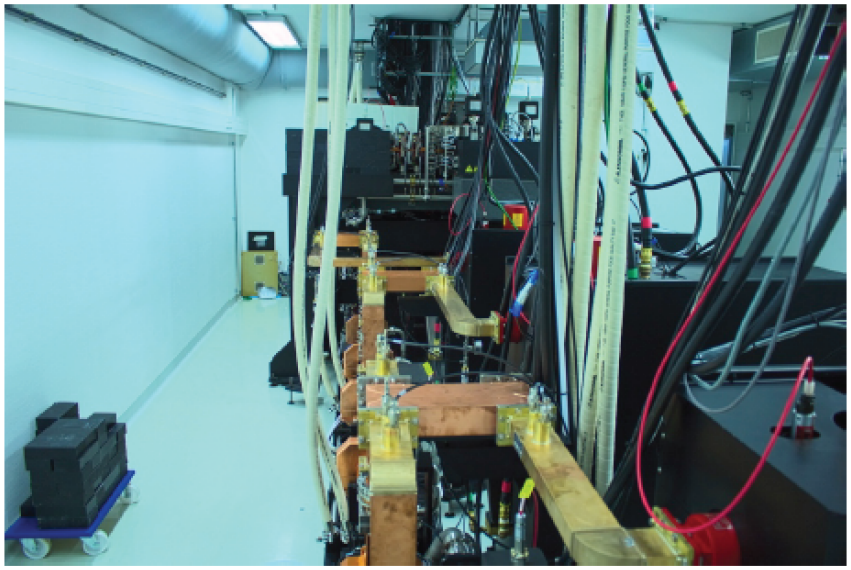

$$E_x\left(\Theta,\alpha,E_L,T\right)=\frac{\left(1+\beta\cos\alpha\right)E_L}{1-\beta\cos\Theta+\left(E_L/mc2\right)\left(1+\cos\left(\Theta+\alpha\right)\right)}$$

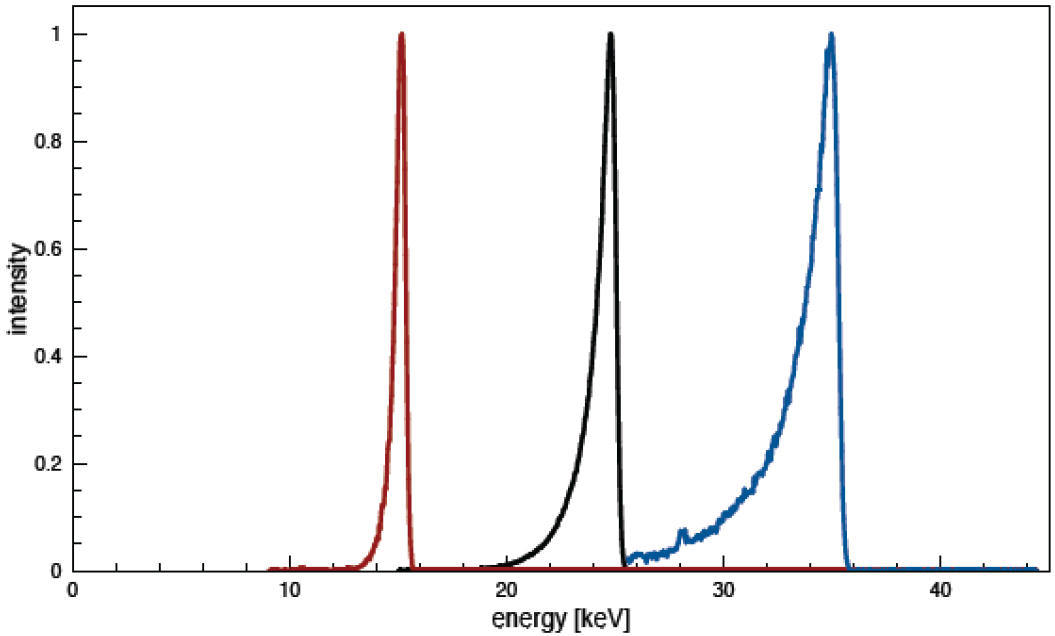

measured
Spectrum of X-rays
into +/- 2 mrad

Bandwidth

$35000+0.0016\cdot\Delta T$ with $\Delta T/T=0.3\%$
$35000+30000\cdot\Delta E_L$ with $\Delta E_L/E_L=10^{-12}$

$35000-9000\cdot\Delta\alpha^2$ with $\Delta\alpha=0.03$

Measured $5\cdot10^{10}$ ph/sec with 20 mA

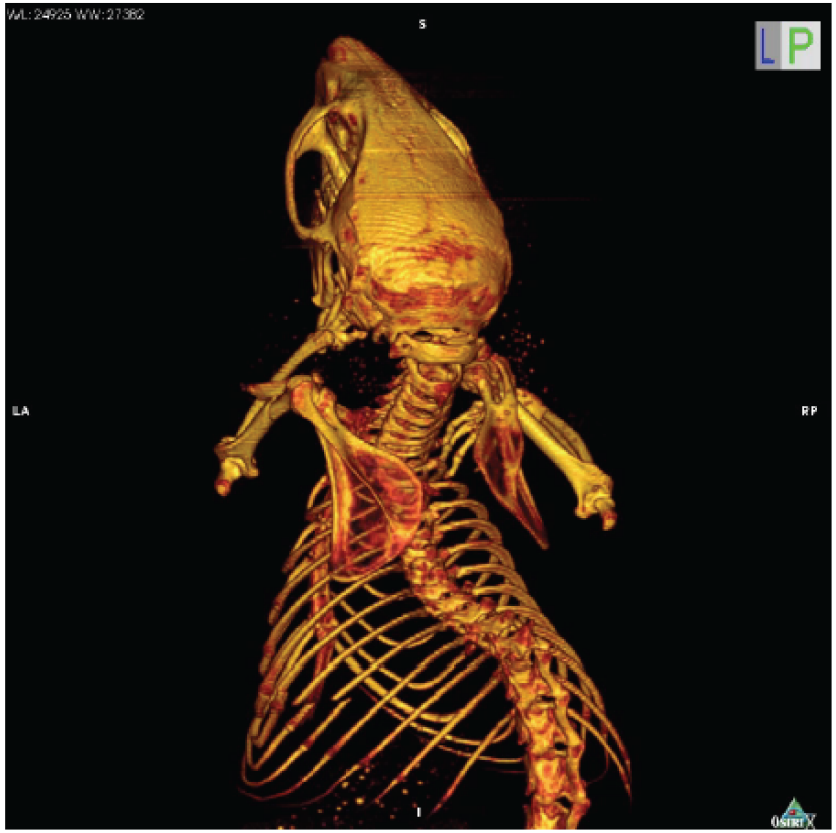

small source size → high resolution (81 μm)
monochromatic → no beam hardening artefacts

Klaus.Achterhold@tum.de

Phase Contrast Imaging made possible by small round source spot size (< 20 μm)

courtesy of A. Bravin (ESRF)

Bio-Medical Advanced Imaging with Mono-chromatic X-rays, demonstrated at Synchrotrons, is possible also with High Flux Thomson X-ray Sources in 20 keV-100 keV energy range

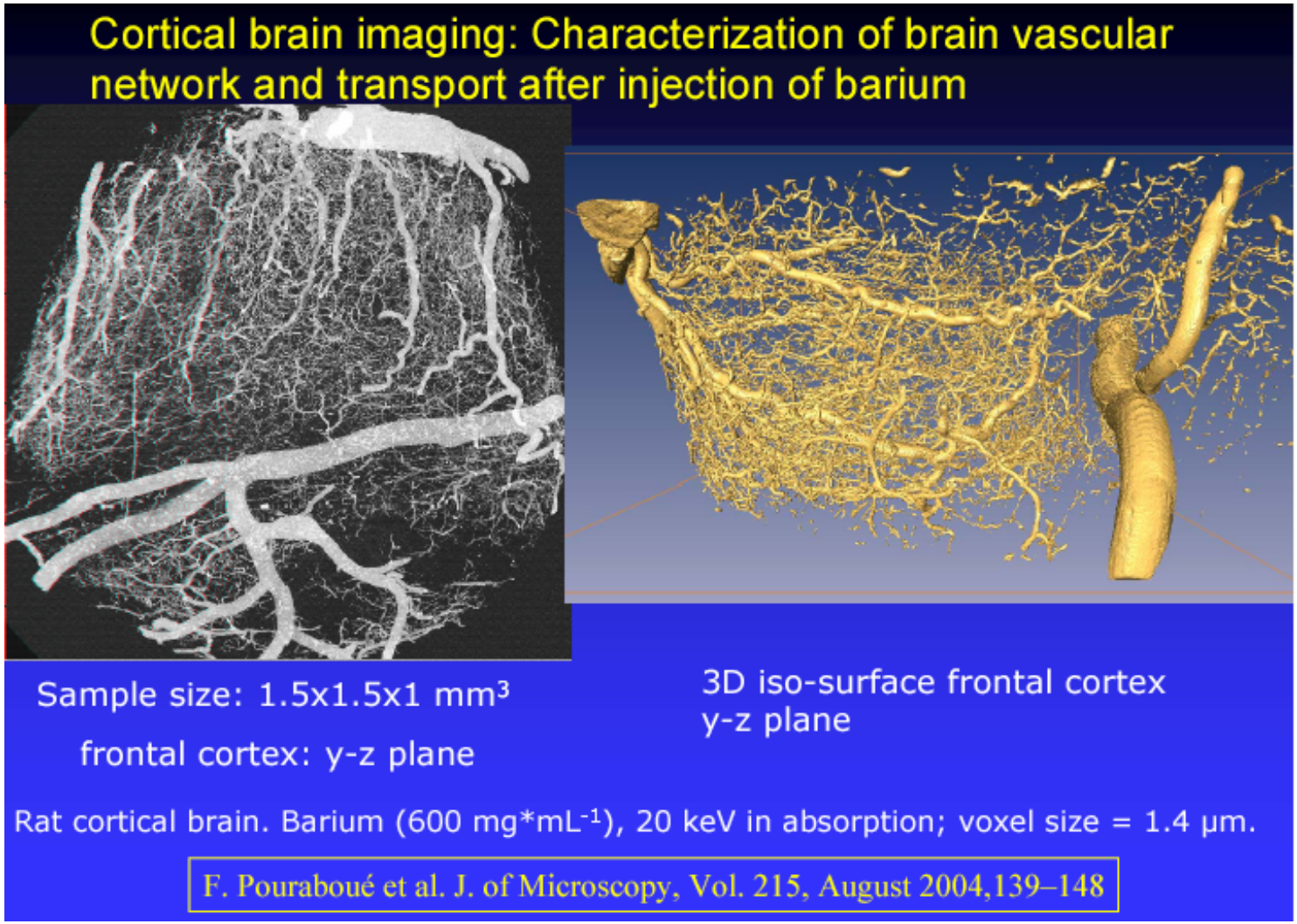

Bio-Medical Advanced Imaging with Digital Subtraction of Mono-chromatic X-ray shots are also possible with High Flux Thomson X-ray Sources with picosecond to millisecond time resolution

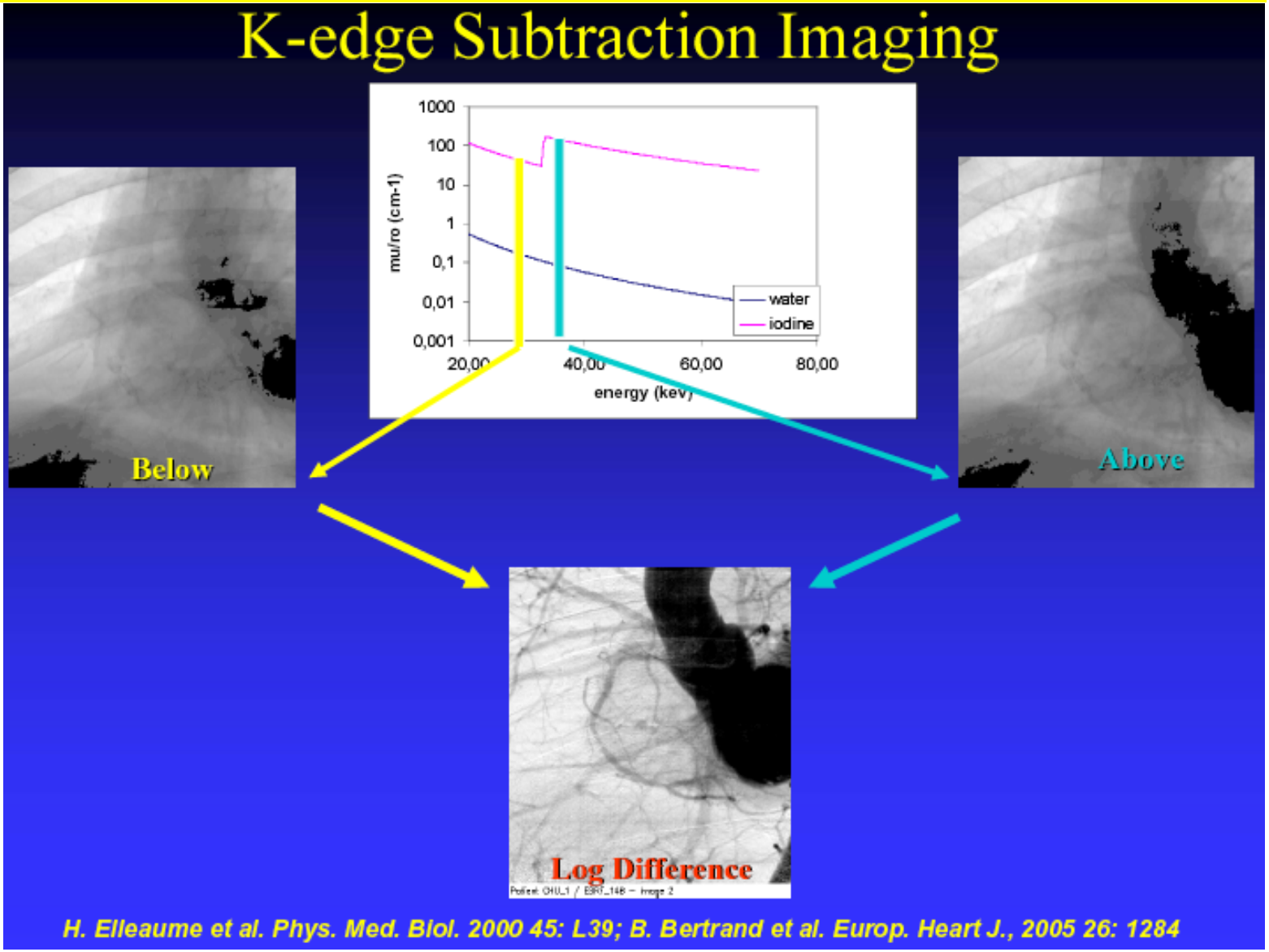

Also Mammography with Mono-chromatic X-rays at 20-30 keV has been proven far superior in Signal-to-Noise-Ratio w.r.t. conventional mammographic tubes, with a considerably lower radiation dose to the tissue

IOP Publishing | Institute of Physics and Engineering in Medicine — Physics in Medicine & Biology

Phys. Med. Biol. 61 (2016) 1634–1649 — doi:10.1088/0031-9155/61/4/1634

Compact Thomson X-ray Sources could be located inside hospitals to diagnose and treat patients directly at the hospital site (unlike Synchrotrons…)

Towards breast tomography with synchrotron radiation at Elettra: first images

R Longo[1,2], F Arfelli[1,2], R Bellazzini[3,4], U Bottigli[5], A Brez[3,4], F Brun[2,6], A Brunetti[7], P Delogu[4,8], F Di Lillo[9], D Dreossi[10], V Fanti[11], C Fedon[1,2], B Golosio[7], N Lanconelli[12], G Mettivier[9], M Minuti[3,4], P Oliva[7], M Pinchera[3,4], L Rigon[1,2], P Russo[9], A Sarno[9], G Spandre[3,4], G Tromba[10] and F Zanconati[13]

For Radio-logical Imaging and Radio-therapy Applications
The Key Issue is Flux (Photons/s) with a reasonable bandwidth
(3-10%, avoid low energy tail of bremmstrahlung spectrum!)

The entry level is 10^{12} photons/s for Imaging
and 10^{13} for Therapy

10^{13} – 10^{14} and over would open the era of clinical applications,
i.e. treatment of patients inside hospital

UH-FLUX
Advanced Compton/THz source based on novel design of coupled SC RF cavities

A. Seryi, JAI

Collaboration of UK centers JAI, CI, STFC and UK industry

- Three patents on the technology, publication prepared
- Develop in collaboration
  - With Cockcroft and STFC, most recently with Fermilab
- Working with ISIS Innovation and companies
  - Niowave company USA and Sheakespear Engineering, UK
- Developing IPS, PRD, Innovate UK grant proposals
- Positive review by JAI AB and peers

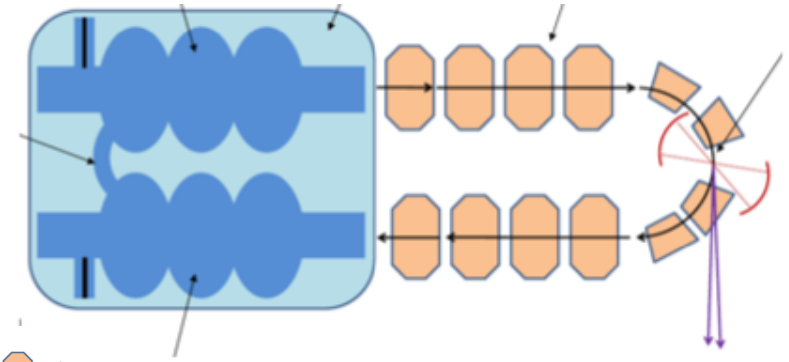

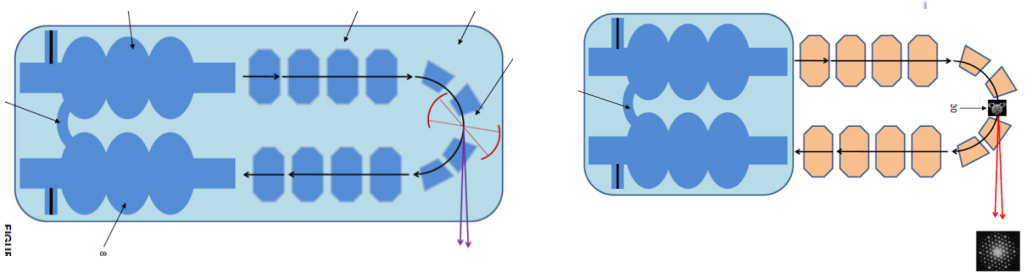

Compton or Coherent Smith Purcell (THz)
Recovery linac

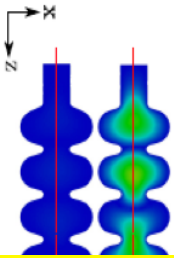

[1] International (PCT) Patent Application No. PCT/GB2012/052632 (WO2013/061051) filed on the 26th October 2012

[2] Oxford University Isis Project No. 11330 – "Asymmetric superconducting RF structure" (UK Priority patent application 1420936.5 titled 'Asymmetric superconducting RF structure' filed on the 25th November 2014

New Generation High Flux (10^{14}-10^{15} ph/s) Sources in the US (BNL), Japan (KEK) and UK (STFC) based on Energy Recovery Super-Conducting CW electron linacs

UH-FLUX
Advanced Compton/THz source based on novel design of coupled SC RF cavities

A. Seryi, JAI

Possible parameters

Typical parameters, range	[		]	
Electron beam E, MeV	10	20	30	
Electron bunch charge, nC	0.2	0.5	1	
e-bunch repetition rage, MHz	50	200	1000	
e-beam average current, A	0.01	0.1	1	
e-beam reactive power, MW	0.1	2	30	
e-beam energy at dump, MeV	0.2	0.1	0.1	
laser wavelength	1000	600	300	
X-ray max energy, keV	2	12	60	
X-ray min wavelength, nm	0.6	0.1	0.02	
X-ray flux, ray/s	1.E+15	8.E+15	4.E+16	
approx peak brilliance	2.E+20	2.E+21	8.E+21	ph/(s mm^2 mrad^2 0.1%bw)
approx RF power, kW	2	10	100	
e-Energy recovery coefficient	50	200	300	

Table from the Patent No. PCT/GB2012/052632 (WO2013/061051) filed on 26th October 2012

High flux X-ray/THz compact SCRF Compton Light Source

With unprecedented and outstanding foreseen performances, at all similar to Synchrotrons, but with higher energy X-rays

-- developing plans for realization of the prototypes of key systems *m manipulation, Luca Serafini, Marie-Emmanuelle Couprie*

Quantum beam project – KEK/ATF

Compact (less than 10m) quasi-monochromatic (less than 1%)
High Flux (100 times than Compact normal Linac X-ray : 10^{11} photons/sec 1% b.w.)
High Brightness (10^{17} photons/sec mrad^2 mm^2 0.1% b.w.)
Ultra-short pulse X-ray (40 fs ~)

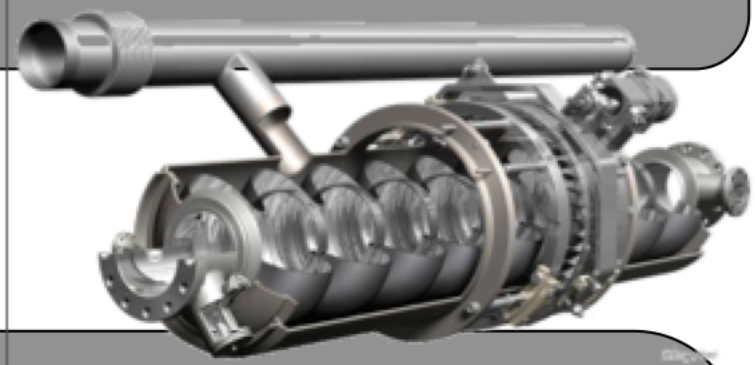

J. Urakawa, Quantum Beam Project

Key: SCRF acceleration technology

Structural genetic analysis,

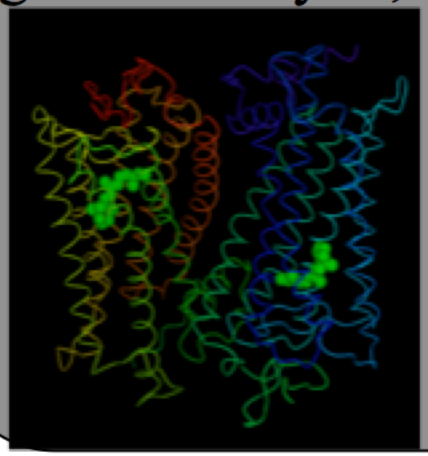

Nano-material evaluation,

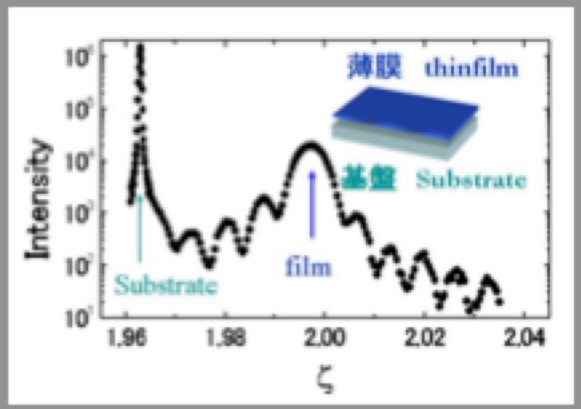

Highly fine X-ray Imaging

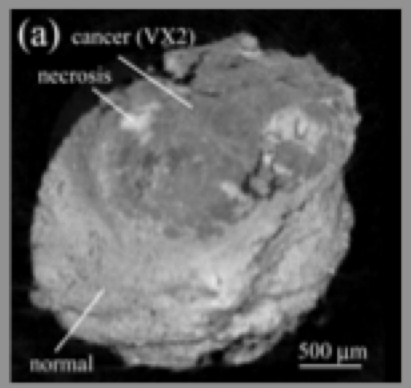

http://mml.k.u-tokyo.ac.jp/

J. Urakawa at KEK-ATF

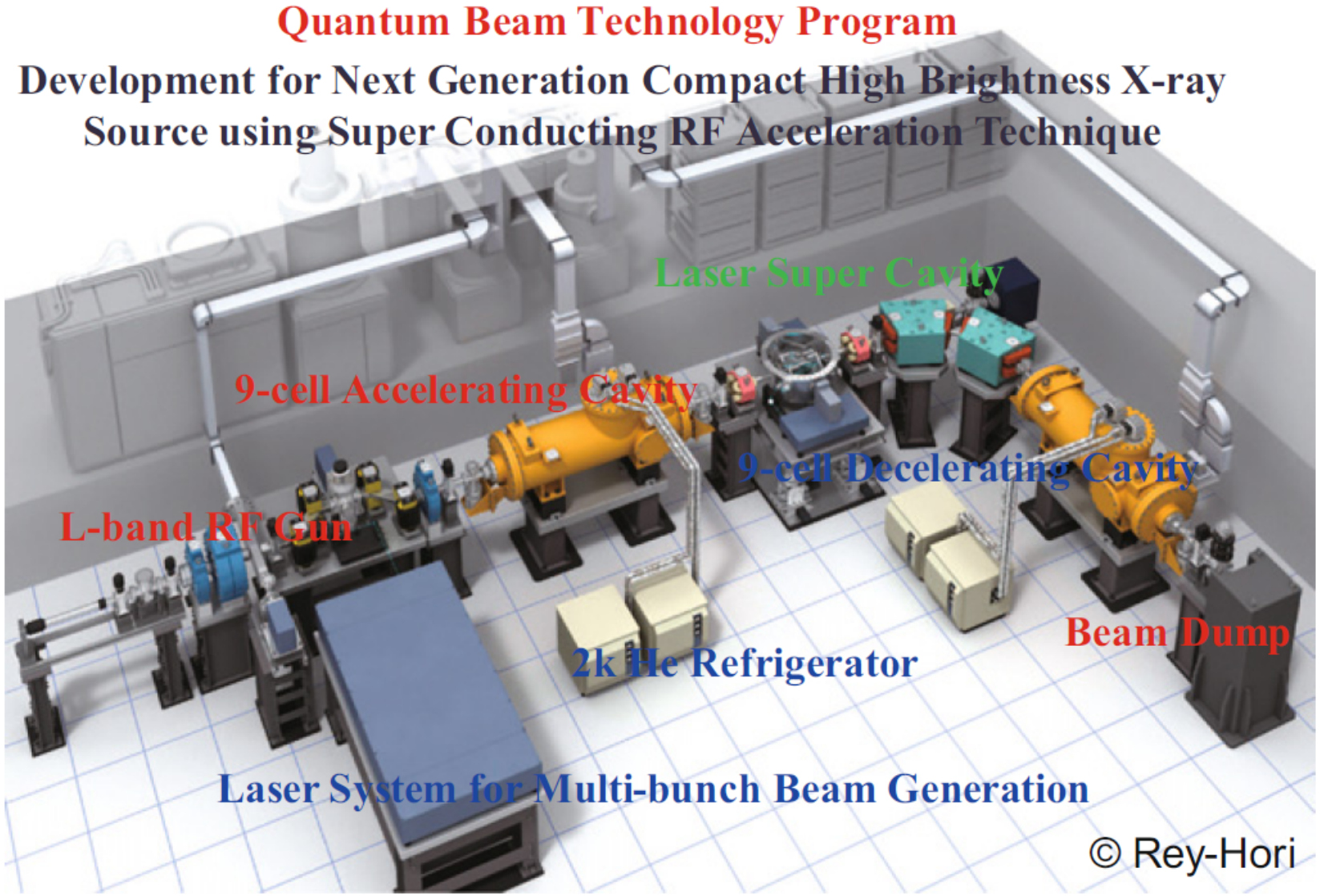

J. Urakawa, Nucl. Instr. and Meth. A (2010), doi:10.1016/j.nima.2010.02.019

ICS vs. other sources

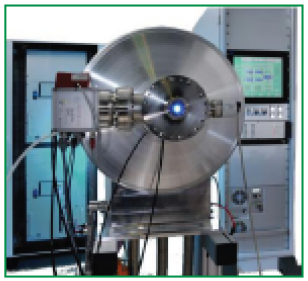

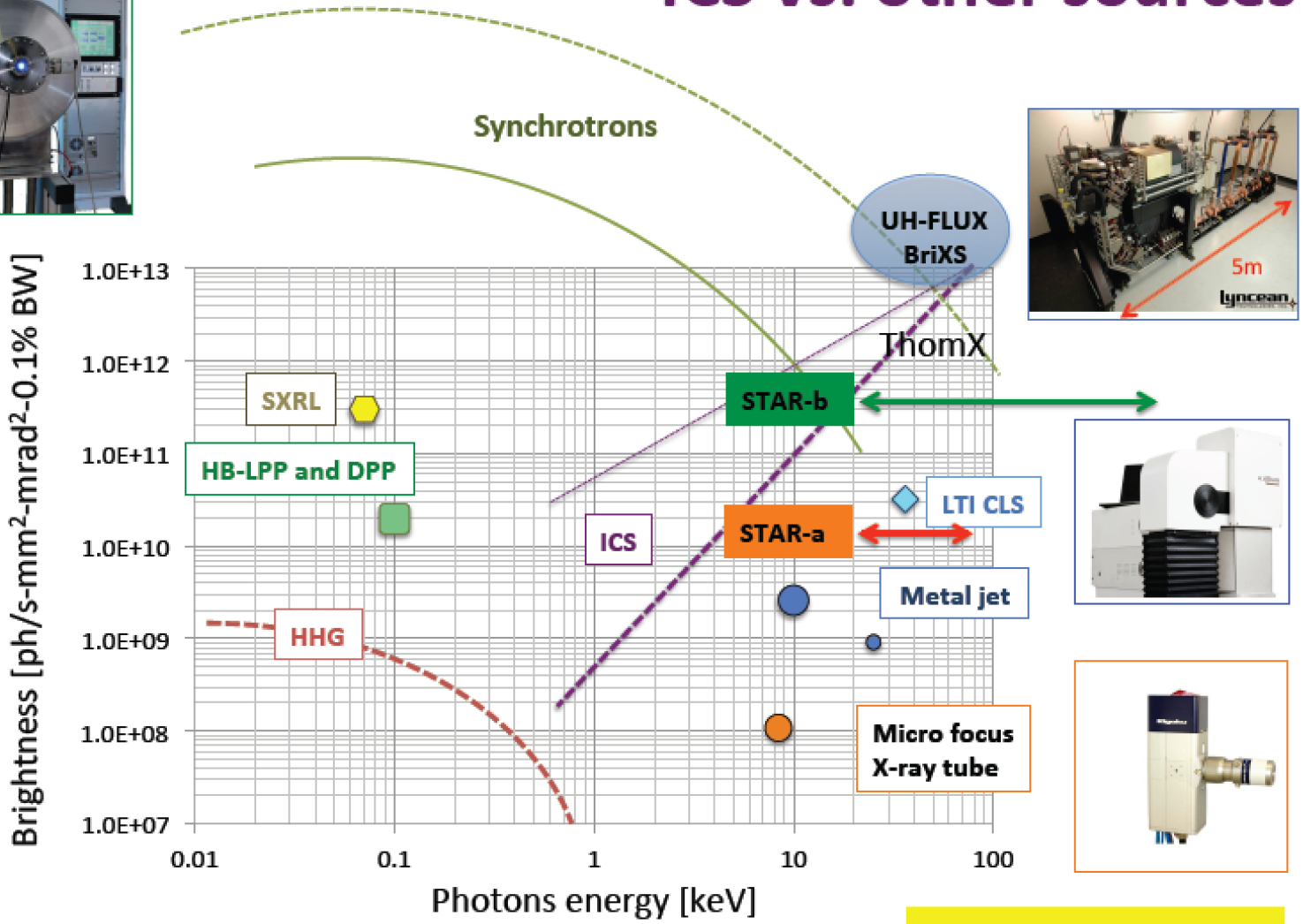

Courtesy of A. Murokh
RadiaBeamTechnology

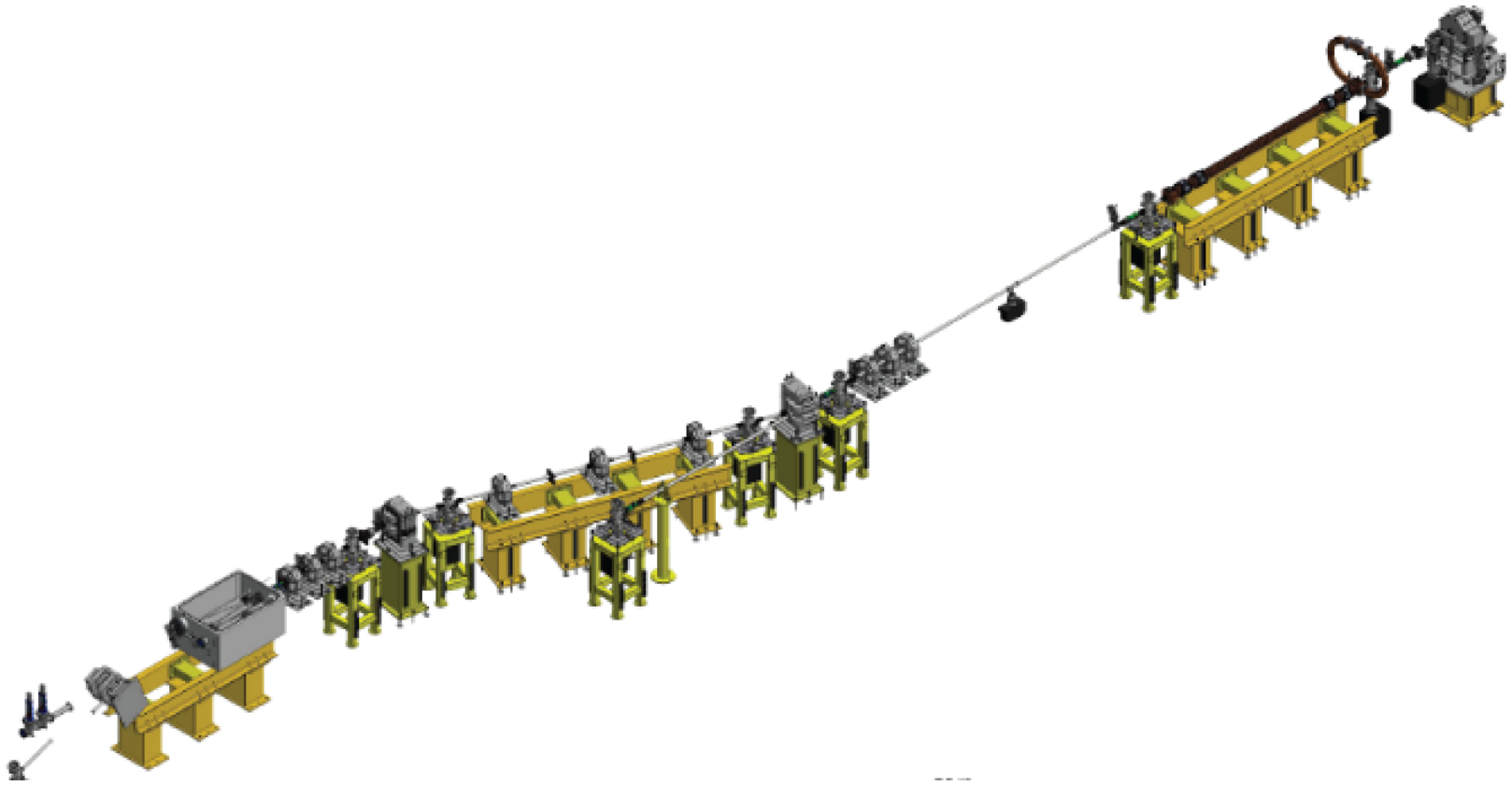

Fig.2 *– STAR machine as an example of Paradigm A. Overall length about 12 m.*

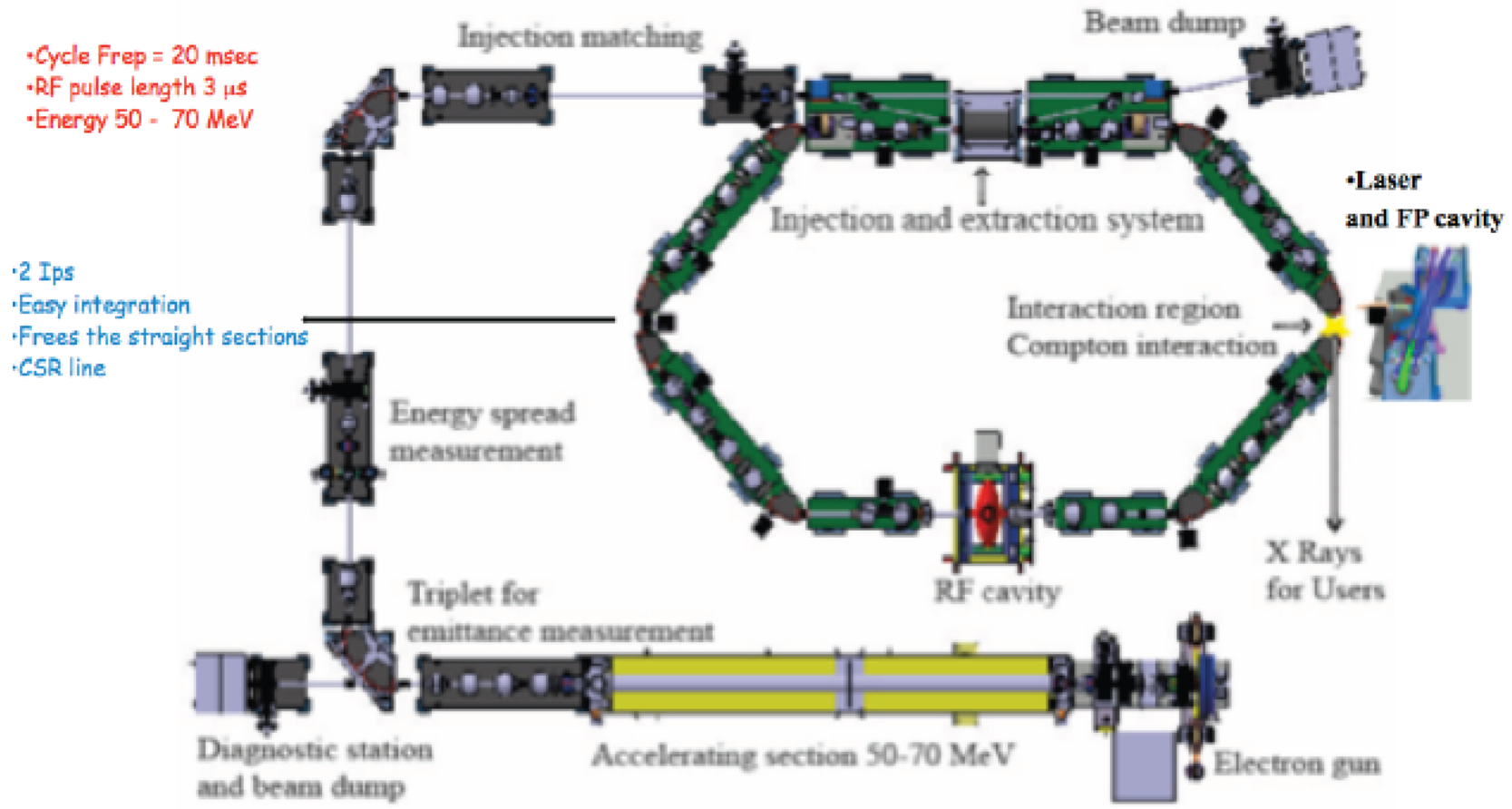

***Fig.3** – ThomX as an example of Paradigm B. Size is about 10x10 m^2.*

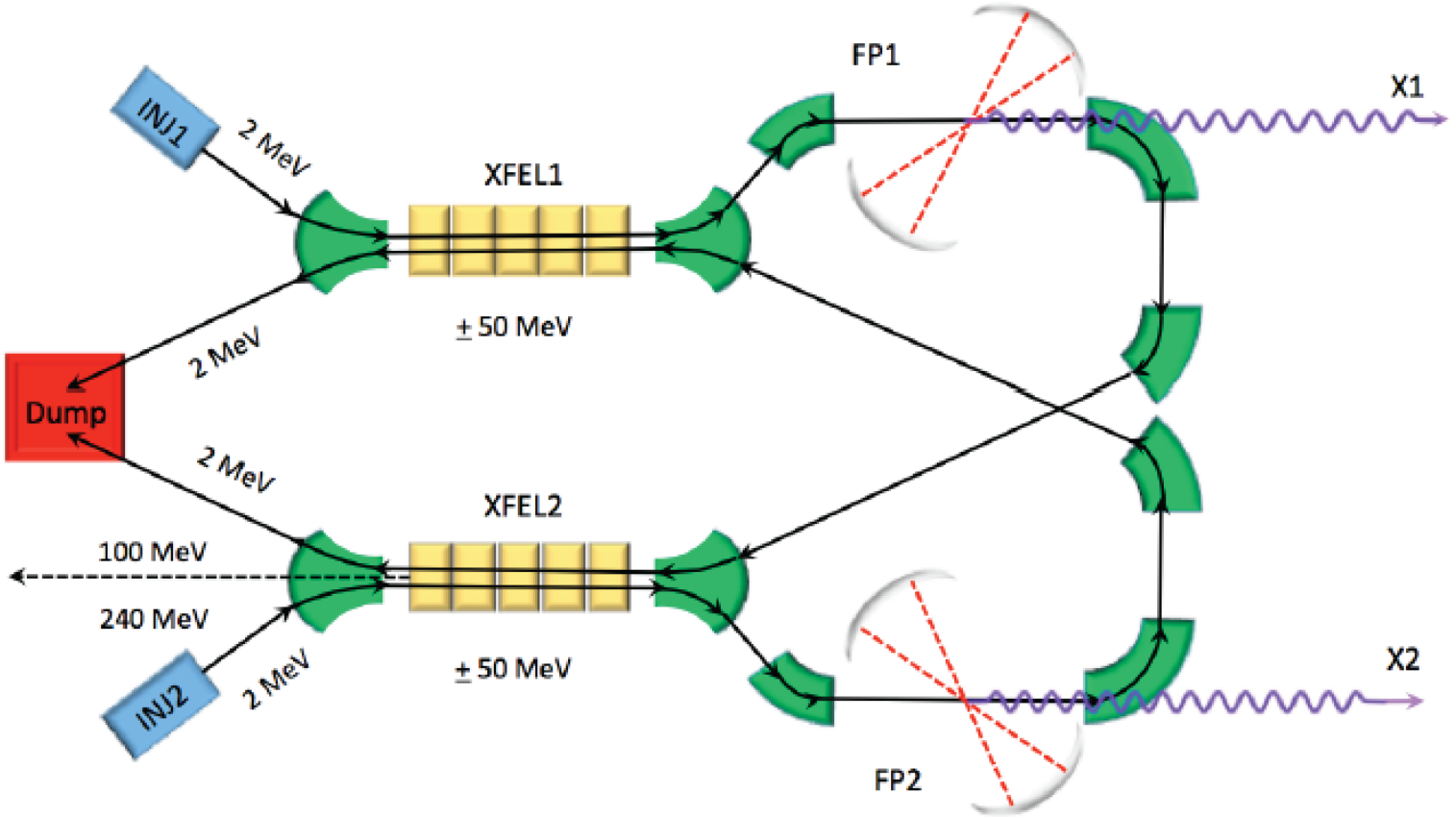

***Fig.6** – BriXS conceptual lay-out, based on a wrapped push-and-pull modified Tigner-Variola scheme.*

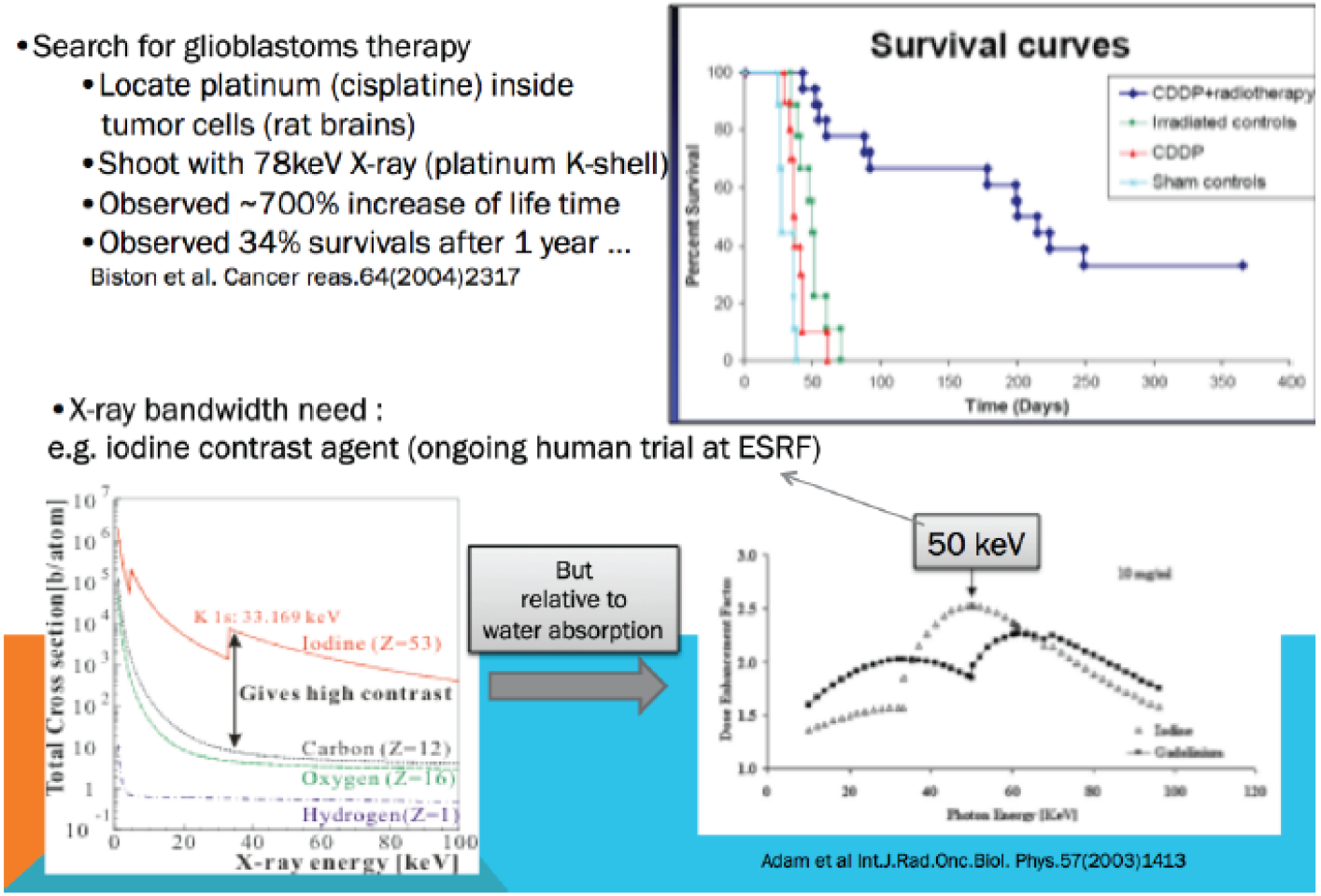

Fig.10 *– Radio-Therapy using mono-chromatic X-rays joined to cisplatine chemio-therapy for selected X-ray absorption inside tumoral cells.*

comprehensive overview recently presented at the PAHBB-2016 Workshop (see https://conferences.pa.ucla.edu/hbb/index.html) by A. Variola (INFN-LNF)

Compton sources for the observation of elastic photon-photon scattering events

D. Micieli[1], I. Drebot[2], A. Bacci[2], E. Milotti[3], V. Petrillo[4,2], M. Rossetti Conti[4,2], A. R. Rossi[2], E. Tassi[1] and L. Serafini[2]

[1] *Università degli Studi della Calabria, Arcavata di Rende (Cosenza), Italy*

[2] *INFN-Sezione di Milano, via Celoria 16, 20133, Milano, Italy*

[3] *Università di Trieste and INFN-Sezione di Trieste, Via Valerio 2, 34127 Trieste, Italy and*

[4] *Università degli Studi di Milano, via Celoria 16, 20133, Milano, Italy*

We present the design of a photon-photon collider based on conventional Compton gamma sources for the observation of elastic $\gamma\gamma$ scattering. Two symmetric electron beams, generated by photocathodes and accelerated in linacs, produce two primary gamma rays through Compton back scattering with two high energy lasers. The elastic photon-photon scattering is analyzed by start-to-end simulations from the photocathodes to the detector. A new Monte Carlo code has been developed *ad hoc* for the counting of the QED events. Realistic numbers of the secondary gamma yield, obtained by using the parameters of existing or approved Compton devices, a discussion of the feasibility of the experiment and of the nature of the background are presented.

I. INTRODUCTION

The scattering of light by light ($\gamma\gamma \longrightarrow \gamma\gamma$), a phenomenon which is precluded in Classical Electrodynamics *in vacuo*, is one of the most elusive effects foreseen by Quantum Electrodynamics (QED). Immediately after the appearence the Dirac's theory of the electrons it became clear that the existence of antiparticles opened the way to $\gamma\gamma$ scattering [1], that has never been observed so far, except as radiative correction to other processes. Apart from some early misdirected or technologically immature attempts, the first experimental proposals, dated back to the 1960's, all involved the use of low-energy photons, with energies that were mostly not higher than a few keV [2–4]. Low-energy photon-photon scattering can be described by the effective Euler-Heisenberg-Weisskopf Lagrangian [5], which allows the calculation of the propagation properties of light in vacuum, either in the presence of other real photons, or within the sea of virtual photons produced by external static fields. The measurement of photon-field scattering appears to be advantageous with high-field magnets, and, in this case, the phenomenon manifests itself as an effective birefringence of vacuum produced by the magnetic field [6–9]. The

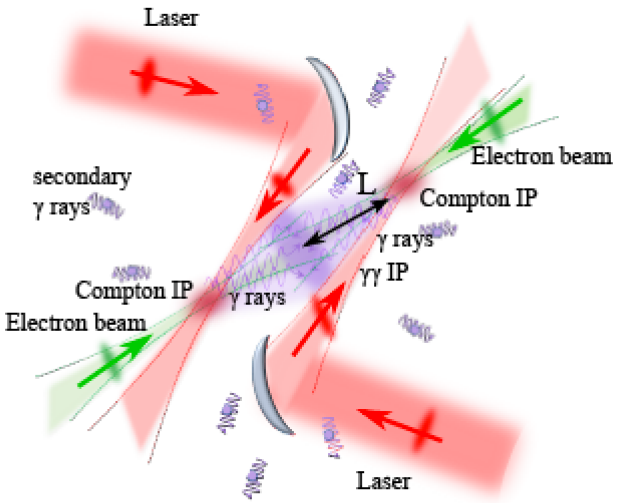

Figure 1: Scheme of the $\gamma\gamma$ interaction. Two lasers (in red) impinge on two electron beams (in green) in two interaction points Compton IP, generating primary gamma rays (in violet). The primary gamma rays interact in the $\gamma\gamma$ IP, generating secondary gammas.

submitted for publication

Low emittance pion beams generation from bright photons and relativistic protons

L. Serafini, C. Curatolo and V. Petrillo
INFN-Milan and Università degli Studi di Milano, via Celoria 16, 20133 Milano, Italy
(Dated: July 11th, 2015)

Present availability of high brilliance photon beams as those produced by X-ray Free Electron Lasers in combination with intense TeV proton beams typical of the Large Hadron Collider makes it possible to conceive the generation of pion beams via photo-production in a highly relativistic Lorentz boosted frame: the main advantage is the low emittance attainable and a TeV-class energy for the generated pions, that may be an interesting option for the production of low emittance muon and neutrino beams. We will describe the kinematics of the two classes of dominant events, i.e. the pion photo-production and the electron/positron pair production, neglecting other small cross-section possible events like Compton and muon pair production. Based on the phase space distributions of the pion and muon beams we will analyze the pion beam brightness achievable in three examples, based on advanced high efficiency high repetition rate FELs coupled to LHC or Future Circular Collider (FCC) proton beams, together with the study of a possible small scale demonstrator based on a Compton Source coupled to a Super Proton Synchrotron (SPS) proton beam.

I. INTRODUCTION

One of the main challenges of present muon collider design studies is the capture/cooling stage of muons after generation by intense GeV-class proton beams impinging on solid targets: this mechanism produces pions further decaying into muons and neutrinos. As extensively analyzed in Ref. [1, 2], the large emittance of the generated pion beams, which is mapped into the muon beam, is mainly given by the mm-size beam source at the target (i.e. the proton beam focal spot size) and by Coulomb scattering of protons and pions propagating through the target itself, inducing large transverse momenta which in

Their combined capability of producing ultra-high phase space density particle beams is the base of our strategy for generating low emittance pion, muon and neutrino beams, using collisions between two counter-propagating beams of highly relativistic protons and ultra-high intensity photons. The extremely high luminosity achievable by such a collider (10^{38} cm^{-2}s^{-1}) can compensate for the low efficiency of the pion photo-production which has a total cross section of $\simeq 220$ μbarn with 300 MeV photons, much smaller than GeV-proton based pion production ($\simeq 20$ mbarn).

There are two crucial aspects in such a collision scheme. The first is the much higher energy of the X-ray

Many Thanks to my Colleagues/Friends:

Vittoria Petrillo, Camilla Curatolo, Cristina Vaccarezza, Alberto Bacci, Andrea Rossi, Illya Drebot, Ezio Puppin, Alessandro Variola, Alex Murokh, Fabian Zomer, for many helpful and stimulating discussions and for providing material for this talk


INFN

A MeV-class Photon-Photon Scattering Machine based on twin Photo-Injectors and Compton Sources

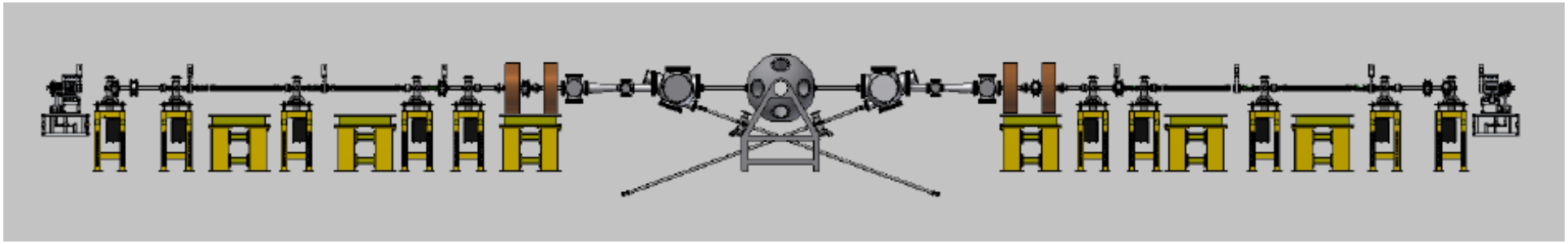

- **γ-ray beams similar to those generated by Compton Sources for Nuclear Physics/Photonics**
- **issue with photon beam diffraction at low energy!**
- **Best option: twin system of high gradient *X-band* 200 *MeV* photo-injectors with *J-class ps* lasers (ELI-NP-GBS)**

$$\sigma \approx 0.13\left(\frac{\hbar\omega}{m_e c^2}\right)^6 \mu\text{barn}$$

peak cross-section, $\approx 1.6\ \mu$barn
at $\hbar\omega \approx 1.5 m_e c^2$

$$\sigma \approx 20\left(\frac{m_e c^2}{\hbar\omega}\right)^2 \mu\text{barn}$$

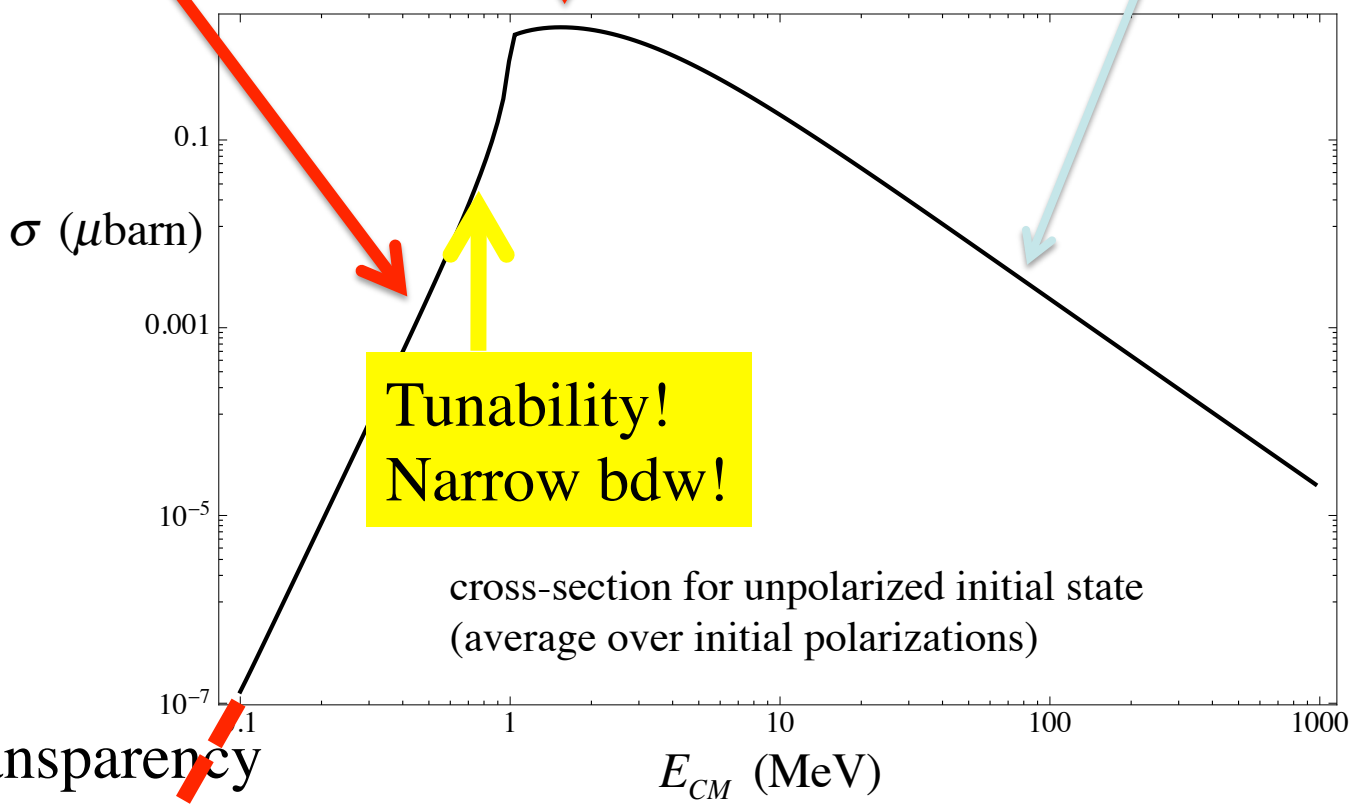

Tunability!
Narrow bdw!

optical transparency
of the Universe

courtesy E. Milotti

The cosmological constant problem is related to the zero-point energy, i.e., to the fluctuations of quantum vacuum, and therefore also to the renormalization procedure in QFT.

Photon-photon scattering directly probes the fluctuations of quantum vacuum.

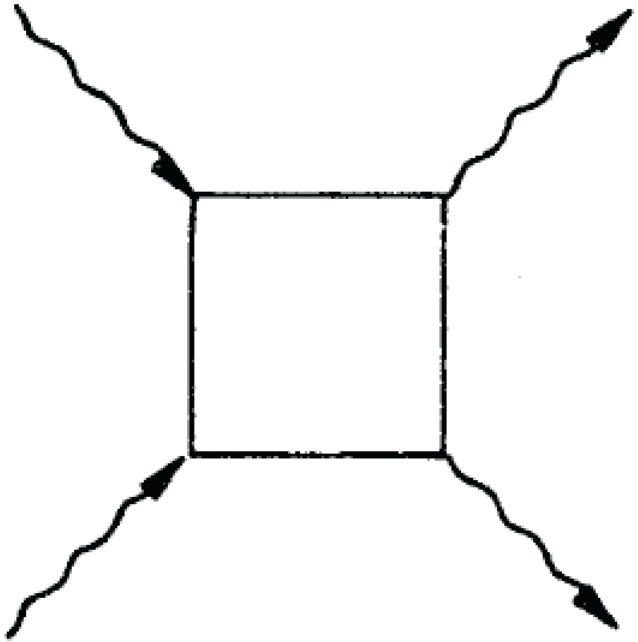

This is the first nonvanishing diagram: there are no tree-level diagrams

All the involved photons are real particles

courtesy E. Milotti

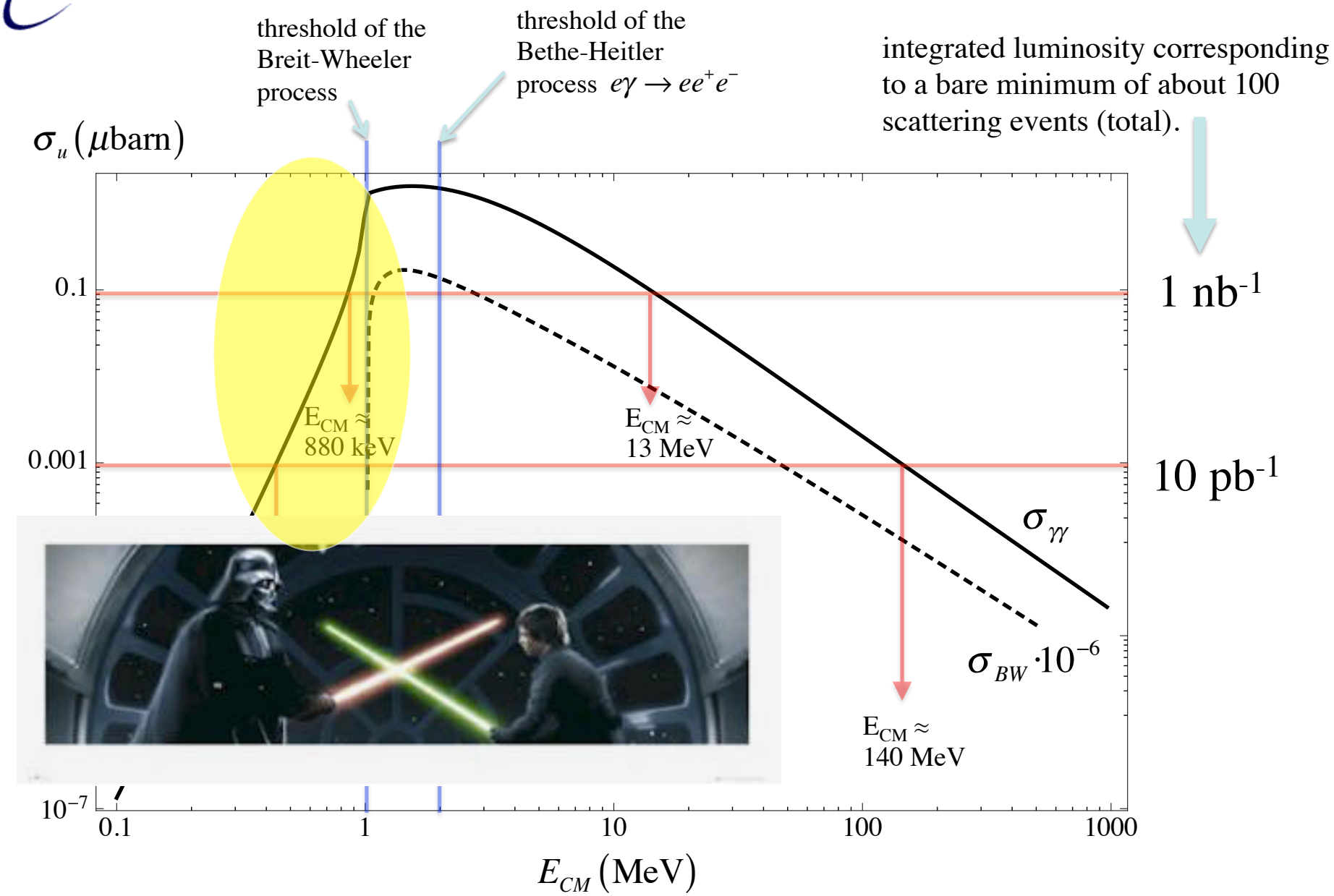

courtesy E. Milotti

We evaluated the event production rate of several schemes for photon-photon scattering, based on *ultra-intense lasers*, *bremsstralhung machines*, *Nuclear Photonics gamma-ray machines*, etc, in all possible combinations: collision of 0.5 MeV photon beams is the only viable solution to achieve 1 nbarn^{-1} in a reasonable measurement time.

1)Colliding 2 ELI-NP 10 PW lasers under construction (ready in 2018), *hν=1.2 eV*, *f=1/60 Hz*, we achieve (E_{cm}=3 eV): $L_{SC}=6.10^{45}$, cross section= 6.10^{-64}, events/sec=10^{-19}
2)Colliding 1 ELI-NP 10 PW laser with the 20 MeV gamma-ray beam of ELI-NP-GBS we achieve (E_{cm}=5.5 keV): $L_{SC}=6.10^{33}$, cross section=10^{-41}, events/sec = 10^{-8}

3)Colliding a high power Bremsstralhung 50 keV X-ray beam (unpolarized, 100 kW on a mm spot size) with ELI-NP-GBS 20 MeV gamma-ray beam (E_{cm}=2 MeV) we achieve: $L_{SC}=6.10^{22}$, cross section=1 μbarn, events/s = 10^{-8}

4) **Colliding 2 gamma-ray 0.5 MeV beams, carrying 10^9 photons per pulse at 100 Hz rep rate, with focal spot size at the collision point of about 2 μm, we achieve: $L_{SC}=2.10^{26}$, cross section = 1 $\mu barn$, events/s=2.10^{-4}, events/day=18, 1 $nanobarn^{-1}$ accumulated after 3 months of machine running.**


INFN

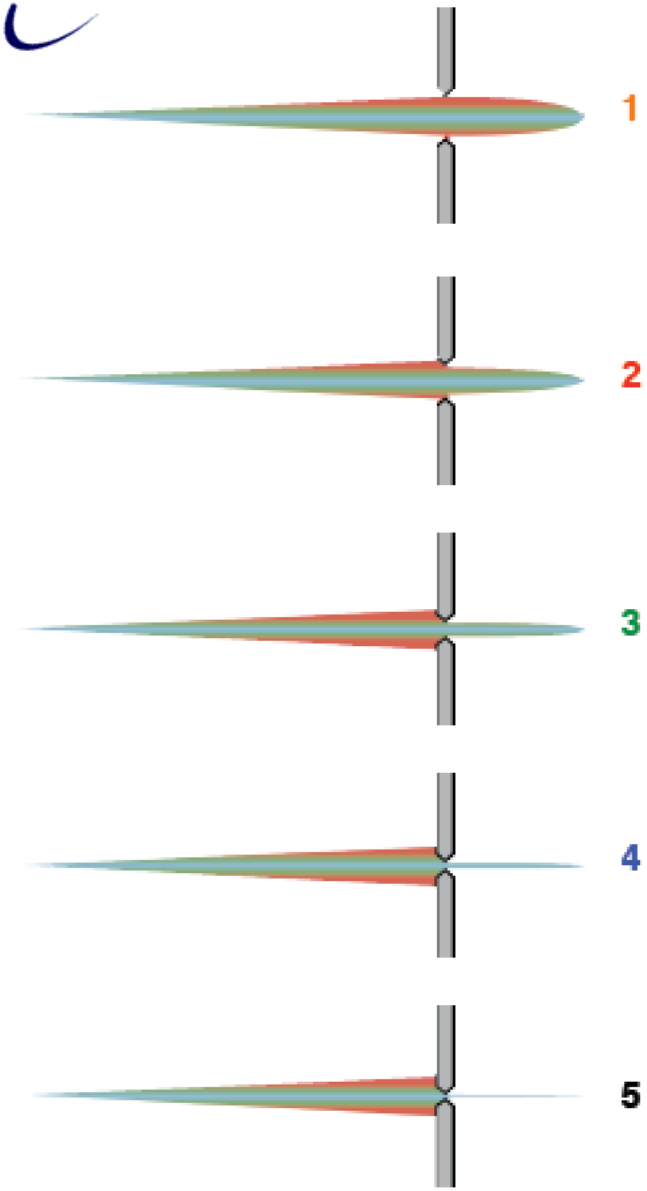

$$\Delta\theta \approx \frac{1}{\gamma} \; ; \; \Delta\nu_\gamma \approx 50\%$$

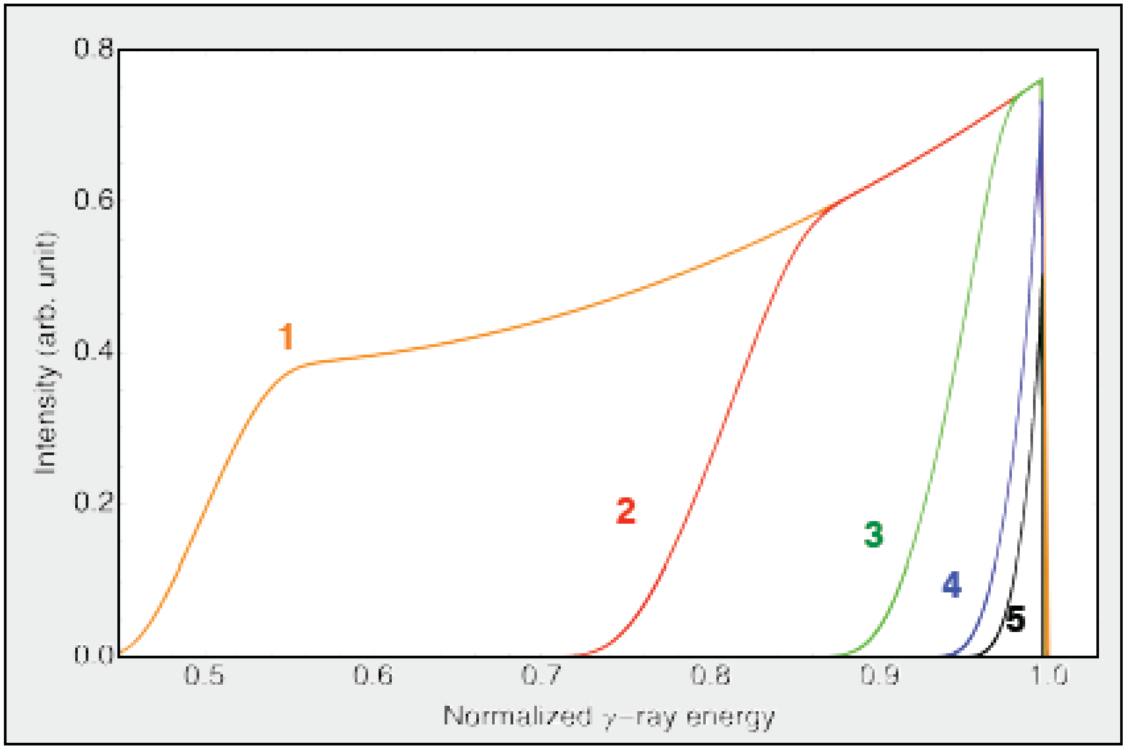

$$\Delta\theta \approx \sigma_{x'} = \frac{\varepsilon_n}{\gamma\sigma_x} \; ; \; \Delta\nu_\gamma \approx \left(\frac{\varepsilon_n^2}{\sigma_x^2}\right)$$

Courtesy C. Barty - LLNL

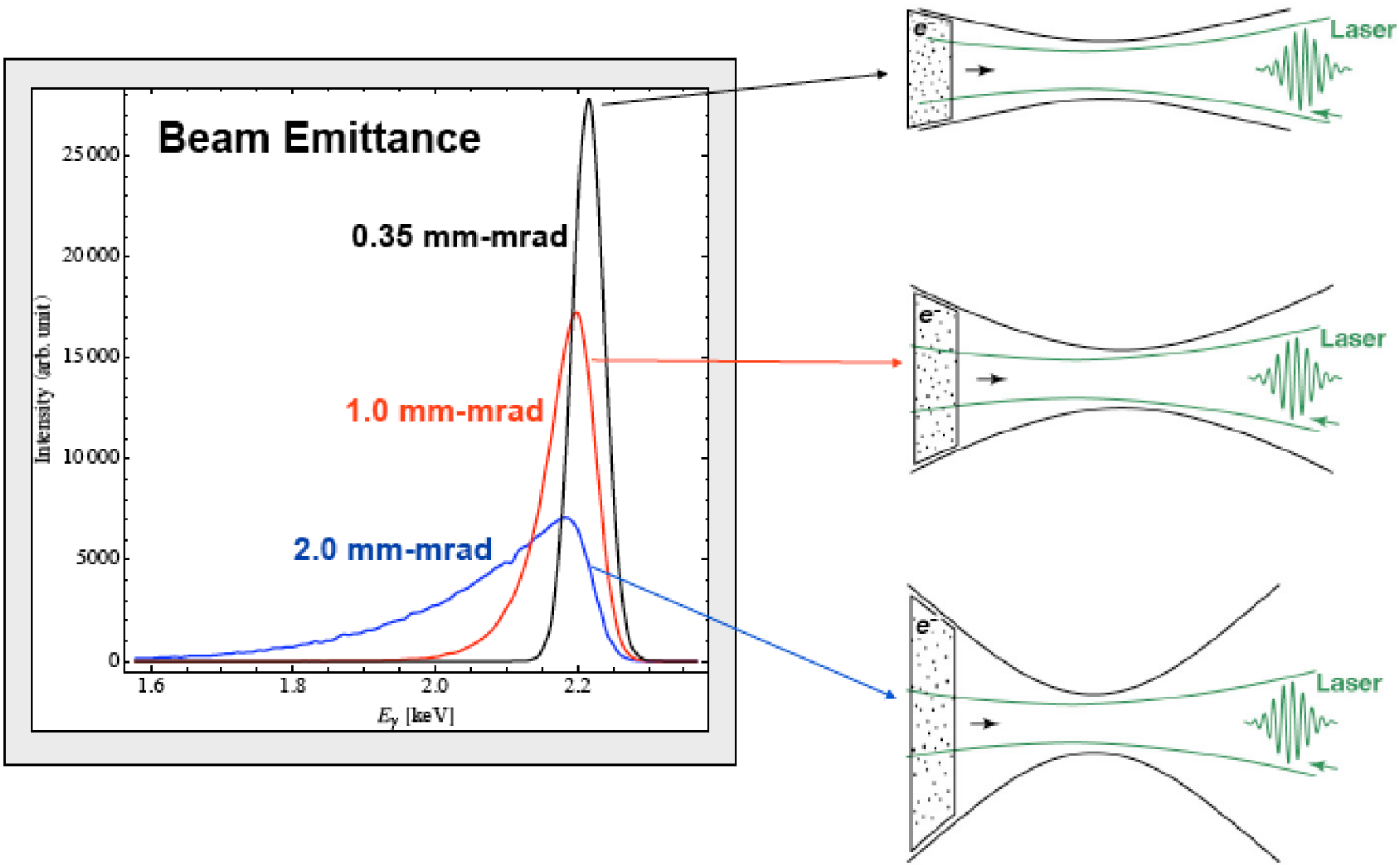

Courtesy C. Barty - LLNL

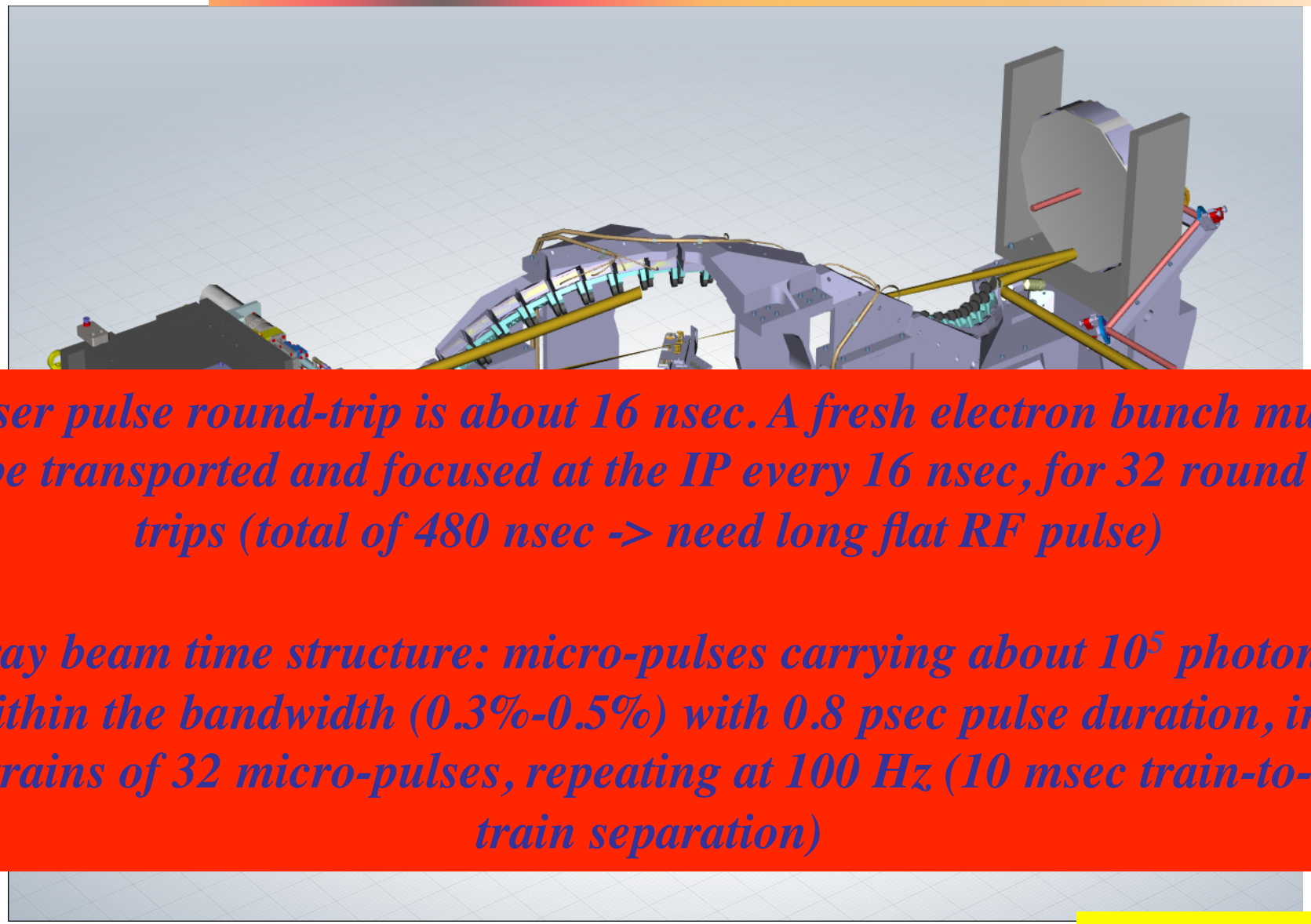

Laser pulse round-trip is about 16 nsec. A fresh electron bunch must be transported and focused at the IP every 16 nsec, for 32 round trips (total of 480 nsec -> need long flat RF pulse)

γ-ray beam time structure: micro-pulses carrying about 10^5 photons within the bandwidth (0.3%-0.5%) with 0.8 psec pulse duration, in trains of 32 micro-pulses, repeating at 100 Hz (10 msec train-to-train separation)

courtesy K. Cassou

Full Control of Polarization and switch from Linear (H, V) to Circular (up to 98% polarization)

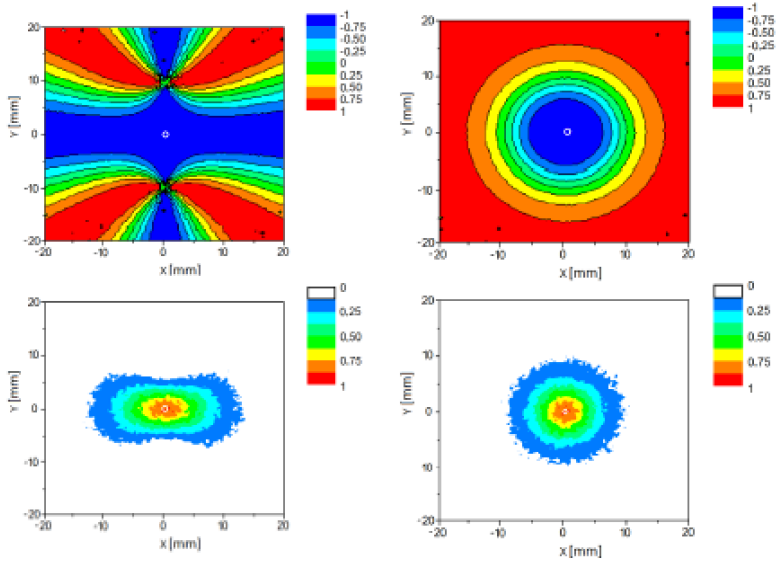

Figure 6: Stokes parameter S_3 and S_2 (top) and photon distribution (bottom) for linear (left) and circular (right) polarization, photon energy $10\,MeV$ at $z = 10\,m$. The white circle delimits the region of the collimated photons.

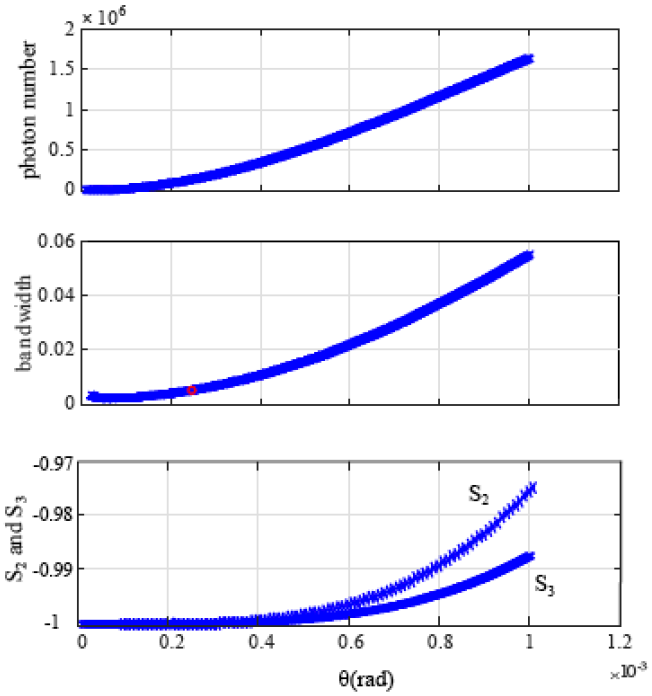

Figure 7: Photon number, relative bandwidth and Stokes parameters for gamma rays at 2 MeV, linear and circular laser polarizations.

- **Final Formula including acceptance angle and electron recoil is:**

$$P_\gamma \cong P_{las}\left(1-\frac{3}{2}\Delta^2\right)\left(1-\frac{\gamma^4\theta^4}{3}\right) \quad \Rightarrow \quad P_{\gamma-ELI-NP-GBS} > 0.995 P_{las-ELI-NP-GBS}$$

very favourable scaling with bandwidth

dominated by recoil: gift of quasi-Thomson elastic regime (no polarized electrons needed!)

$$\nu_\gamma = \nu \frac{4\gamma^2}{1+\gamma^2\theta^2+a_0^2/2}(1-\Delta)$$

$$\Delta = \frac{4\gamma\, h\nu/mc^2}{1+2\gamma\, h\nu/mc^2} \qquad 0.005 < \Delta_{ELI-NP-GBS} < 0.025$$

Formula valid also for diagonal and circular polarizations

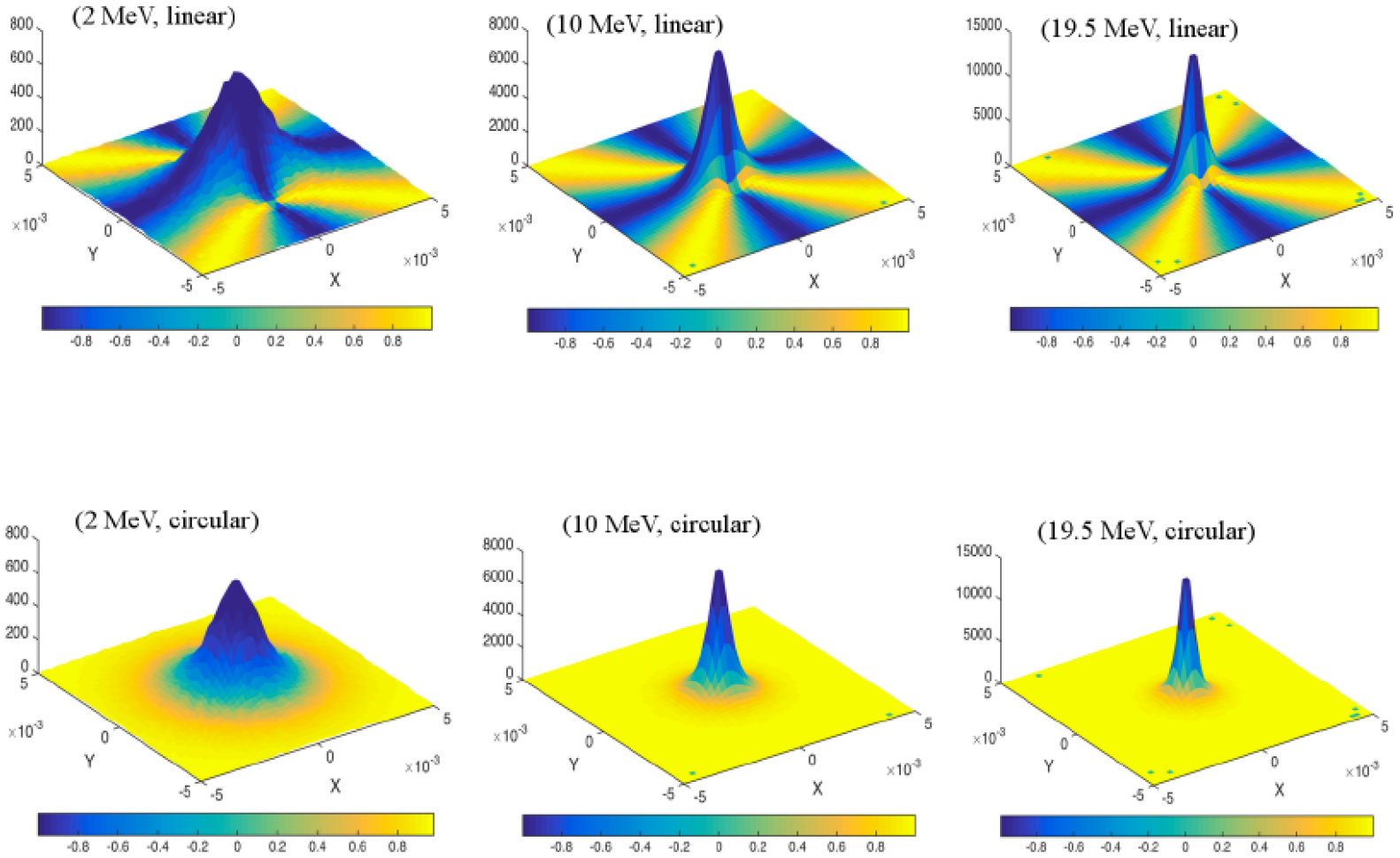

Figure 9: Intensity-polarization graphs for photons at 2, 10 and 19.5 MeV, with linear and circular laser polarization.

Polarization of X-gamma radiation produced by a Thomson/Compton inverse scattering

V.Petrillo[1,2], A. Bacci[2], C. Curatolo[1,2], I. Drebot[2], A. Girobono[3], C. Maroli[1], A.R. Rossi[2], L. Serafini[2], P. Tomassini[1], C. Vaccarezza[3], A. Variola[3]

[1] *Università degli Studi di Milano, via Celoria 16, 20133 Milano, Italy*

[2] *INFN-Sezione di Milano, via Celoria 16, 20133 Milano, Italy and*

[3] *INFN Laboratori Nazionali di Frascati, Via E. Fermi 44, 00044 Frascati, Roma, Italy*

I. INTRODUCTION

The development of X and gamma-ray sources with large spectral flux and high tunability opens the way to applications at the frontier of science [1, 2], allowing to deepen the fundamental knowledge and understanding of the properties of materials and living systems by probing the matter on microscopic-to-atomic and nuclear scales in space and time [2]. Thomson [3–10] and Compton sources [11, 12] are among the most performing devices in producing radiation with short wavelength, high power, ultra-short time duration, large transverse coherence and tunability. The characteristics of contained dimensions of the set-up and limited costs of construction and maintenance of the sources. The sources operated on the second beam of the photoinjector SPARC [27]. Since the main application of this source is in the field of mammographic images, the electron beam is driven at a final electron energy E_e of about $30\,MeV$, producing Doppler blue shifted hard x-rays with energy $E_p \approx 4E_0\gamma^2$ ($E_0 = 1.55eV$ is the photon energy of FLAME and the electron Lorentz factor $\gamma = 60$) of about $20\,keV$. The e-beam operations can be however easily extended in energy up to $180\,MeV$, with the emission of radiation covering the range between 20 and $500\,keV$.

As regards existing gamma Compton sources, the facility Higs [11], which represents the state of the art up to now, relies on the emission produced by the scattering of an electron beam and its FEL radiation. It can produce gamma rays between 2 and $100\,MeV$ with linear and circular polarizations. The total gamma ray intensities are

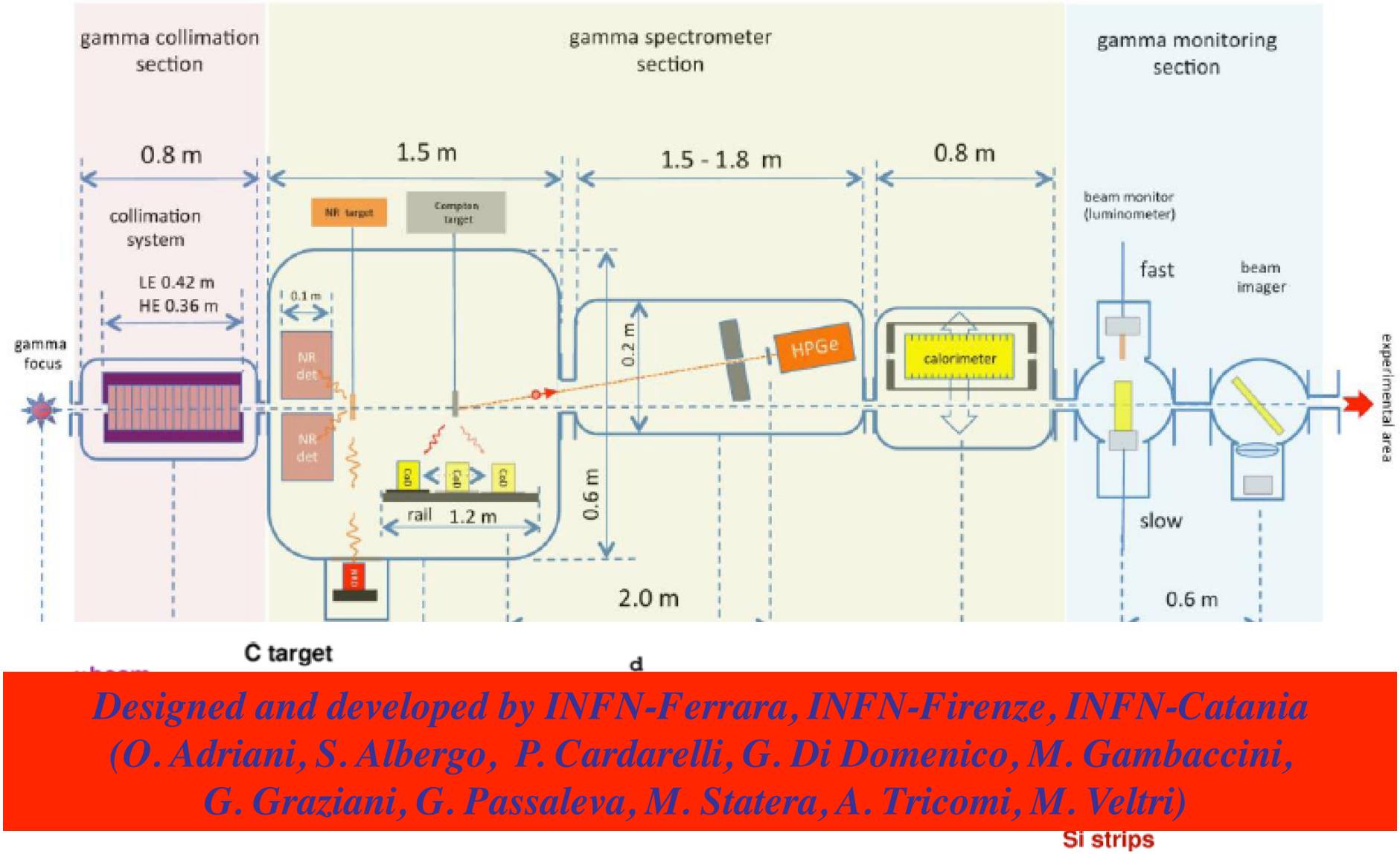

Fig. 193. **Schematic view of the Compton spectrometer. The HPGe and Si strips detectors are used to measure the scattered electron at small angles. The scattered photon is measured by a movable device, to be placed according to the beam energy.**


INFN

Matching Laser Pulse Length and Focus Size

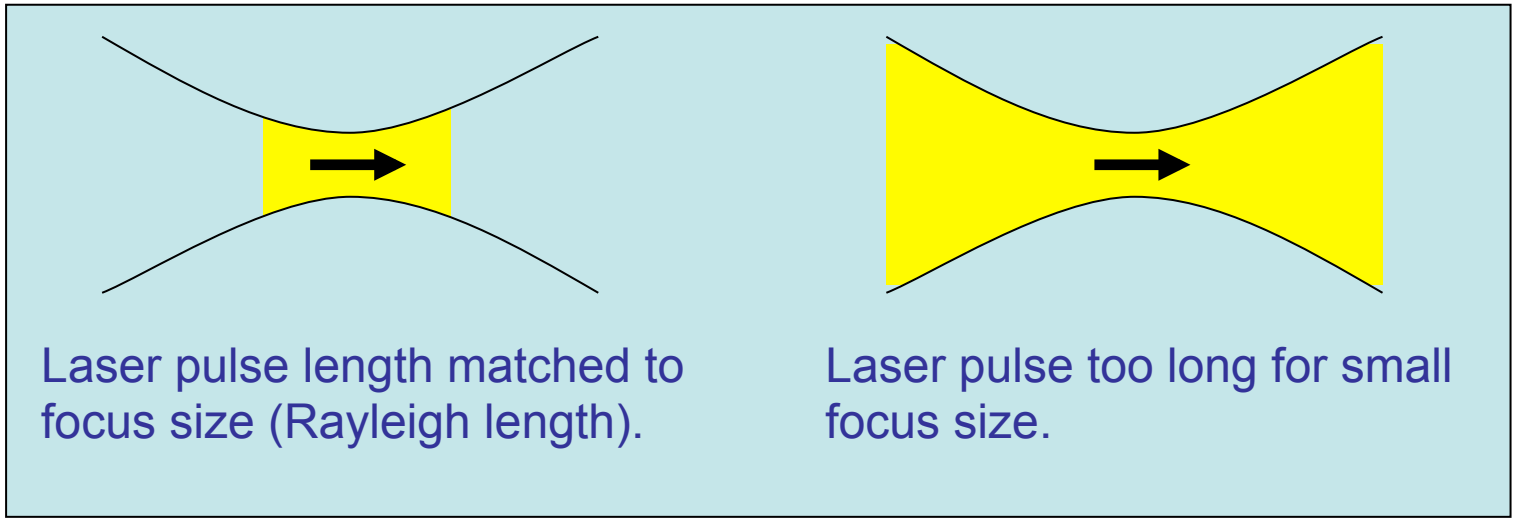

Laser pulse length matched to focus size (Rayleigh length).

Laser pulse too long for small focus size.

Laser pulse must be short compared to Rayleigh length so that whole pulse is focused simultaneously.

Laser may be shorter than Rayleigh length, but less than 0.5 ps is not practical, and could lead to non-linear effects not included in our spectral model.

courtesy D. Moncton

Electron Bunch Length Matched to Rayleigh Length

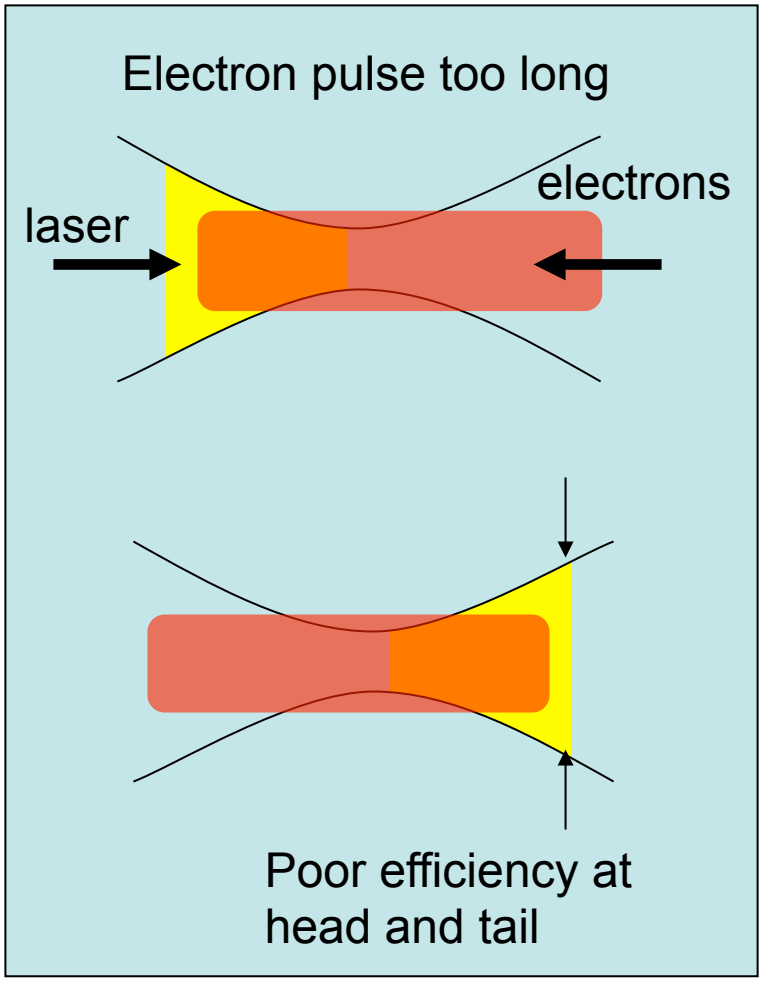

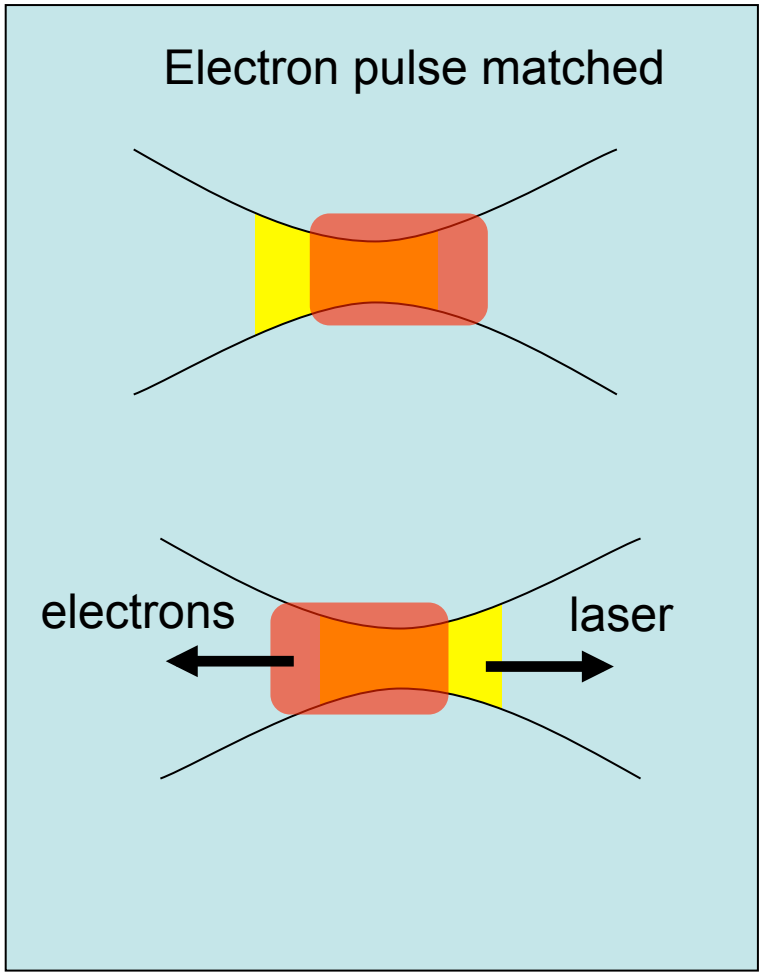

courtesy D. Moncton

The peak brilliance of an optimized MEGa-ray source is both revolutionary and transformative

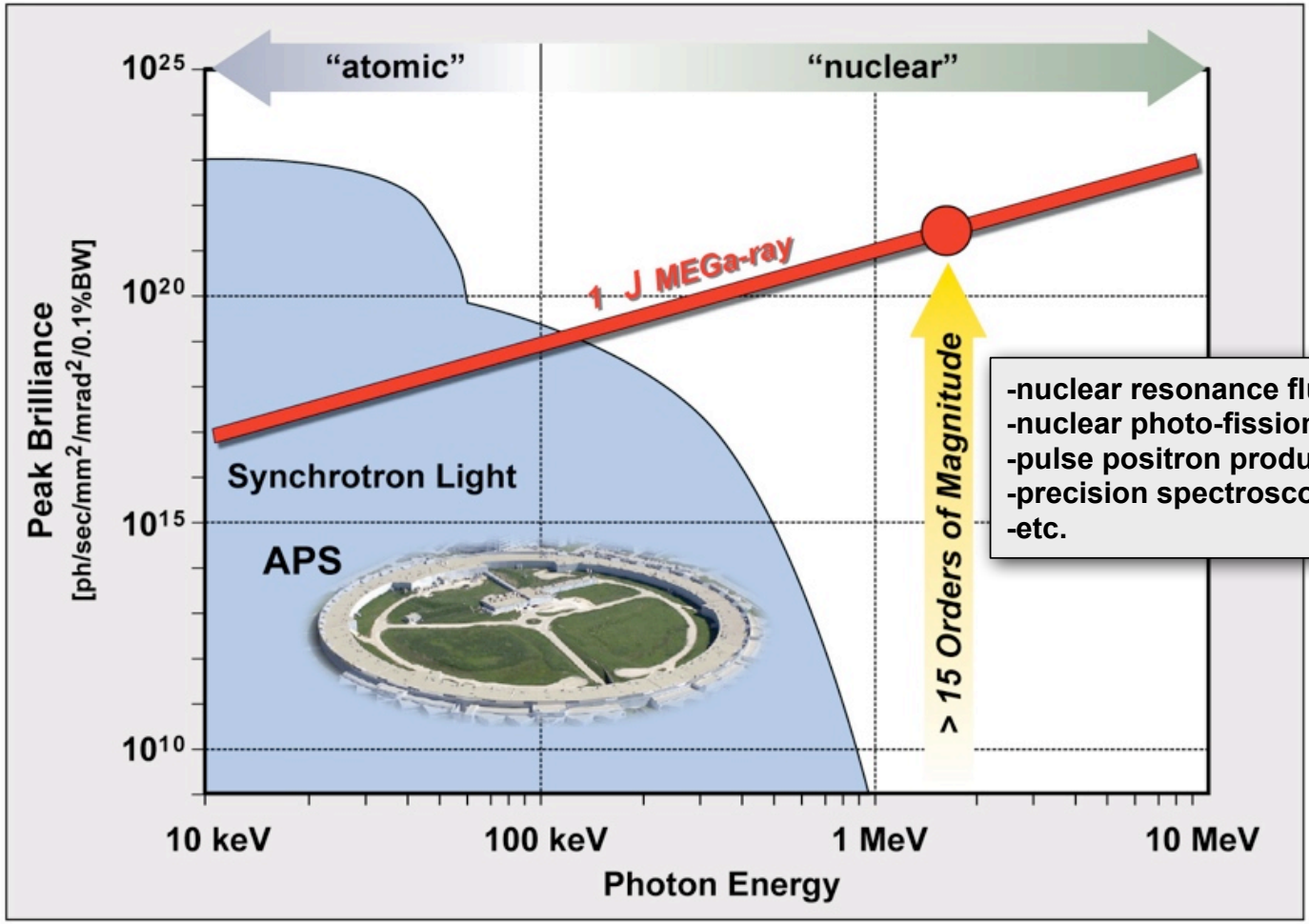

Courtesy C. Barty - LLNL

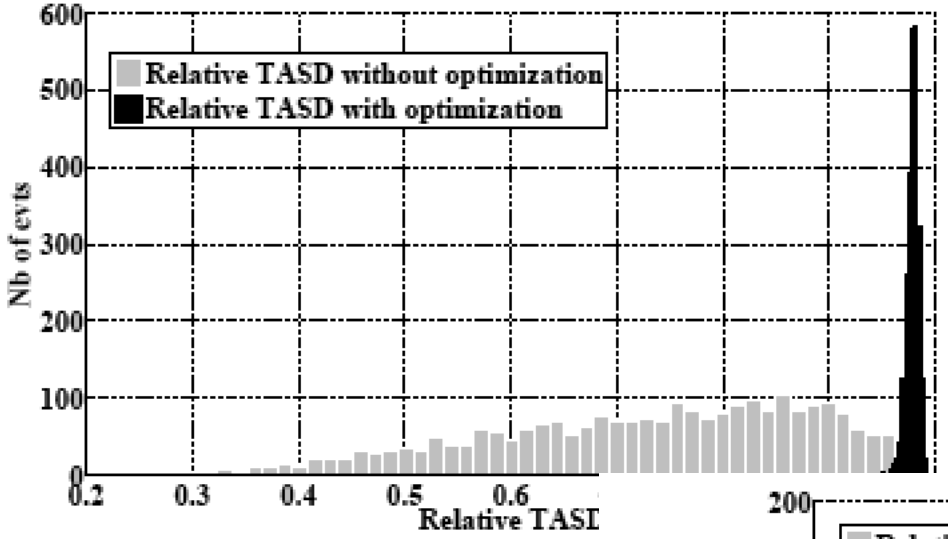

FIG. 16. Relative
$\xi_{2500}(3.8\ \mu\text{rad}, 20\ \mu\text{rad}, 20\ \mu\text{m})$ sim
The histogram in grey show the
the alignment procedure (SIMPLI
black histogram show the relative
optimization.

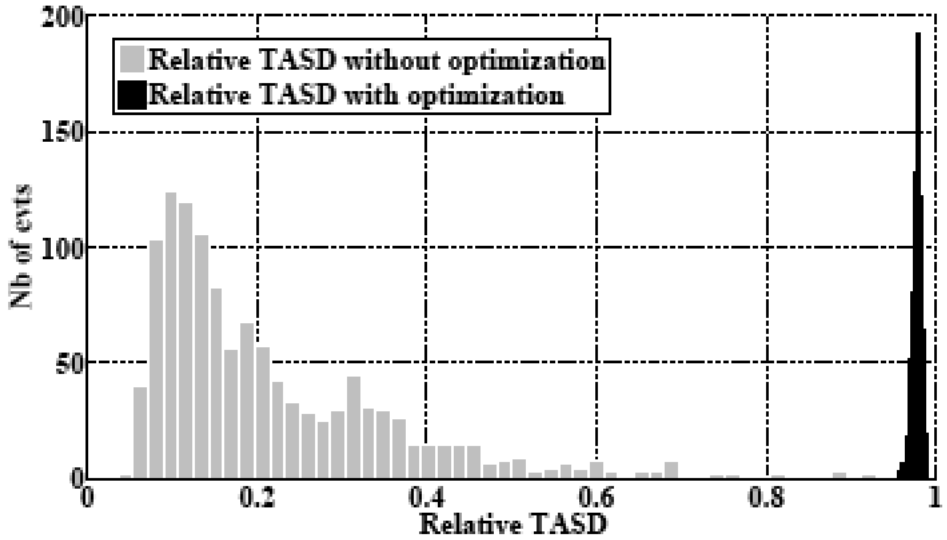

FIG. 17. Relative TASD results for $\xi_{1200}(3.8\ \mu\text{rad}, 100\ \mu\text{rad}, 100\ \mu\text{m})$ simulated and optimized. The histogram in grey show the relative TASD before the alignment procedure (SIMPLEX algorithm) and the black histogram show the relative TASD reached after the optimization.


INFN

Photon-photon scattering is a probe into the structure of the vacuum of QFT

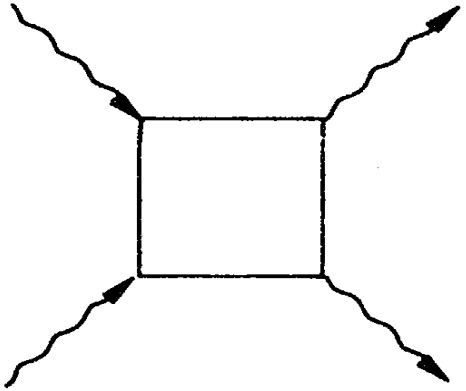

The QFT vacuum holds the key to the understanding of renormalization in QFTs.

Different vacua are possible, and the observation of photon-photon scattering would provide important clues on the actual structure of the QFT vacuum.

Photon-photon scattering at low energy is very difficult to observe, the total cross-section is extremely small. The total unpolarized scattering cross section predicted by QED is

$$\sigma_{\gamma\gamma}^{(QED)} = \frac{973\mu_0^2(\hbar\omega)^6}{20\pi\hbar^4c^4}A_e^2$$

Where

$$A_e = \frac{2\alpha^2\lambda\!\!\!^{-3}_e}{45\mu_0 m_e c^2} \approx 1.32\ 10^{-24}\mathrm{T}^{-2}$$

This evaluates to a very small number with low energy (≈ 1 eV) photons, however it increases as the sixth power of photon energy.

SLAC E-144 experiment: first sign of positron production in light-by-light scattering

PHYSICAL REVIEW D, VOLUME 60, 092004

Studies of nonlinear QED in collisions of 46.6 GeV electrons with intense laser pulses

C. Bamber,* S. J. Boege,† T. Koffas, T. Kotseroglou,‡ A. C. Melissinos, D. D. Meyerhofer,§ D. A. Reis, and W. Ragg‖
Department of Physics and Astronomy, University of Rochester, Rochester, New York 14627

C. Bula,¶ K. T. McDonald, and E. J. Prebys
Joseph Henry Laboratories, Princeton University, Princeton, New Jersey 08544

D. L. Burke, R. C. Field, G. Horton-Smith,** J. E. Spencer, and D. Walz
Stanford Linear Accelerator Center, Stanford University, Stanford, California 94309

S. C. Berridge, W. M. Bugg, K. Shmakov,†† and A. W. Weidemann
Department of Physics and Astronomy, University of Tennessee, Knoxville, Tennessee 37996

(Received 1 February 1999; published 8 October 1999)

- Recently shown that, on average, $n = 6.44$ laser photons were absorbed.

Burke et al., *PRL* **79,** 1626 (1997)
Hu & Müller, *PRL* **107,** 090402 (2010)

Courtesy Oliver Pike

Multiphoton Breit-Wheeler scattering was observed at SLAC. However, as clearly stated also in the paper, "The multiphoton Breit-Wheeler reaction becomes accessible for n > 3 laser photons of wavelength 527 nm colliding with a 29.2 GeV photon".

Indeed, the straghtforward two-photon Breit-Wheeler reaction has never been observed. The difference may appear minor, however it isn't. Multi photon scattering has a considerably more complex kinematics, and the dynamical calculation clearly requires more than one internal propagator in the Feynman diagram.

But more than that, Breit-Wheeler scattering — be it multi photon or not — is described by a simple tree-level diagram at the lowest perturbative order, while photon+photon —> photon+photon, needs a fermion loop at the lowest level, and thus is a true probe of the quantal nature of field theory.

Edoardo Milotti - INFN-Trieste

Unpolarized and (circularly) polarized initial photons.

The scattering of polarized photons yields additional information

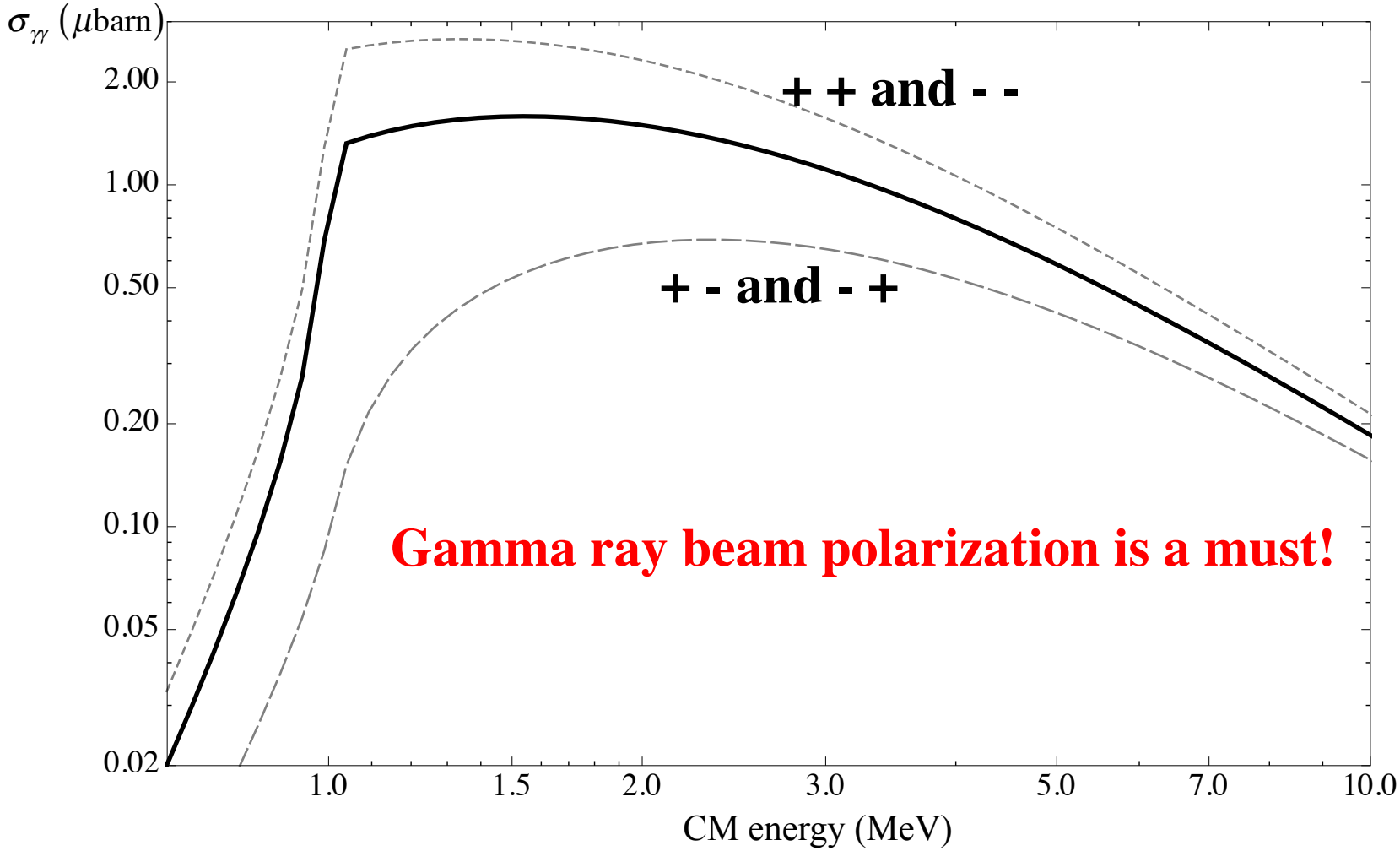

For $\hbar\omega \leq 0.7 m_e c^2$, the differential photon-photon scattering cross-section is

$$\frac{d\sigma}{d\Omega} = \frac{139\alpha^4}{(180\pi)^2}\frac{\omega^6}{m^8}\left(3+\cos^2\theta\right)^2$$

This cross-section is derived from a genuine non-linear QED effect (loop) and its value is critically dependent on the regularization procedure.

The importance of regularization has recently been emphasized by the a couple of wrong preprints, that claimed that the photon-photon cross section is actually

$$\frac{d\sigma_{\mathrm{FK}}}{d\Omega} = \frac{\alpha^4}{(12\pi)^2\omega^2}\left(3+2\cos^2\theta+\cos^4\theta\right)$$

(see N. Kanda, arXiv:1106.0592, and T. Fujita and N. Kanda, arXiv:1106.0465, and the refutation by Y. Liang and A. Czarnecki, arXiv:1111.6126)

Differential cross-section at ECM = 1.6 MeV (peak)

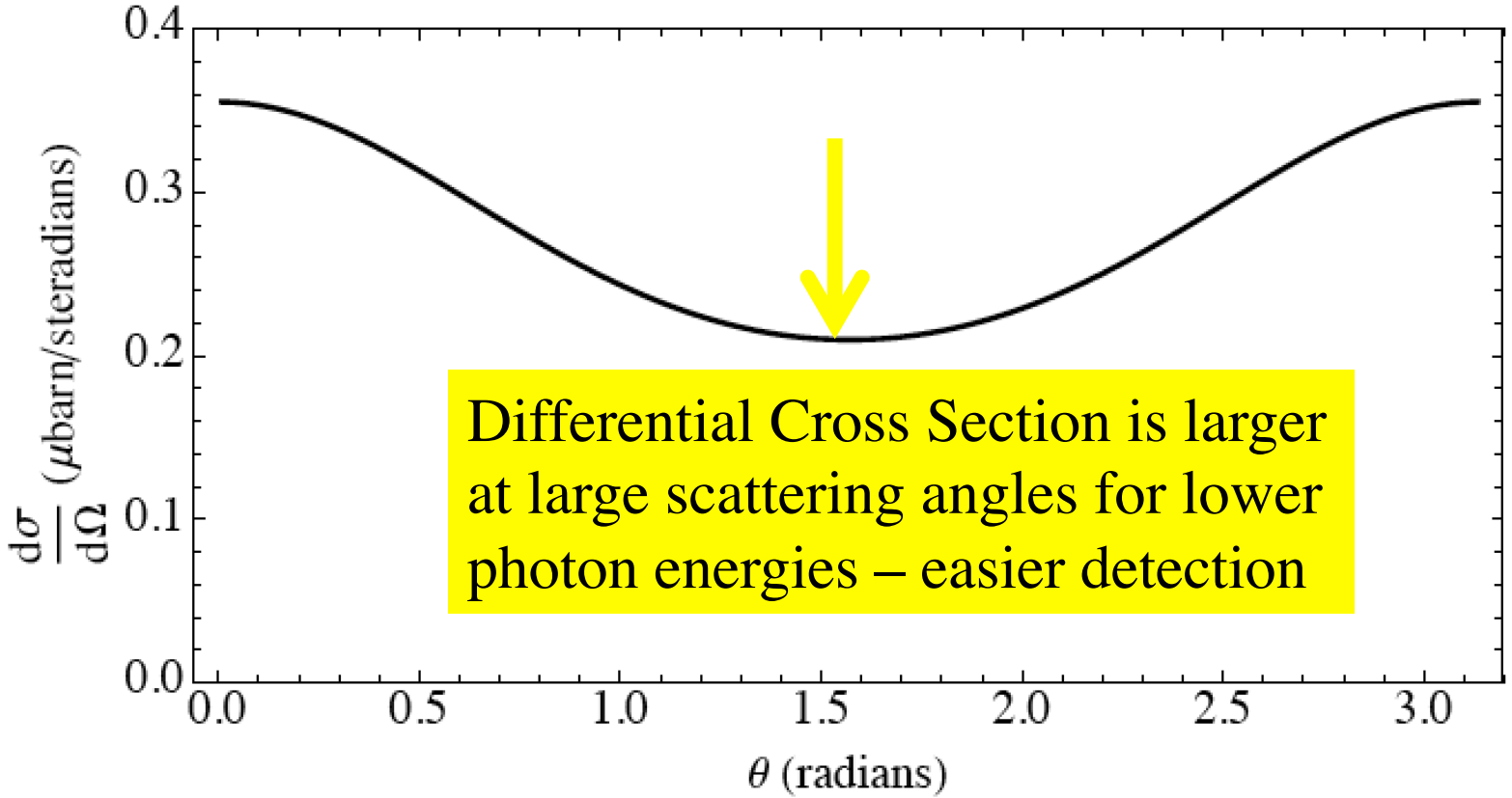

Differential Cross Section is larger at large scattering angles for lower photon energies – easier detection

$$\frac{d\sigma}{d\Omega} \approx \frac{139}{(180\pi)^2}\alpha^2 r_0^2 \left(\frac{\hbar\omega}{mc^2}\right)^6 \left(3+\cos^2\theta\right)^2$$

Differential cross-section at ECM = 10 MeV

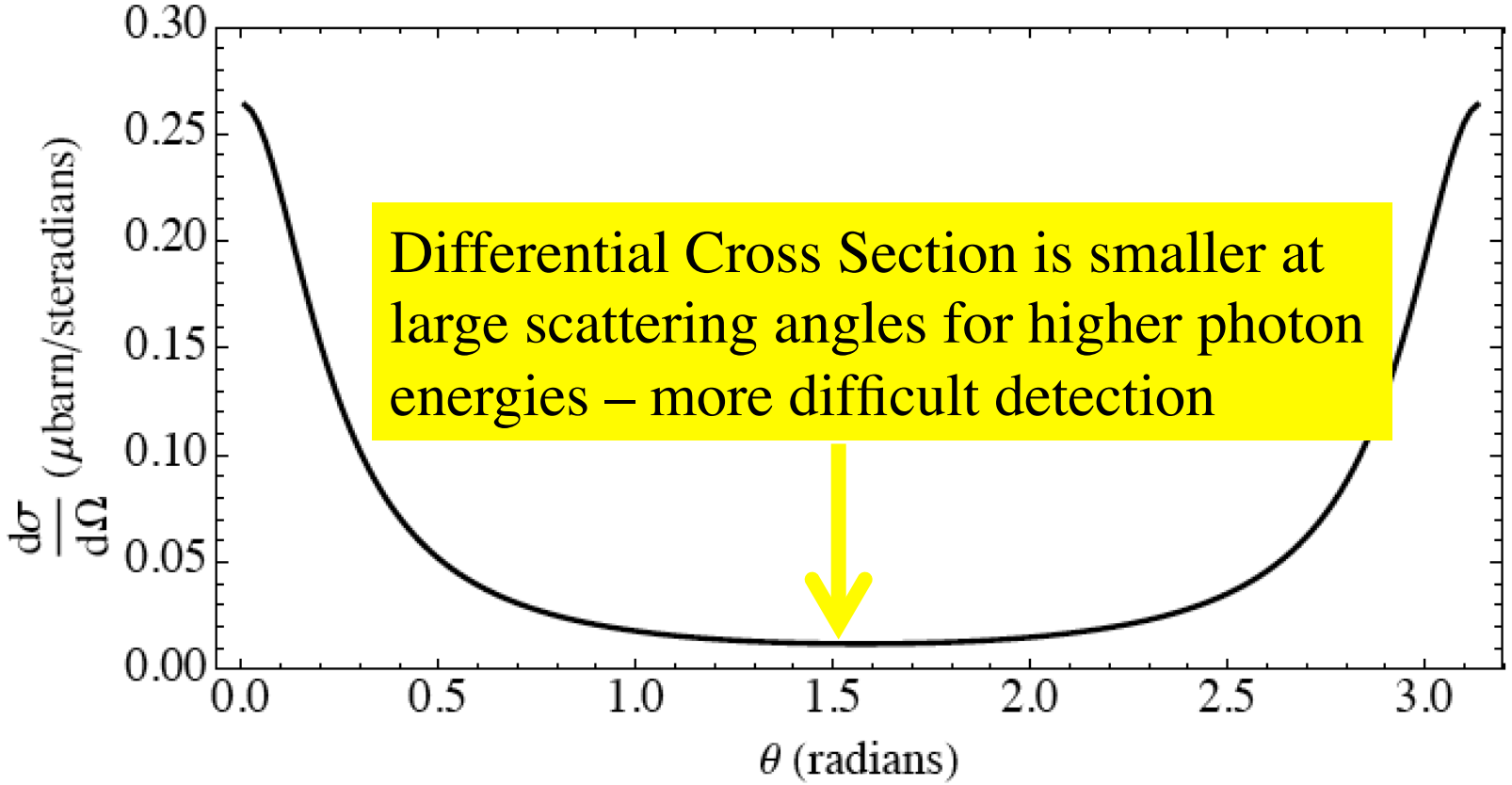

Differential Cross Section is smaller at large scattering angles for higher photon energies – more difficult detection

$$\left.\frac{d\sigma}{d\Omega}\right|_{\theta=0} \approx \frac{\alpha^2}{\pi^2} r_0^2 \left(\frac{\hbar\omega}{mc^2}\right)^2 \left(\ln\frac{\hbar\omega}{mc^2}\right)^4 \qquad \left.\frac{d\sigma}{d\Omega}\right|_{\theta=\pi/2} \approx \frac{\alpha^2}{\pi^2} r_0^2 \left(\frac{\hbar\omega}{mc^2}\right)^2$$

Recent references on low-energy light-magnetic field scattering (photon-photon scattering between real infrared photons and virtual magnetic field photons)

•F. Della Valle, E. Milotti, A. Ejlli, G. Messineo, L. Piemontese, G. Zavattini, U. Gastaldi, R. Pengo, G. Ruoso: "First results from the new PVLAS apparatus: A new limit on vacuum magnetic birefringence", accepted for publication in Physical Review D

•F. Della Valle, U. Gastaldi, G. Messineo, E. Milotti, R. Pengo, L. Piemontese, G. Ruoso, G. Zavattini: "Measurements of vacuum magnetic birefringence using permanent dipole magnets: the PVLAS experiment", New J. Phys. 15 (2013) 053026

Recent references on possible photon-photon scattering schemes

•A. Torre, G. Dattoli, I. Spassovsky, V. Surrenti, M. Ferrario, and E. Milotti: "A double FEL oscillator for photon-photon collisions", Journal of the Optical Society of America B 30 (2013) 2906-2914

•E. Milotti, F. Della Valle, G. Zavattini, G. Messineo, U. Gastaldi, R. Pengo, G. Ruoso, D. Babusci, C .Curceanu, M. Iliescu, C. Milardi: "Exploring quantum vacuum with low-energy photons", Int. J. of Quantum Information 10 (2012) 1241002

Historical reference on photon-photon scattering opportunities

•Paul L. Csonka, “Are photon-photon scattering experiments feasible?”, Phys. Lett. 24B (1967) 625

a) 200 MeV/m peak cathode field of X-Band SLAC RF Photo-Injector (recently proven)

b) 100 MeV/m SLAC (Tantawi/Dolgashev/Spataro) new X-band RF cavities (recently demonstrated)

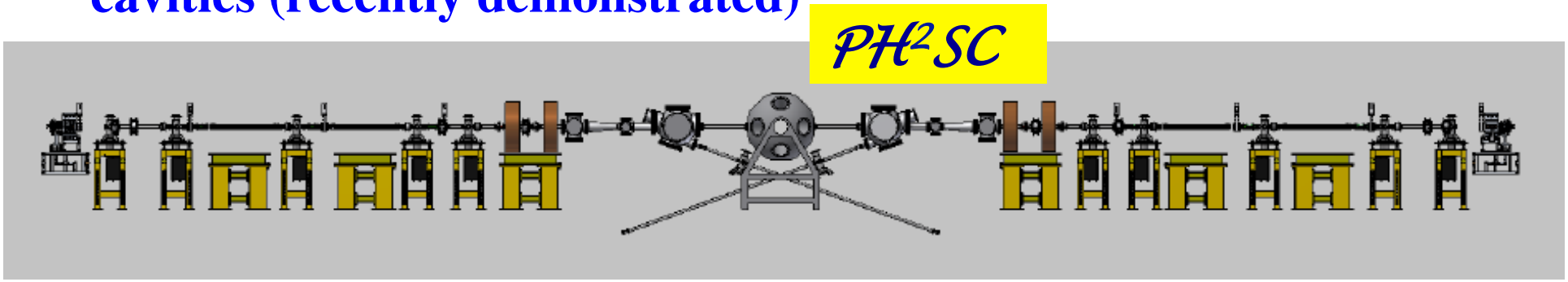

1) Electron beam operation in single bunch – focusability to 3 micron spot size at Compton Interaction Point
2) Pointing stability at 2 Compton Sources
3) Deflection of counter-propagating electron bunches to avoid e-/e- interactions

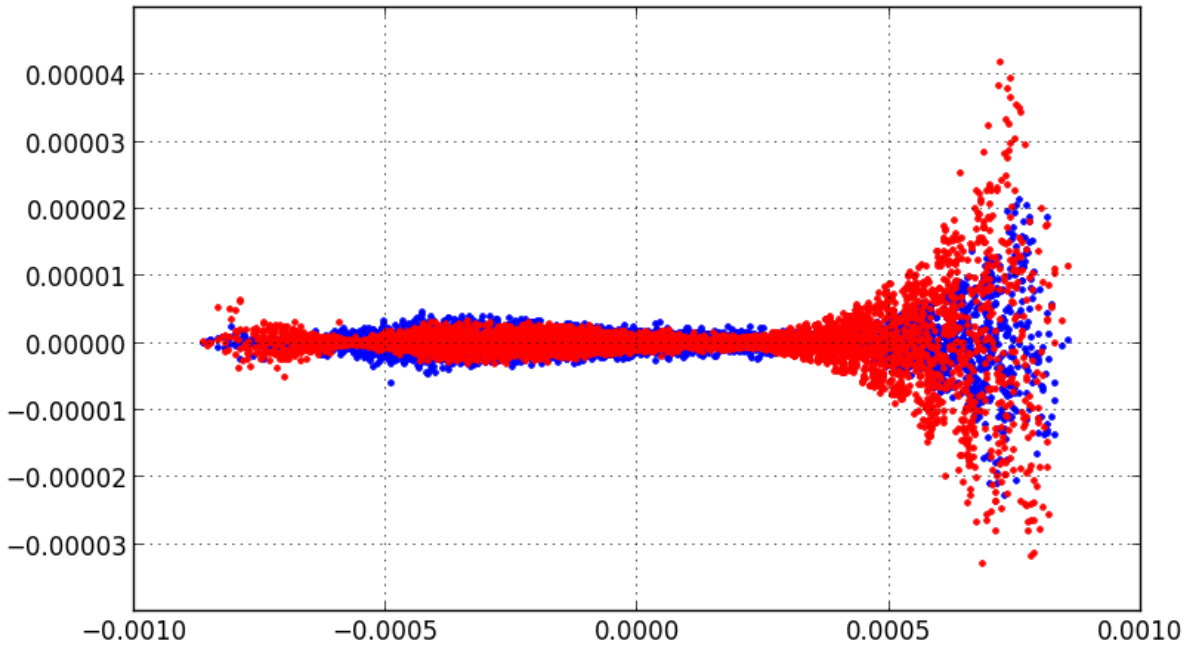

A.Bacci – first attempt SLAC X-band RF gun and SLAC X-band RF structures

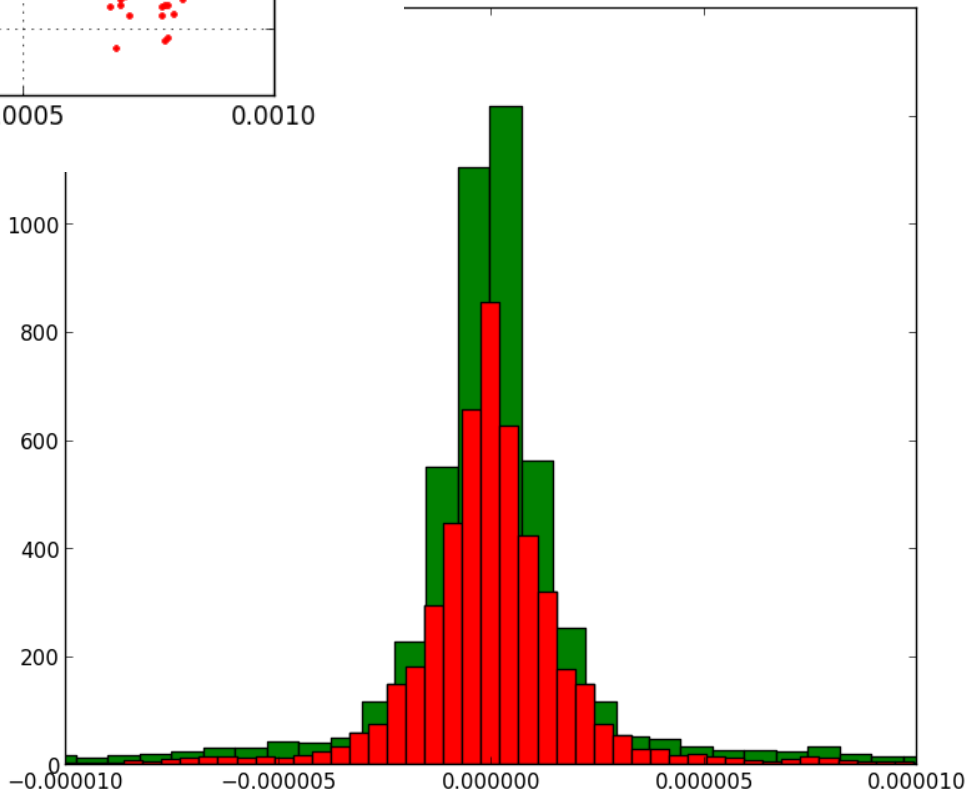

250 pC, 3 μm spot size

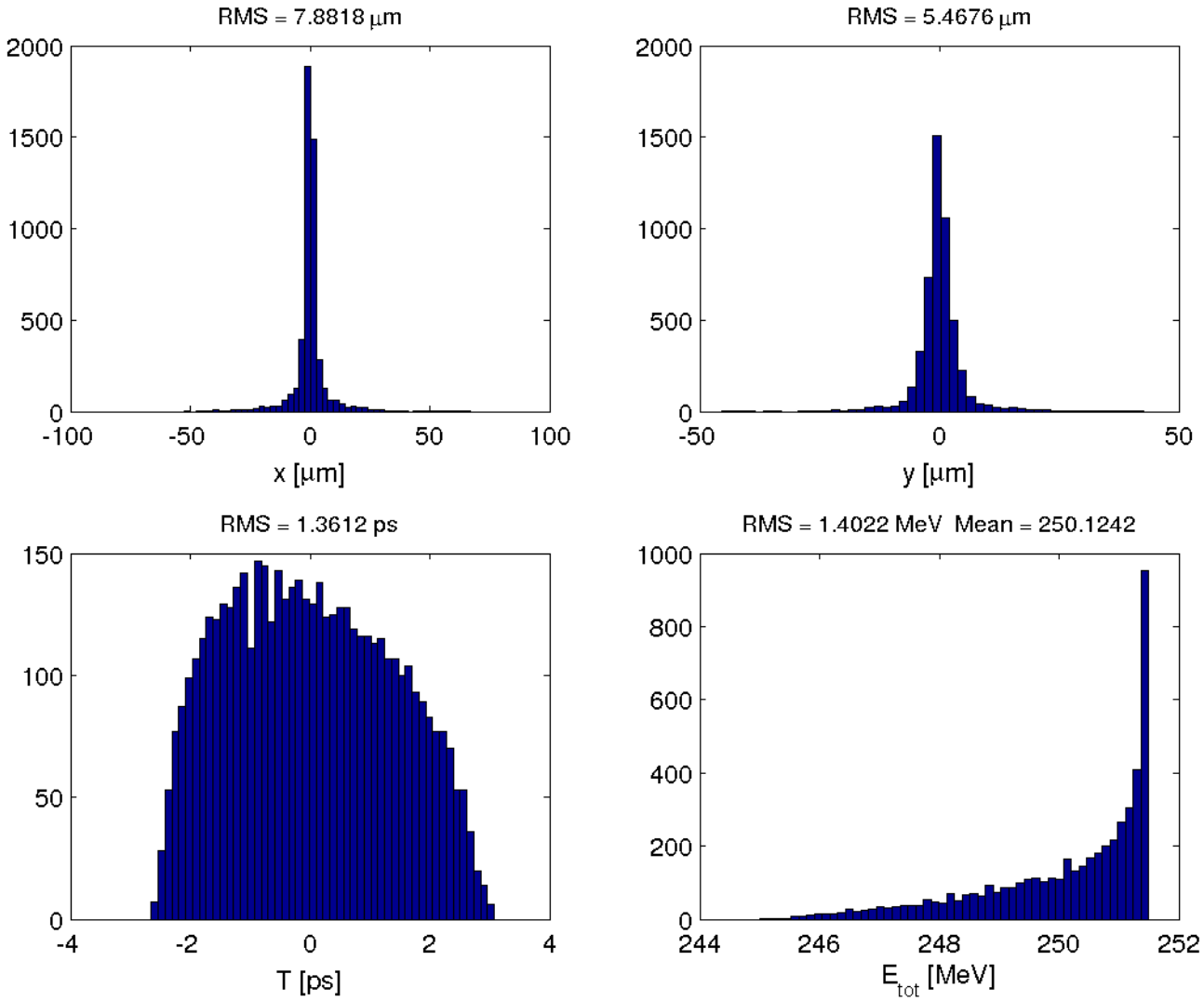
RMS = 7.8818 μm
2000
1500
1000
500
0
-100
-50
0
50
100
x [μm]
RMS = 5.4676 μm
2000
1500
1000
500
0
-50
0
50
y [μm]
RMS = 1.3612 ps
150
100
50
0
-4
-2
0
2
4
T [ps]
RMS = 1.4022 MeV Mean = 250.1242
1000
800
600
400
200
0
244
246
248
250
252
E_tot [MeV]

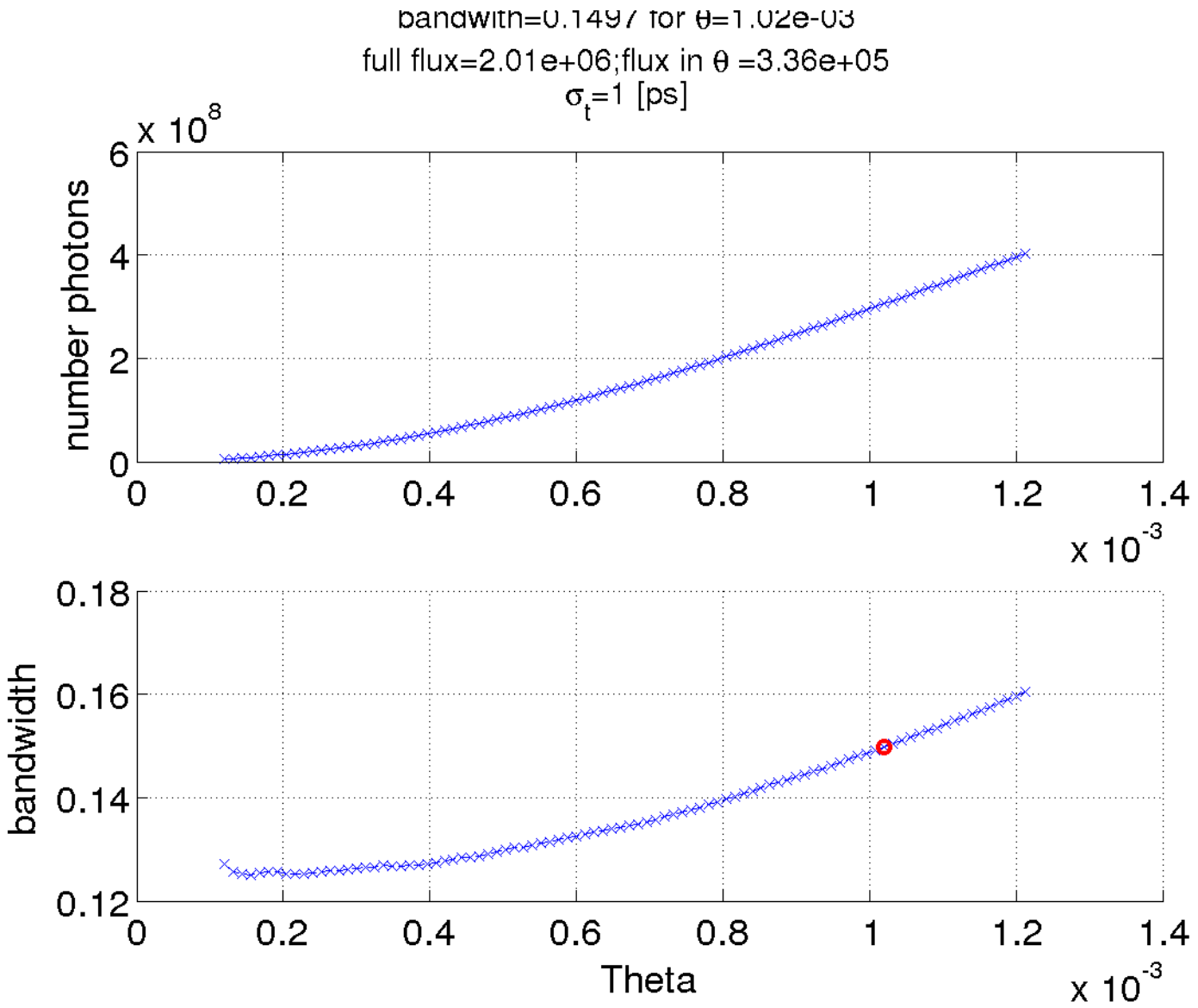

Illya Drebot with CAIN – single bunch mode 100 Hz no laser re-circul.

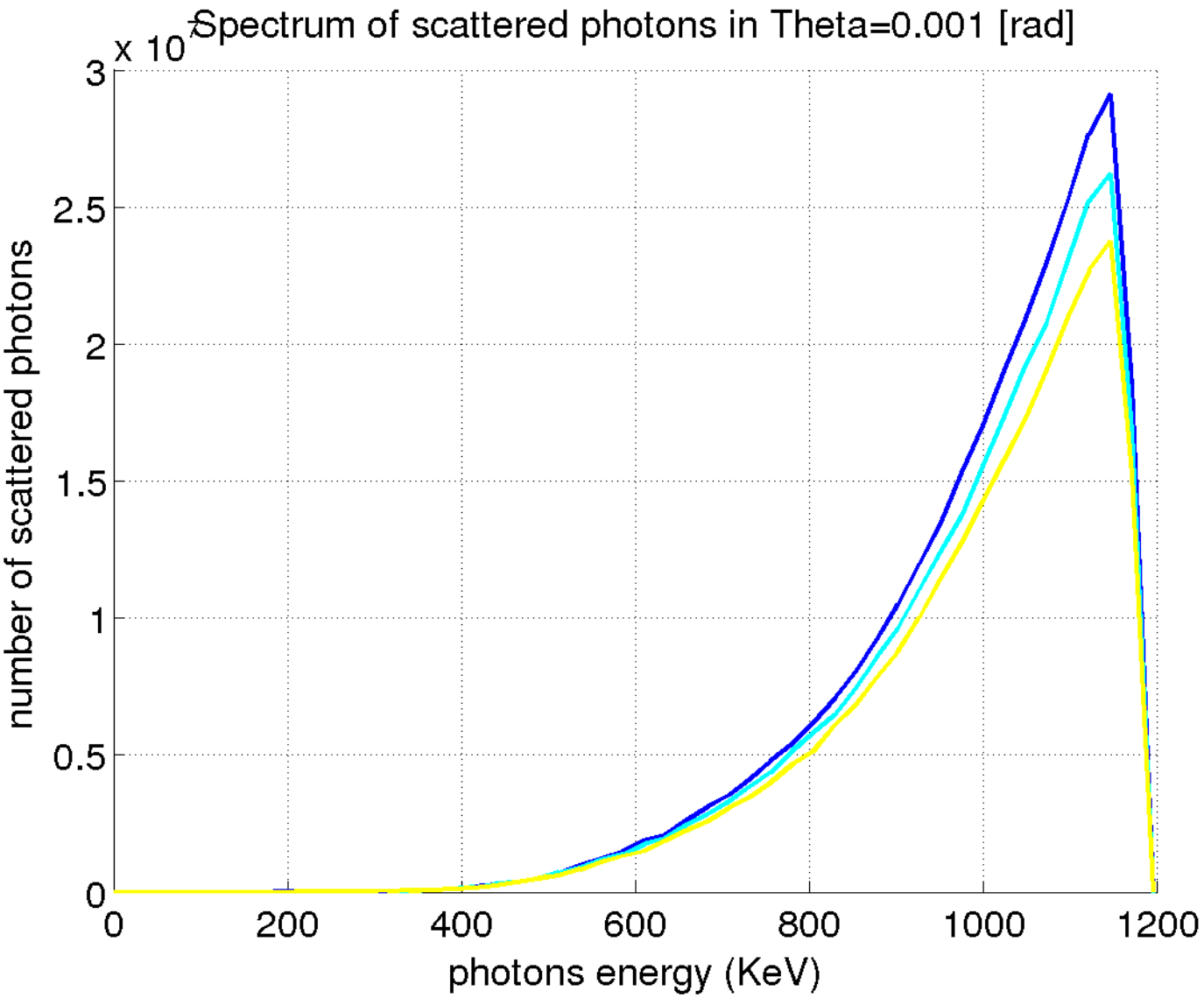

$$L_{SC} \approx 3 \cdot 10^{25} - 1 \cdot 10^{26} \quad \textit{uncollimated}$$